Entropic measures and magnetospheric dynamics

Georgios Balasis

IAASARS – National Observatory of Athens

Acknowledgements: **C. Papadimitriou, I. A. Daglis, A. Z. Boutsi, S. Potirakis, K. Eftaxias**

ISSS 2021
Web School, **1-5 February 2021**

Outline

- Investigating dynamical complexity in the magnetosphere using various entropy measures (and its significance for Space Weather)
  - Dynamical complexity in Dst time series using non-extensive Tsallis entropy
  - Signatures of discrete scale invariance in Dst time series
  - Dynamical Complexity of the 2015 St. Patrick's Day Magnetic Storm at Swarm Altitudes Using Entropy Measures
  - Dynamical Complexity in Swarm Electron Density Time Series using Block Entropy

- Multivariate information-theoretic causality analysis: disentangling the storm-substorm relationship

Motivation

An extreme coronal mass ejection and consequences for the magnetosphere and Earth

(Tsurutani & Lakhina, *GRL* 2014)

- A "perfect" interplanetary coronal mass ejection could create a magnetic storm with intensity up to the saturation limit (Dst ~2500 nT), a value greater than the Carrington storm.
- The interplanetary shock would arrive at Earth within ~12 h with a magnetosonic Mach number ~45, comparable to astrophysical shocks.
- The associated magnetospheric electric field will form a new relativistic electron radiation belt.

Welling et al., *Space Weather* in press

Table 1. Comparison of simulation results to other extreme space weather events & simulations. Values for the March 24, 1991 event are taken from the Moshiri magnetometer station (MSR) at 37.9° magnetic latitude.

Event/Simulation	D_{ST} Impulse	Standoff	Max dB/dt	Max $\lvert E \rvert$
T & L Estimates[1]	245 nT	5 R_E	30 nT/s	N/A
Present Results: NB_Z	234.0 nT	4 R_E	260 nT/s 12nT/s at 0°	$0.34 - 34.3\ V/km$ $11.2 - 15.8\ V/km$ at 55°
Present Results: SB_Z	268.7 nT	$< 3R_E$	290 nT/s 12 nT/s at 0°	$0.48 - 47.7\ V/km$ $16.7 - 23.5\ V/km$ at 55°
Synthetic Carrington[2]	$< 200\ nT$	>2 R_E	N/A	$> 30\ V/km$ $> 17\ V/km$ at 55°
July 2012 near-miss[3,4]	N/A	N/A	$\sim 10\ nT/s$	$\sim 15\ V/km$ $\sim 15\ V/km$ at 55°
September 1909 Storm[5]	$\sim 70.0\ nT$	5.9 R_E	N/A	N/A
May 1921 Storm[6]	$\sim 107.0\ nT$	5.3 R_E	N/A	N/A
March 1989 Storm[7,8,9]	$\sim 70\ nT$	N/A	$\sim 20\ nT/s$	$> 3\ V/km$ at 55°
March 1991 Storm[10,11]	202 nT	N/A	$\sim 20\ nT/s$ at MSR	N/A

[1]Tsurutani and Lakhina (2014), [2]Ngwira et al. (2014), [3]Baker et al. (2013), [4]Ngwira et al. (2013), [5]Love, Hayakawa, and Cliver (2019b), [6]Love, Hayakawa, and Cliver (2019a), [7]Kappenman (2005), [8]Boteler (2019), [9]Allen, Sauer, Frank, and Reiff (1989), [10]Araki et al. (1997), [11]Araki (2014)

Motivation

- The solar wind-magnetosphere and solar wind-radiation belt systems have been shown to be nonlinear [e.g., Johnson and Wing, *JGR* 2005; Reeves et al., *JGR* 2011; Wing et al., *JGR* 2016 and references therein].

- The Earth's magnetosphere corresponds to an open spatially extended nonequilibrium (input-output) dynamical complex system [Baker, 1990; Tsurutani et al., 1990; Vasssiliadis et al., 1990; Sharma et al., 1993; Sitnov et al., 2001; Consolini et al., 2008].

Motivation

- ***Dynamical complexity detection*** for output time series of complex systems is one of the foremost problems in physics, biology, engineering, and economic sciences.

- Especially in geomagnetism and magnetospheric physics, ***accurate detection of the dissimilarity between normal and abnormal states (e.g. pre-storm activity and magnetic storms)*** can vastly improve space weather diagnosis and, consequently, the mitigation of space weather hazards.

- The data sets obtained from most space physics studies are usually ***nonstationary, rather short, and stochastic.***

- One of our objectives is to find an ***effective complexity measure*** that requires short data sets for statistically significant results, provides the ability to make fast and robust calculations, and can be used to analyze nonstationary and noisy data, which is convenient for the analysis of geomagnetic and magnetospheric time series.

Information-Theoretical Measures

- **Linear Time Series Analysis Techniques**
  - Spectral Methods (Fourier Transform, Wavelets)
  - Rescaled Range Analysis

[Balasis et al., ANGEO 2006]

- **Non-linear Time Series Analysis Techniques**
  - Entropies
    - Shannon, Hartley, Rényi, etc.
  - Symbolic Dynamics
  - Non-extensive Statistical Mechanics (Tsallis entropy)
  - Approximate Entropy, Fuzzy Entropy, Sample Entropy etc.

[Balasis et al., GRL 2008, JGR 2009, Entropy 2013, Frontiers 2016, EPL 2020]

IAASARS

ΕΘΝΙΚΟΝ ΑΣΤΕΡΟΣΚΟΠΕΙΟΝ ΑΘΗΝΩΝ * NATIONAL OBSERVATORY OF ATHENS *

Power-law

- If a time series is a temporal fractal then a power law of the form:

$$S(f) \sim f^{-\beta}$$

is obeyed with

- *S(f)* - power spectral density
- *f* - frequency
- *β* - spectral scaling exponent, a measure of the strength of time correlations
- *r* - linear correlation coefficient, the fit of the time series to a power-law

In general, $-1<\beta<3$, but it describes 2 classes of signal: fractional Gaussian noise (fGn) or fractional Brownian motion (fBm)

The Hurst exponent - *H* is calculated using different formulas for fGn ($-1<\beta<1$) or fBm ($1<\beta<3$)

Spectral Methods – beta Exponent

If a time series is a temporal fractal then a power law of the form **$S(f) \sim f^{-\beta}$** is obeyed with S(f) the power spectral density, f the frequency and 'β' the spectral scaling exponent, a measure of the strength of time correlations.

In general, $-1<\beta<3$, but it describes 2 classes of signal:

- **$-1<\beta<1$**: fractional Gaussian noise (**fGn**)
- **$1<\beta<3$**: fractional Brownian motion (**fBm**)

For the fBm case, **$\beta > 2$** marks the transition from anti-persistent to persistent behaviour.

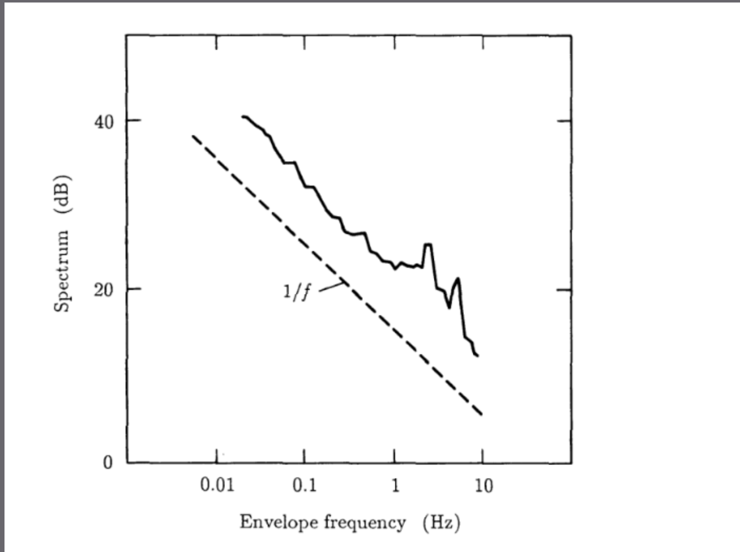

Spectrum of amplitude variations for Bach's First Brandenburg Concerto [VC 78].

"Fractals, Chaos, Power Laws: Minutes from an Infinite Paradise" by Manfred Schroeder

β exponent and its relation to Hurst

β** = 2**H**+1*, where ***H is the Hurst exponent for the fBm case (1 < ***β*** < 3)

- The exponent ***H*** characterizes the ***persistent/anti-persistent*** properties of the signal. The range *0<**H**<0.5 (1<**β**<2)* during the normal period indicates ***anti-persistency***, reflecting that if the fluctuations increase in a period, it is likely to decreasing in the interval immediately following and vice versa.
- We pay attention to the fact that the time series appears ***persistent*** properties, *0.5<**H**<1 (2<**β**<3)*. This means that if the amplitude of fluctuations increases in a time interval it is likely to continue increasing in the interval immediately following.
- ***H****=0.5 (**β**=2)* suggests no correlation between the repeated increments. Consequently, this particular value takes on a special physical meaning:

  It marks the transition between persistent and anti-persistent behavior in the time series.

Dst Index

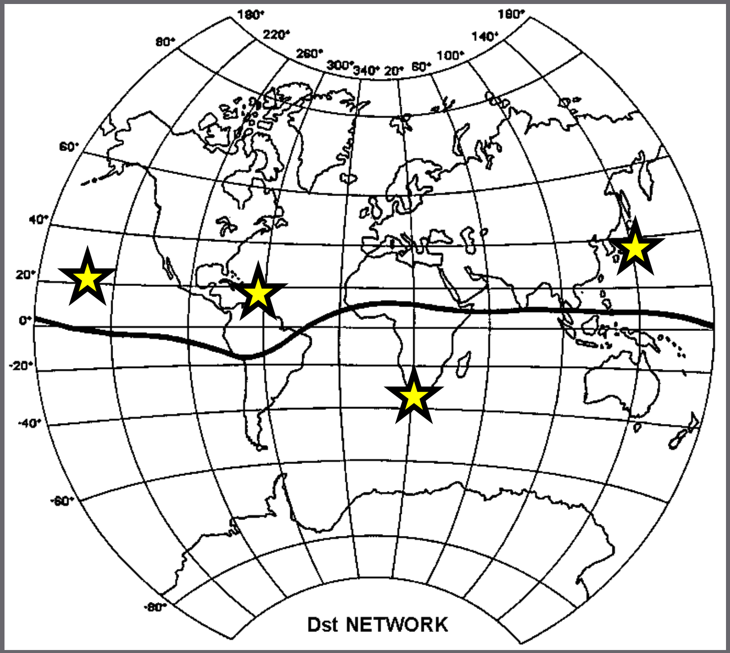

- Represents the axially symmetric disturbance (of the horizontal component) of the magnetic field at the dipole equator on the Earth's surface.
- Derived using data from 4 stations
  - Hermanus (South Africa)
  - Kakioka (Japan)
  - Honolulu (US-HI)
  - San Juan (Puerto Rico)

IAGA Bulletin N°40: http://wdc.kugi.kyoto-u.ac.jp/dstdir/dst2/onDstindex.html

D_{st} index time series

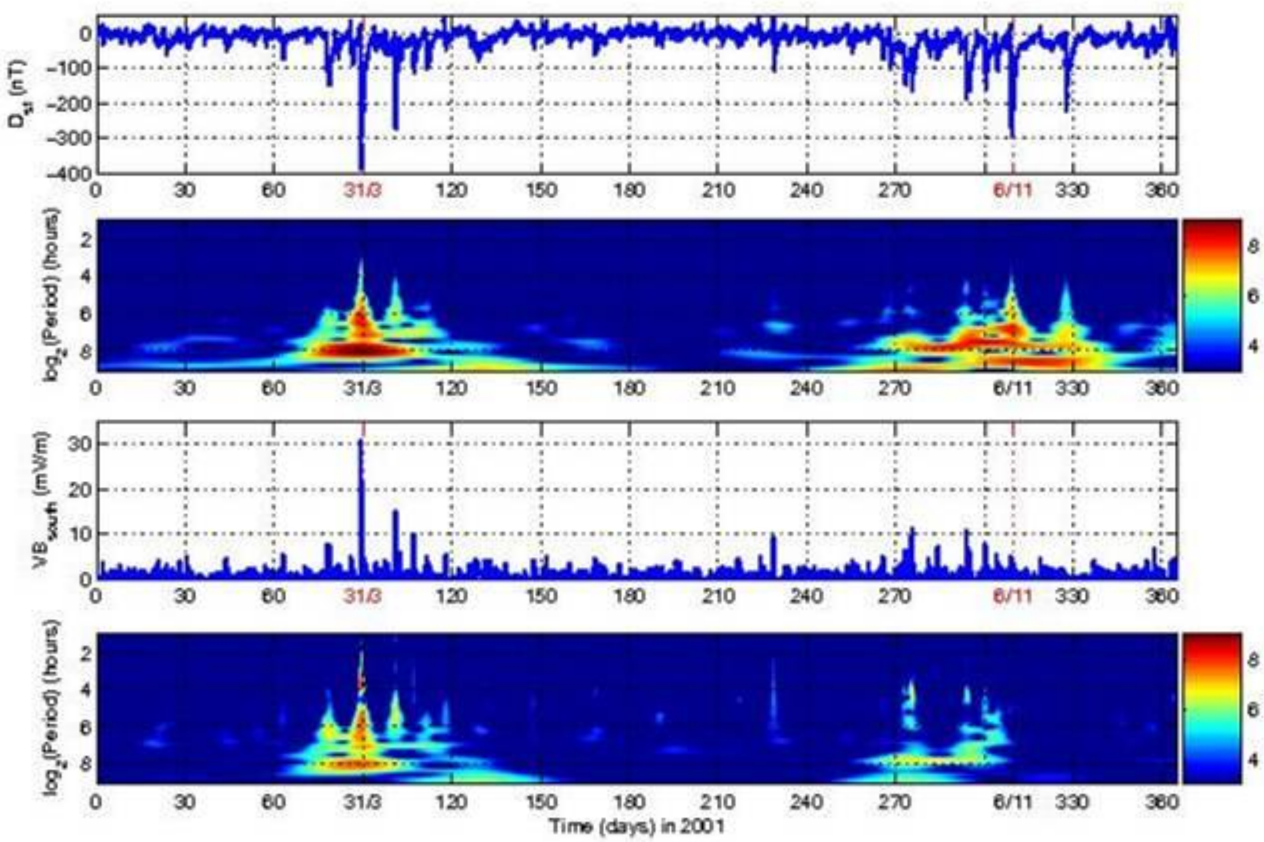

(Balasis et al., *Ann. Geophys.* 2006)

Scaling parameters of the D_{st} index

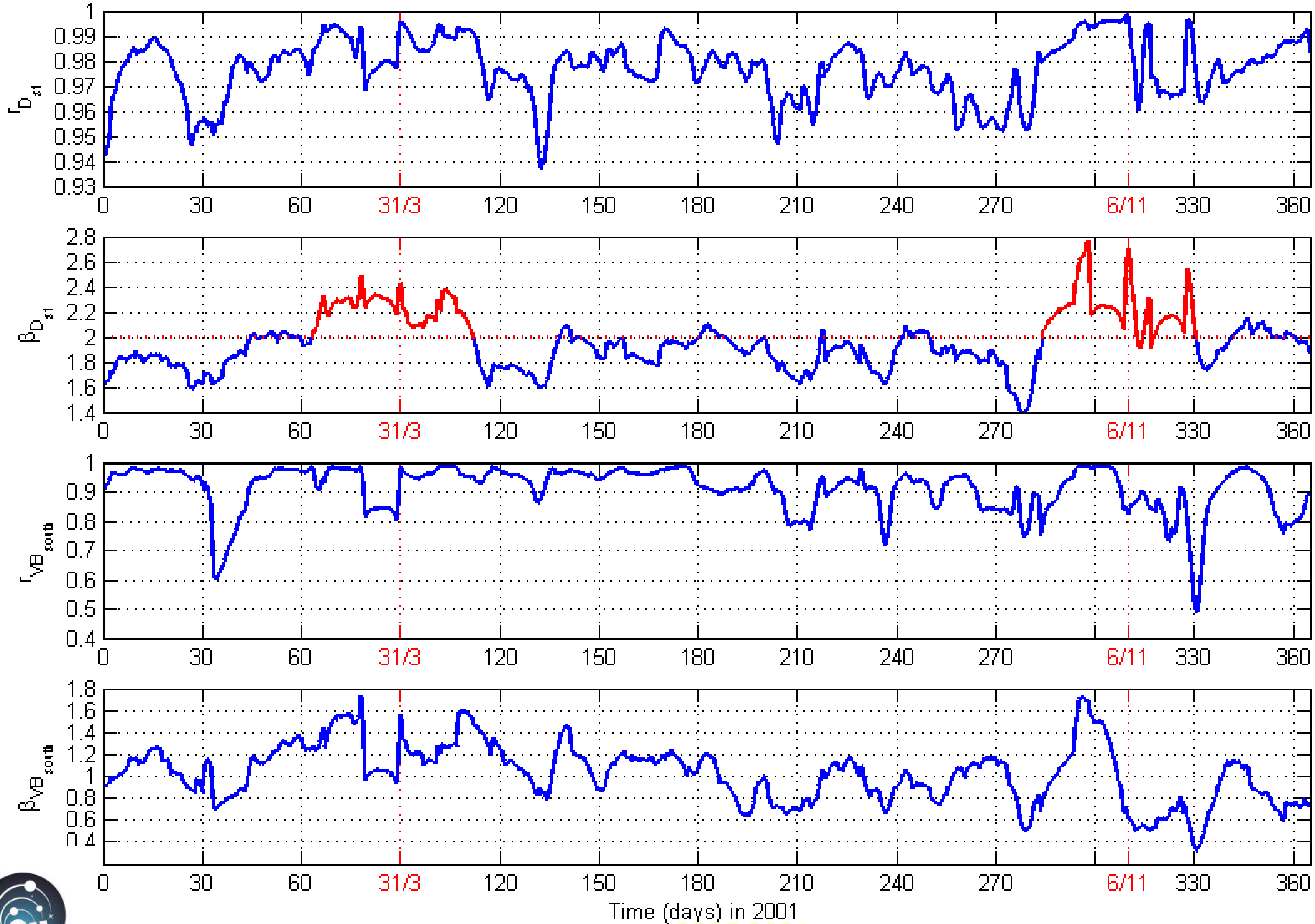

Summary

- We show that distinctive alterations in scaling parameters of D_{st} index time series occur as an intense magnetic storm approaches.
- The transition from anti-persistent to persistent behavior may indicate that the onset of an intense magnetic storm is imminent.
- See also Wanliss (*JGR* 2005) and Wanliss and Dobias (*JASTP* 2007) for SYM-H as well as Zaourar et al. (*EPS* 2013) for observatory data.

The concept of Entropy

- In information theory, **entropy** is the average amount of information contained in each message received.

- Here, message stands for an event, sample or character drawn from a distribution or data stream.

- <u>Entropy thus characterizes our uncertainty about our source of information.</u>

- Generally, "entropy" stands for "disorder" or uncertainty.

- Entropy is a measure of *unpredictability* of *information content*.

- <u>Entropy may characterize the regularity statistics of a signal.</u>

Shannon entropy

[15] Shannon recognized that a similar approach to Boltzmann-Gibbs entropy could be applied to information theory. In his famous 1948 paper [*Shannon*, 1948], he introduced a probabilistic entropy measure H_S:

$$\boxed{H_S(X) = -\sum_{i=1}^{n} p(x_i)\log_b p(x_i),}$$

where b is the base of the logarithm used and p denotes the probability mass function of a discrete random variable X with possible values $\{x_1, \ldots, x_n\}$.

Shannon Entropy

Given p_i the probability of a telecom. system being in a cell 'i' of its phase space, Shannon defined the information produced by it by means of the Boltzmann H theorem, as the entropy

$$H = -\sum_i p_i \cdot \log_b p_i$$

Continuous variables can be "digitized" in order to define these "cells" of the phase space.

This in essence becomes a "histogram entropy" and loses all sense of temporal information.

(Shannon, 1948)

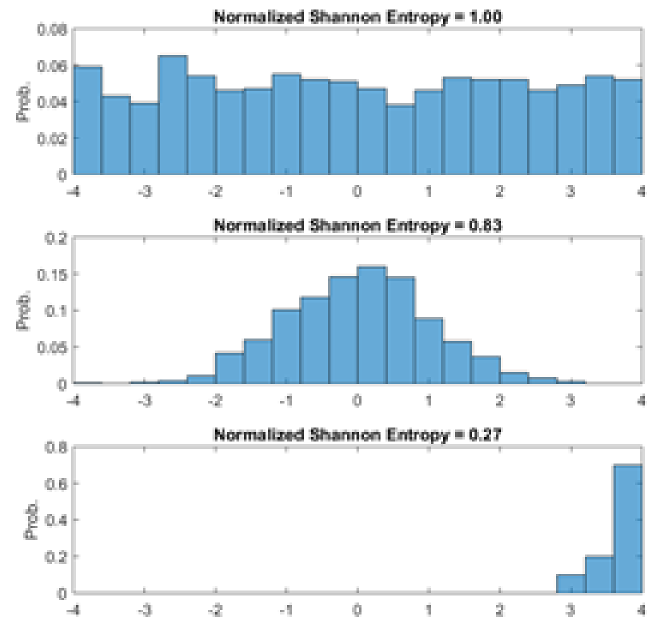

Symbolic dynamics

- Herein, we estimate S_q based on the concept of ***symbolic dynamics***: from the initial measurements we generate a sequence of symbols, where the dynamics of the original (under analysis) system has been projected [Bailin, 1989].

- ***Symbolic dynamics*** is based on a coarse-graining of the measurements, i.e., the original D_{st} time series of length N, $(X_1, X_2, \ldots, X_N)$, is projected to a symbolic time series $(A_1, A_2, \ldots, A_N)$ with An from a finite alphabet of λ letters $(0, \ldots, \lambda - 1)$.

- The simplest possible coarse graining of the D_{st} index is given by choosing a threshold C (usually the mean value of the data considered) and assigning the symbols "1" and "0" to the signal, depending on whether it is above or below the threshold (binary partition).

Dynamical (Shannon-Like) *Block* Entropy

[18] It is useful to transform the initial raw data of the magnetospheric signal into symbolic sequences taking values in the alphabet {0,1}, according to the rules $A_i = 1$ if $A(t_i) > E[A(t_i)]$ and $A_i = 0$ if $A(t_i) < E[A(t_i)]$, where $A(t_i)$ are the values of the measured field at time t_i and $E[A(t_i)] = \langle A(t_i) \rangle$ is the mean value in the particular time windows, as it is nicely stated by *Schwarz et al.* [1993].

[19] Consider a subsequence of length N selected out of a very long (theoretically infinite) symbolic sequence. We stipulate that this subsequence is to be read in terms of distinct "blocks" of length n,

$$\ldots \underbrace{A_1 \ldots A_n}_{B_1} \underbrace{A_{n+1} \ldots A_{2n}}_{B_2} \ldots \underbrace{A_{jn+1} \ldots A_{(j+1)n}}_{B_{j+1}} \ldots \qquad (1)$$

We call this reading procedure "lumping."

[20] The following quantities characterize the information content of the sequence [*Khinchin*, 1957; *Ebeling and Nicolis*, 1992]

[21] 1. The dynamical (Shannon-like) block entropy for blocks of length n

$$\boxed{H(n) = -\sum_{(A_1,\ldots,A_n)} p^{(n)}(A_1,\ldots,A_n) \cdot \ln p^{(n)}(A_1,\ldots,A_n)} \qquad (2)$$

where the probability of occurrence of a block $A_1 \ldots A_n$, denoted $p^{(n)}(A_1,\ldots,A_n)$, is defined by the fraction (when it exists) in the statistical limit as

$$\boxed{\frac{\text{No. of blocks,}\quad A_1 \ldots A_n,\quad \text{encountered when lumping}}{\text{total No. of blocks}}} \qquad (3)$$

starting from the beginning of the sequence, and the associate entropy per letter

$$h^{(n)} = \frac{H(n)}{n}. \qquad (4)$$

[22] 2. The conditional entropy or entropy excess associated with the addition of a symbol to the right of an n block

$$h_{(n)} = H(n+1) - H(n). \qquad (5)$$

[23] 3. The entropy of the source (a topological invariant), defined as the limit (if it exists)

$$\boxed{h = \lim_{n\to\infty} h_{(n)} = \lim_{n\to\infty} h^{(n)}} \qquad (6)$$

which is the discrete analog of metric or Kolmogorov entropy.

Symbolic Dynamics & Block Entropies

Digitization of continuous time series (as an easy example consider the binary case, performed by a simple mean-value thresholding)

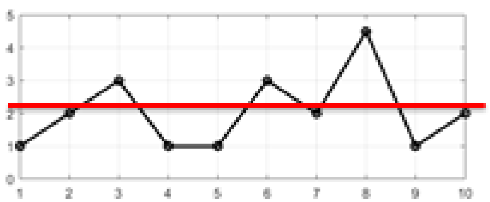

0, 0, 1, 0, 0, 1, 0, 1, 0, 0

Parsing the symbolic series in blocks of length 'm', e.g. for m=3

Gliding/Sliding Method (overlapping)

Lumping Method (non - overlapping)

0, 0, 1, 0, 0, 1, 0, 1, 0, **0, 0, 1,** 0, 0, 1, 0, 1, 0, 0

0, **0, 1, 0,** 0, 1, 0, 1, 0, 0, 0, 1, **0, 0, 1,** 0, 1, 0, 0

0, 0, **1, 0, 0,** 1, 0, 1, 0, 0, 0, 1, 0, 0, 1, **0, 1, 0,** 0

In both cases, count the probability of appearance of each "block of length m" and compute the block entropy H(m).

The entropy of the source is given by $H(m+1) - H(m)$, for $m > 1$

[Karamanos & Nicolis, 1999]

Symbolic Dynamics & Block Entropies

Block entropies are concerned with "**patterns**" of consecutive values (symbols), i.e. with **trajectories** in the system's phase space.

They are better suited to capture the "**dynamics**" of the underlying system and detect changes in its state.

Number of possible blocks scales exponentially with 'm', which means that more data points are needed for meaningful statistics (even more for multi-symbol representations)!

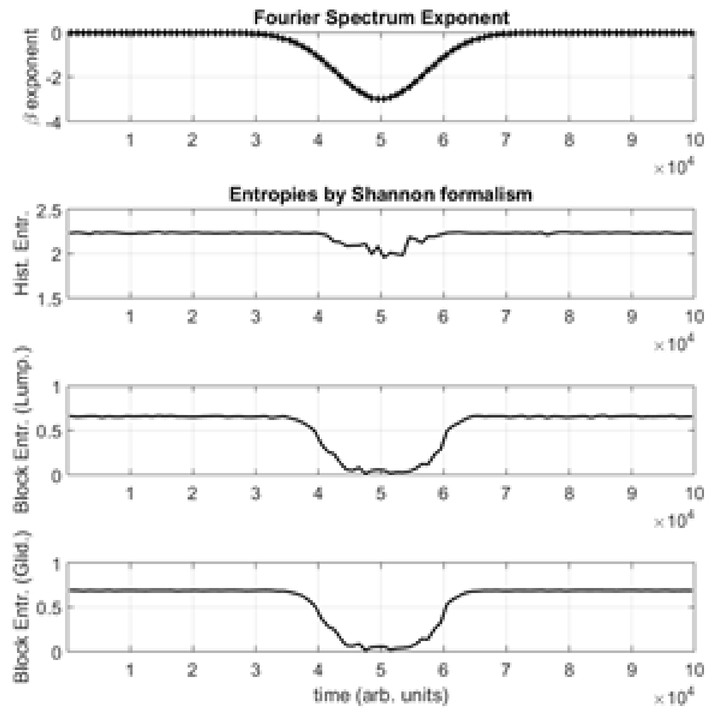

Extensivity

- The uncertainty of an open system state can be quantified by the ***Boltzmann-Gibbs (B-G) entropy***, which is the widest known uncertainty measure in statistical mechanics.
- ***B-G entropy (*** $S_{B\text{–}G}$ ***)*** *cannot, however, describe nonequilibrium physical systems with large variability and multi-fractal structure such as the solar wind [Burlaga et al., 2007].*
- Inspired by multi-fractal concepts, ***Tsallis*** [1988, 1998] has proposed a generalization of the B-G statistics.

Extensivity

- One of the crucial properties of the $\boldsymbol{S_{B-G}}$ in the context of classical thermodynamics is ***extensivity***, namely proportionality with the number of elements of the system.

- The $\boldsymbol{S_{B-G}}$ satisfies this prescription if the subsystems are statistically (quasi-) independent, or typically if the correlations within the system are essentially local. In such cases the system is called ***extensive***.

Tsallis entropy

- In general, however, the situation is not of this type and correlations may be far from negligible at all scales. In such cases the $\boldsymbol{S_{B-G}}$ is ***nonextensive***.
- ***Tsallis*** [1988, 1998] introduced an entropic expression characterized by an index $\boldsymbol{q}$ which leads to a nonextensive statistics,

$$\boxed{S_q = k\frac{1}{q-1}\left(1-\sum_{i=1}^{W} p_i^q\right)}$$

- where p_i^q are the probabilities associated with the microscopic configurations, W is their total number, q is a real number, and k is Boltzmann's constant.

Tsallis entropy and complexity

- The parameter q itself is not a measure of the complexity of the system but measures the degree of nonextensivity of the system.

- It is the time variations of the Tsallis entropy for a given q (S_q) that quantify the dynamic changes of the complexity of the system.

- *Lower S_q values characterize the portions of the signal with lower complexity.*

Tsallis entropy in terms of symbolic dynamics

- *The S_q for the word length L is*

$$S_q(L) = k\frac{1}{q-1}\Big(1 - \sum_{(A_1, A_2, \ldots A_L)} [p(L)_{(A_1, A_2, \ldots A_L)}]^q\Big)$$

- *Broad symbol-sequence frequency distributions produce high entropy values, indicating a low degree of organization.*
- *Conversely, when certain sequences exhibit high frequencies, lower entropy values are produced, indicating a high degree of organization.*

Other Entropy Formulations (Tsallis)

Different mathematical formulas have been proposed as generalizations of Shannon's entropy definition. Some of them incorporating additional free parameters.

Tsallis Entropy: $S_q = k\frac{1}{q-1}\left(1 - \sum_i p_i^q\right)$

[Tsallis, 2009]

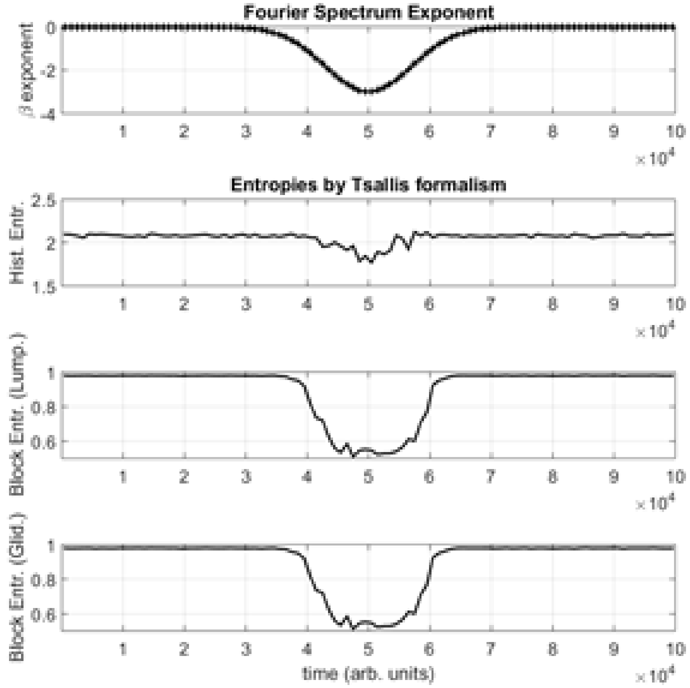

Example with q = 2

Dynamical complexity in Dst time series using non-extensive Tsallis entropy

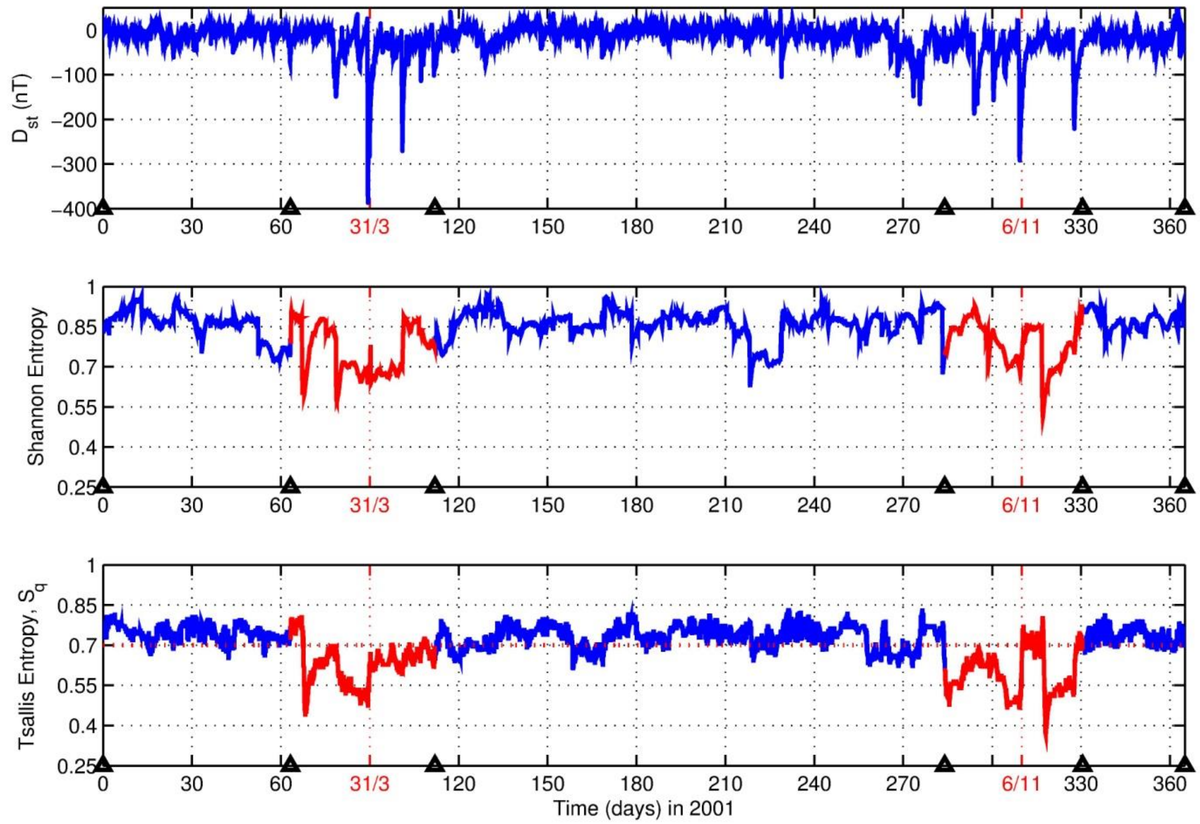

(Balasis et al., *GRL* 2008, *JGR* 2009)

Entropies

- Approximate entropy (ApEn) has been introduced by Pincus as a measure for characterizing the regularity in relatively short and potentially noisy data. More specifically, ApEn examines time series for detecting the presence of similar epochs; more similar and more frequent epochs lead to lower values of ApEn.

- Sample entropy (SampEn) was proposed by Richman and Moorman as an alternative that would provide an improvement of the intrinsic bias of ApEn.

- Fuzzy entropy (FuzzyEn), like its ancestors, ApEn and SampleEn, is a "regularity statistic" that quantifies the (un)predictability of fluctuations in a time series. For the calculation of FuzzyEn, the similarity between vectors is defined based on fuzzy membership functions and the vectors' shapes. FuzzyEn can be considered as an upgraded alternative of SampEn (and ApEn) for the evaluation of complexity, especially for short time series contaminated by noise.

Approximate Entropy (*ApEn*)

[39] The approximate entropy examines time series for similar epochs: more similar and more frequent epochs lead to lower values of *ApEn*. In a more qualitative point of view, given N points, the *ApEn*-like statistics is approximately equal to the negative logarithm of the conditional probability that two sequences that are similar for m points remain similar, that is, within a tolerance r, at the next point. Smaller *ApEn* values indicate a greater chance that a set of data will be followed by similar data (regularity), thus, smaller values indicate greater regularity. Conversely, a greater value for *ApEn* signifies a lesser chance of similar data being repeated (irregularity), hence, greater values convey more disorder, randomness and system complexity. Thus a low/high value of *ApEn* reflects a high/low degree of regularity. The following is a description of the calculation of *ApEn*. Given any sequence of data points $u(i)$ from $i = 1$ to N, it is possible to define vector sequences $x(i)$, which consist of length m and are made up of consecutive $u(i)$, specifically defined by the following:

$$x(i) = (u[i], u[i+1], \ldots, u[i+m-1]). \tag{16}$$

[40] In order to estimate the frequency that vectors $x(i)$ repeat themselves throughout the data set within a tolerance r, the distance $d(x[i], x[j])$ is defined as the maximum difference between the scalar components $x(i)$ and $x(j)$. Explicitly, two vectors $x(i)$ and $x(j)$ are "similar" within the tolerance or filter r, namely $d(x[i], x[j]) \leq r$, if the difference between any two values for $u(i)$ and $u(j)$ within runs of length m are less than r (i.e., $|u(i+k) - u(j+k)| \leq r$ for $0 \leq k \leq m$). Subsequently, $C_i^m(r)$ is defined as the frequency of occurrence of similar runs m within the tolerance r:

$$C_i^m(r) = \frac{[\text{number of } j \text{ such that } d(x[i], x[j]) \leq r]}{(N-m-1)},$$

where $j \leq (N - m - 1)$.

Approximate Entropy (*ApEn*)

[41] Taking the natural logarithm of $C_i^m(r)$, $\Phi^m(r)$ is defined as the average of $ln(C_i^m(r))$:

$$\Phi^m(r) = \sum_i lnC_i^m(r)/(N-m-1) \quad (17)$$

where $\sum_i$ is a sum from $i = 1$ to $(N - m - 1)$. $\Phi^m(r)$ is a measure of the prevalence of repetitive patterns of length m within the filter r.

[42] Finally, approximate entropy, or $ApEn(m, r, N)$, is defined as the natural logarithm of the relative prevalence of repetitive patterns of length m as compared with those of length $m + 1$:

$$\boxed{ApEn(m, r, N) = \Phi^m(r) - \Phi^{m+1}(r).} \quad (18)$$

[43] Thus, $ApEn(m, r, N)$ measures the logarithmic frequency that similar runs (within the filter r) of length m also remain similar when the length of the run is increased by 1. Thus, small values of *ApEn* indicate regularity, given that i increasing run length m by 1 does not decrease the value of $\Phi^m(r)$ significantly (i.e., regularity connotes that $\Phi^m[r] \approx \Phi^{m+1}[r]$). $ApEn(m, r, N)$ is expressed as a difference, but in essence it represents a ratio; note that $\Phi^m[r]$ is a logarithm of the averaged $C_i^m(r)$, and the ratio of logarithms is equivalent to their difference. A more comprehensive description of *ApEn* is given by *Pincus* [1991], *Pincus and Goldberger* [1994], and *Pincus and Singer* [1996].

[44] In summary, *ApEn* is a "regularity statistics" that quantifies the unpredictability of fluctuations in a time series. Intuitively, one may reason that the presence of repetitive patterns of fluctuation in a time series renders it more predictable than a time series in which such patterns are absent. *ApEn* reflects the likelihood that "similar" patterns of observations will not be followed by additional "similar" observations. A time series containing many repetitive patterns has a relatively small *ApEn*; a less predictable (i.e., more complex) process has a higher *ApEn*.

Approximate & Fuzzy Entropy

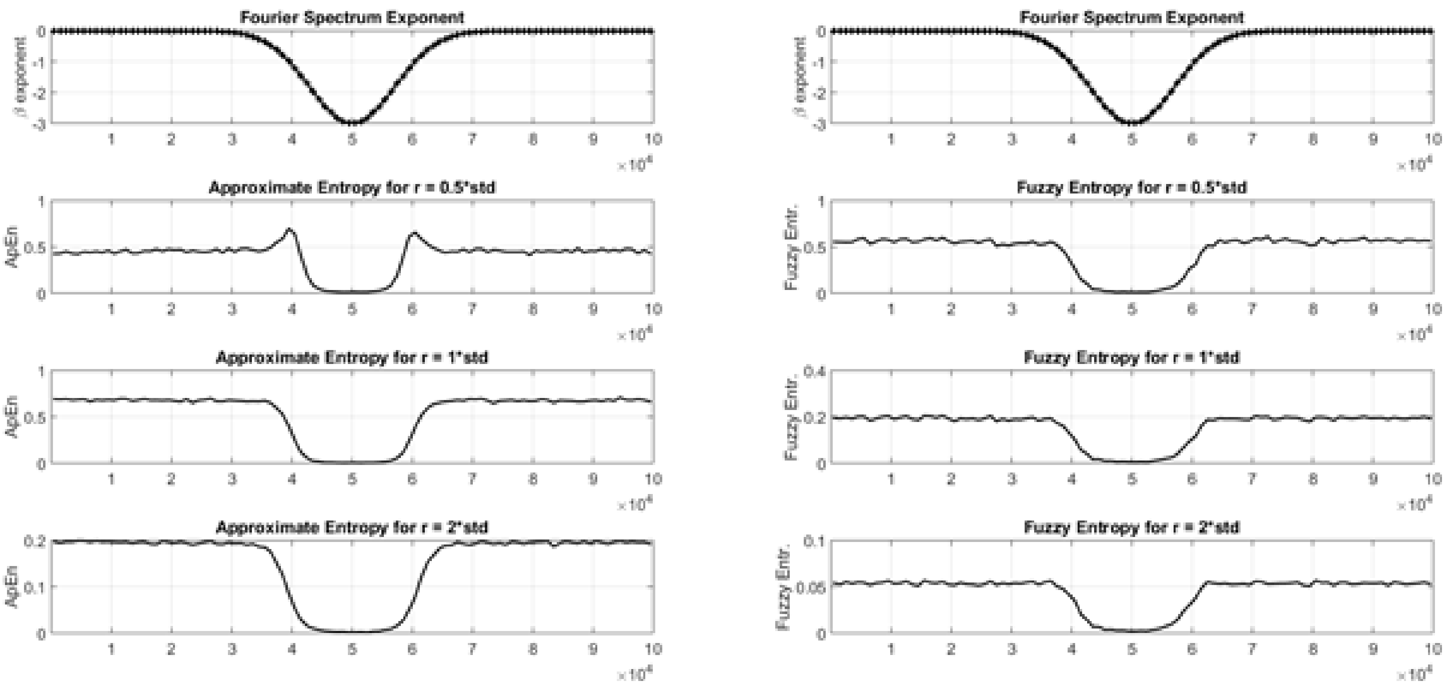

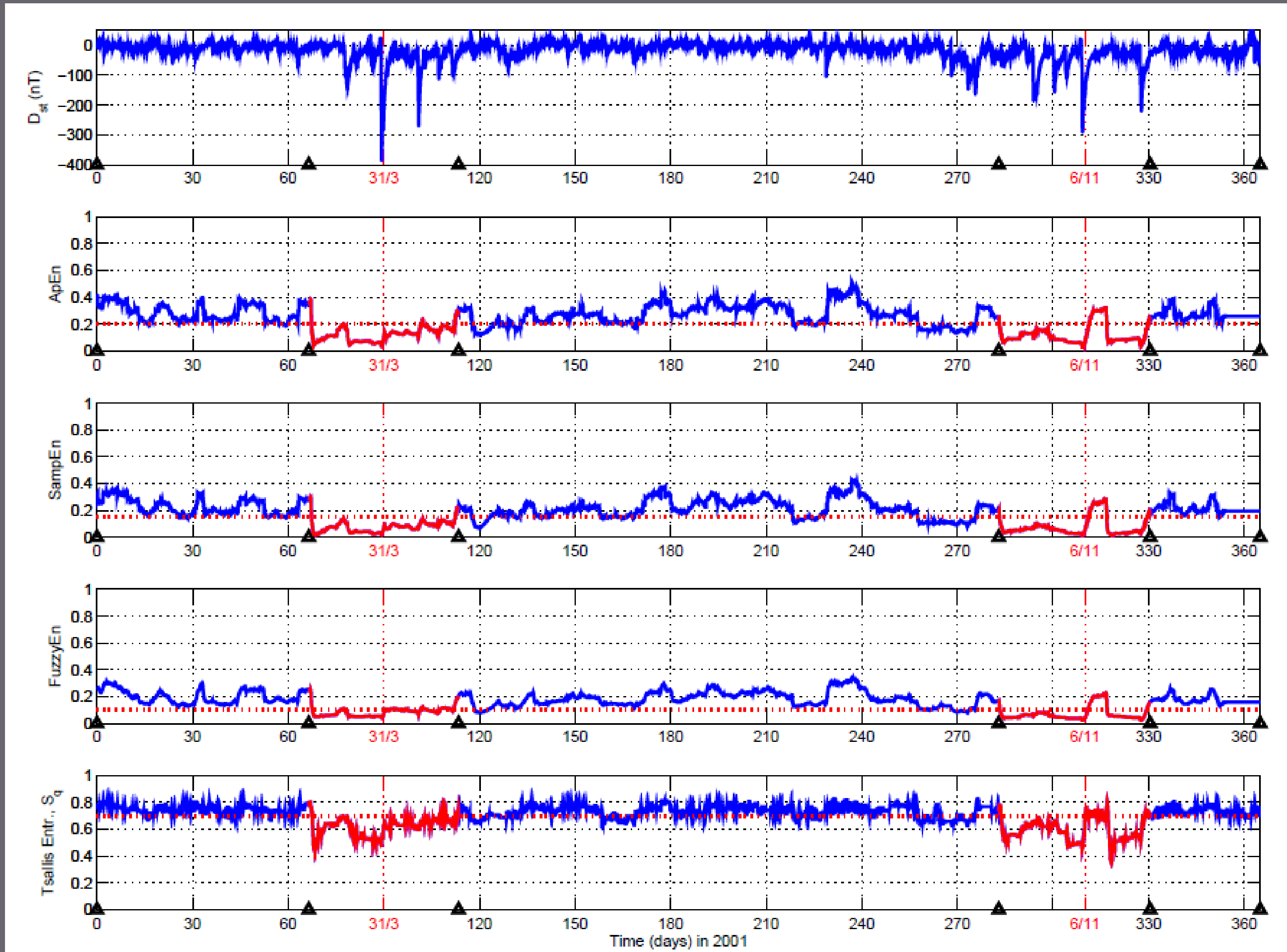

(Balasis et al., *Entropy* 2013)

Which parameter(s) to use for characterizing dynamic complexity of magnetic storms and quiescence periods?

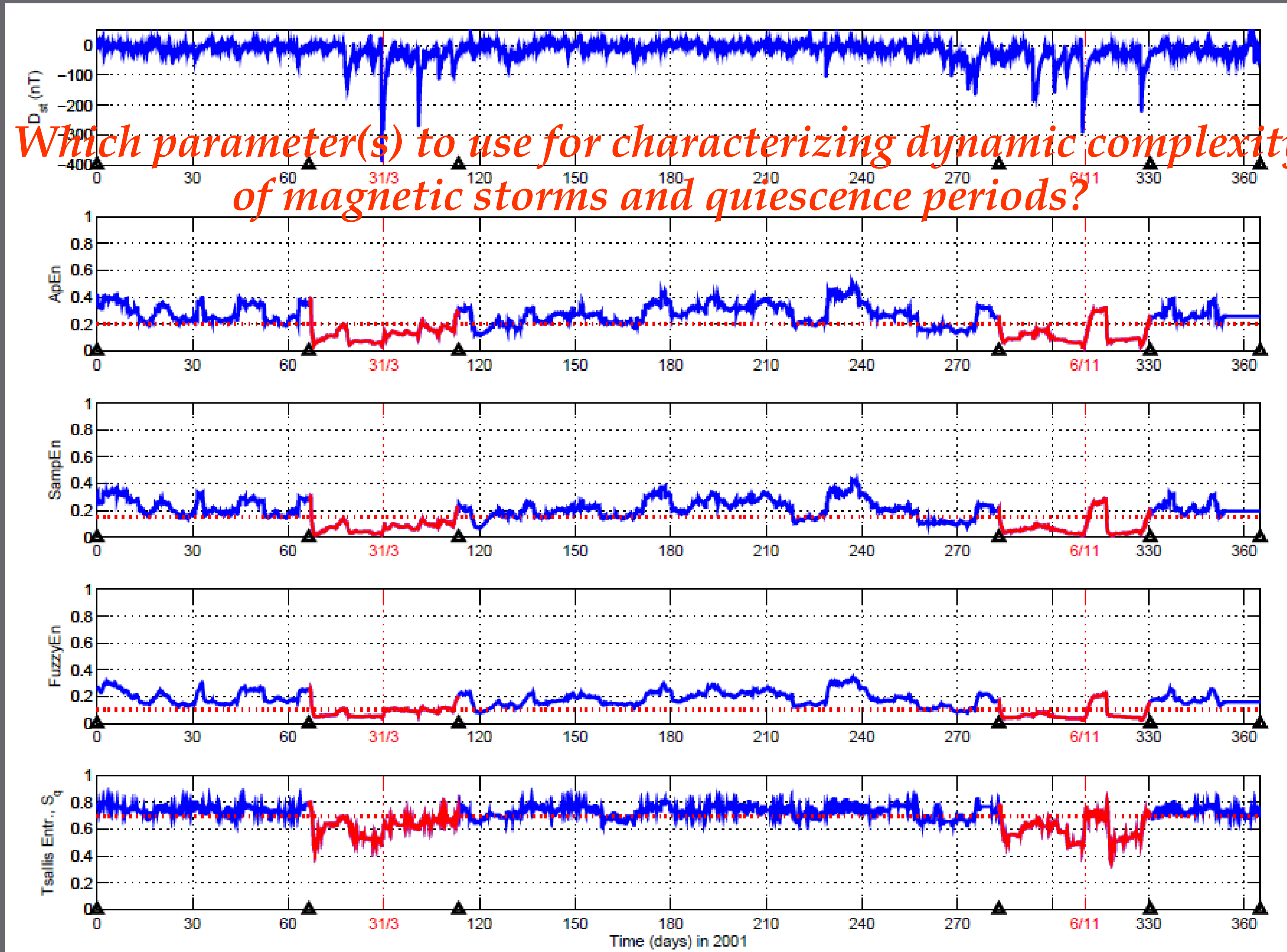

(Balasis et al., *Entropy* 2013)

Discrete scale invariance

- Self-similar systems are characterized by continuous scale invariance and, in response, the existence of power laws.

- However, a significant number of systems exhibits discrete scale invariance (DSI) which in turn leads to log-periodic corrections to scaling that decorate the pure power law.

Discrete Scale Invariance

- DSI manifests itself in data by log-periodic corrections to scaling [Sornette, 1998; 2004].

  - Typically the log-periodicity in time is given by:

$$E(t) = A + B(t_f - t)^m \{1 + C\cos[\omega \log(t_f - t) + \varphi]\}$$

$E(t)$	- the cumulative energy released
t_f	- the time of the main shock (storm peak)
ω	- the frequency
φ	- an offset

(Huang, Y., H. Saleur, and D. Sornette (2000), Reexamination of log periodicity observed in the seismic precursors of the 1989 Loma Prieta earthquake, J. Geophys. Res., 105, 28,111–28,123, doi:10.1029/2000JB900308.)

Dynamical complexity in Dst time series using non-extensive Tsallis entropy

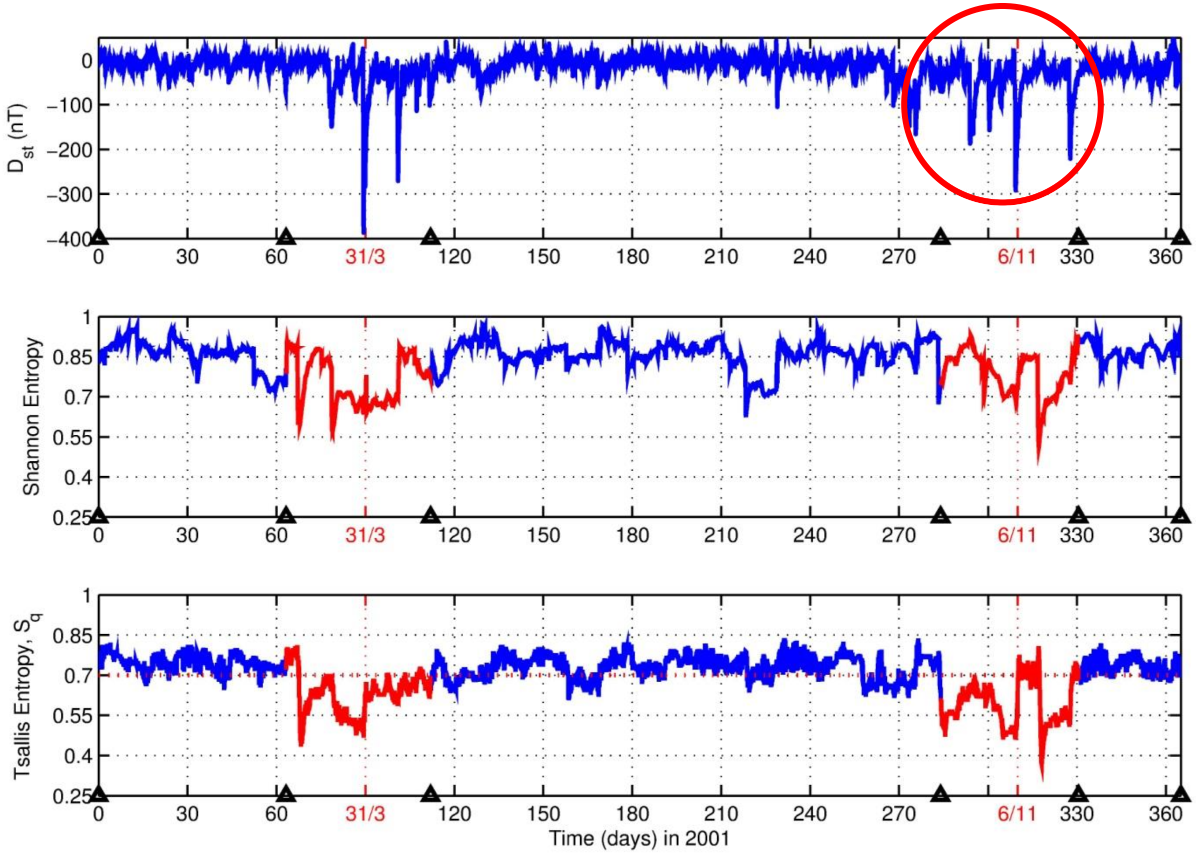

(Balasis et al., *GRL* 2008)

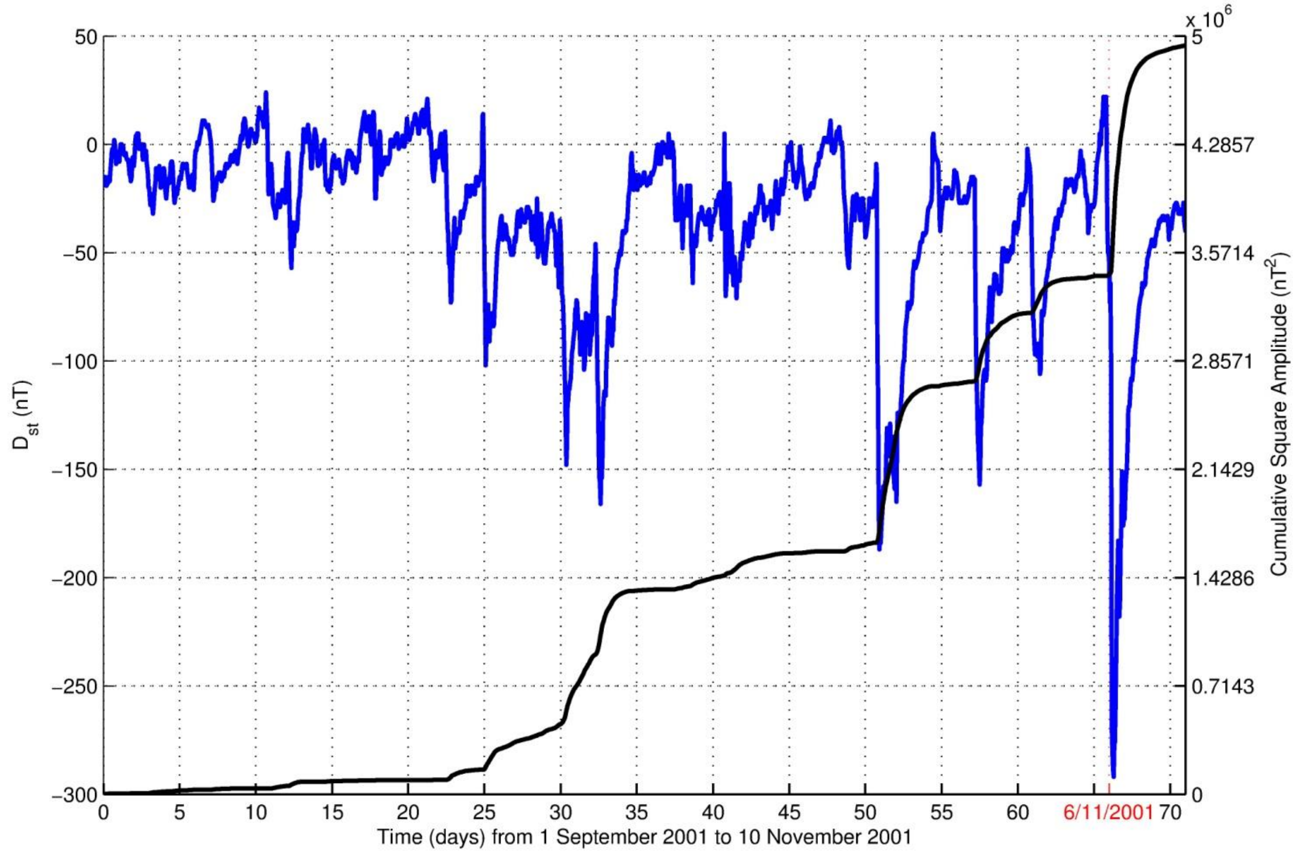
x 10^6
50
0
−50
−100
−150
−200
−250
−300
5
4.2857
3.5714
2.8571
2.1429
1.4286
0.7143
0
0 5 10 15 20 25 30 35 40 45 50 55 60 6/11/2001 70
Time (days) from 1 September 2001 to 10 November 2001
D_st (nT)
Cumulative Square Amplitude (nT^2)

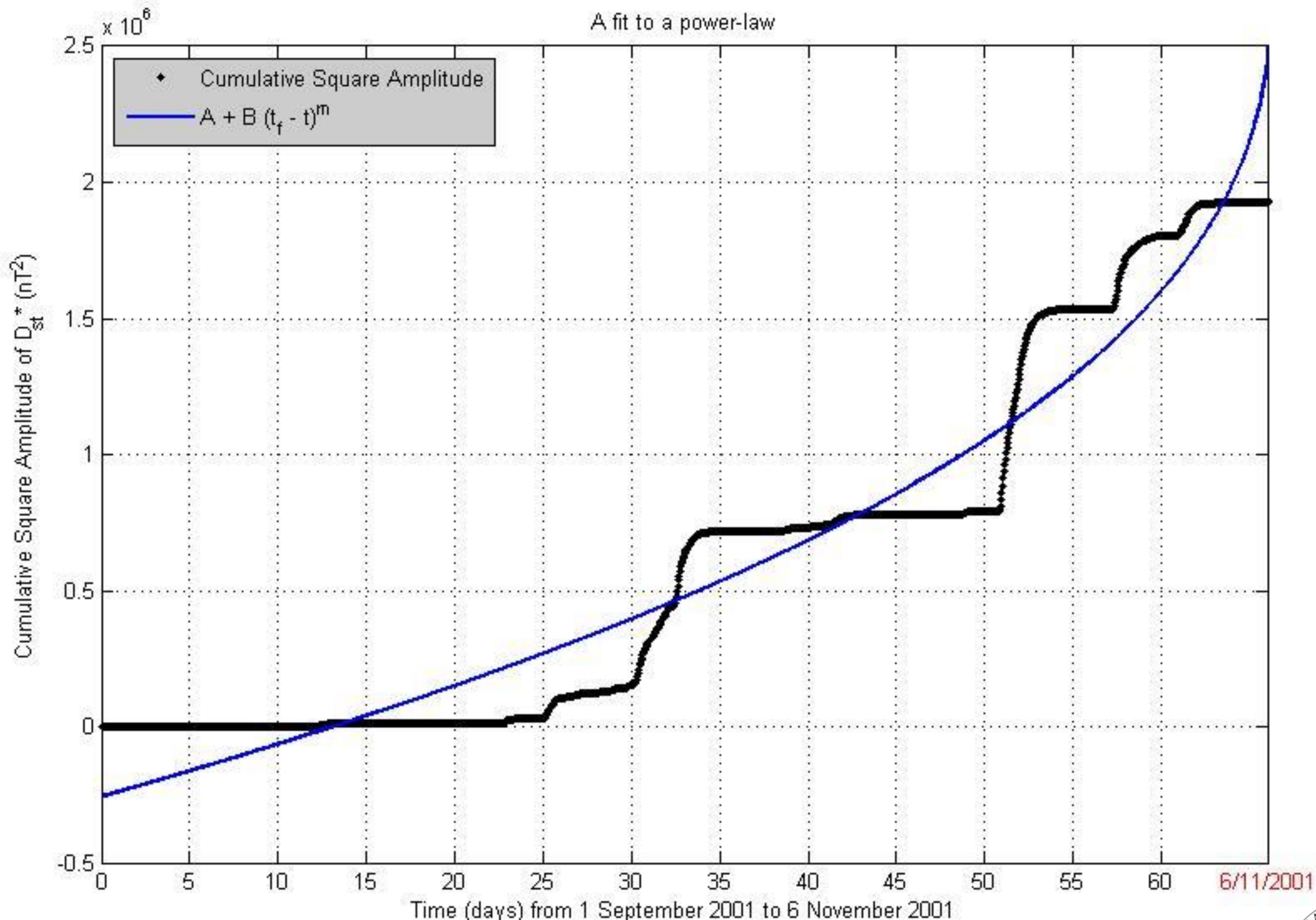
A fit to a power-law
x 10^6
Cumulative Square Amplitude
A + B (t_f - t)^m
Cumulative Square Amplitude of D_st* (nT^2)
2.5
2
1.5
1
0.5
0
-0.5
0
5
10
15
20
25
30
35
40
45
50
55
60
6/11/2001
Time (days) from 1 September 2001 to 6 November 2001

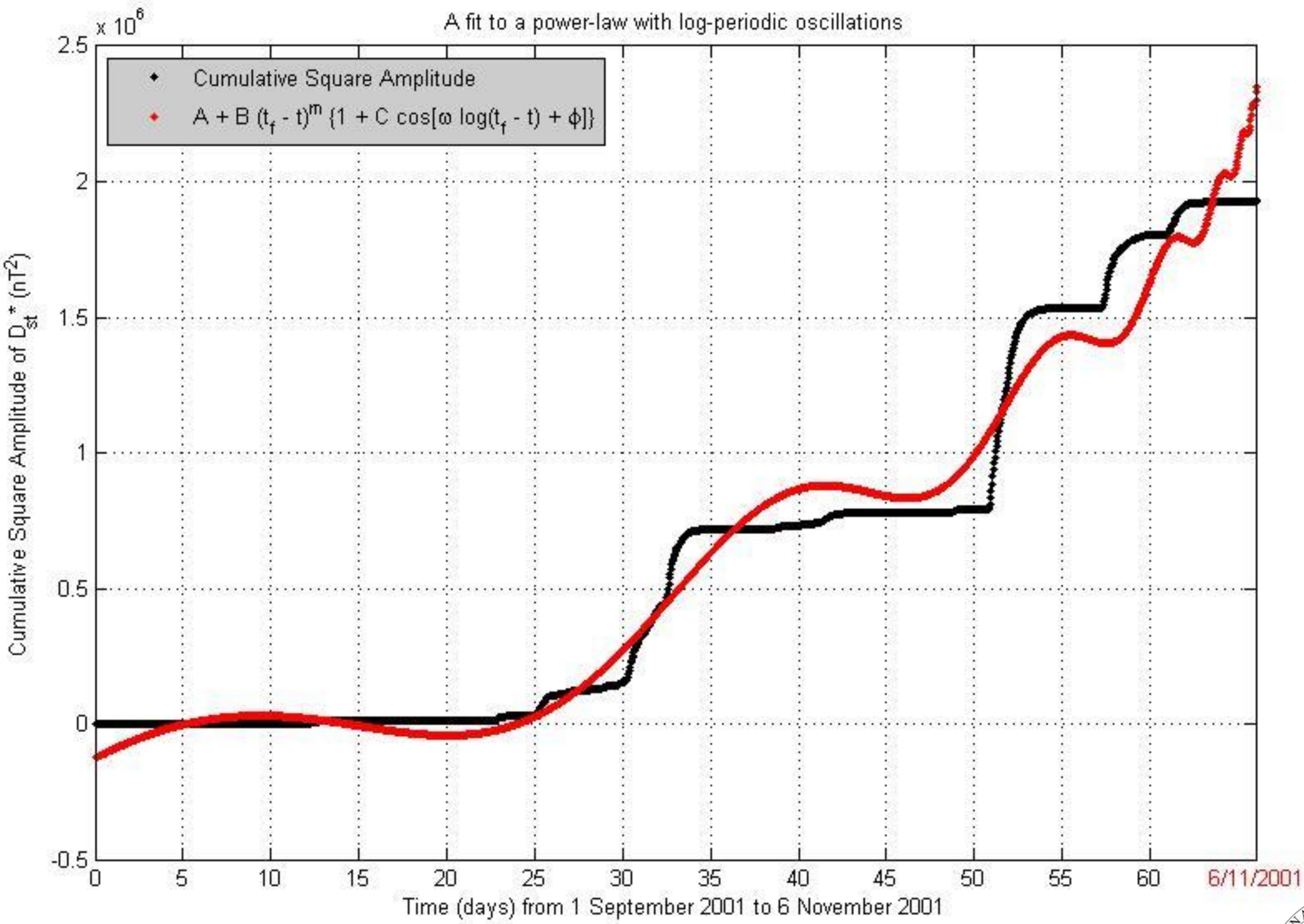
A fit to a power-law with log-periodic oscillations
x 10^6
Cumulative Square Amplitude
A + B (t_f - t)^m {1 + C cos[ω log(t_f - t) + ϕ]}
Cumulative Square Amplitude of D_st* (nT^2)
2.5
2
1.5
1
0.5
0
-0.5
0
5
10
15
20
25
30
35
40
45
50
55
60
6/11/2001
Time (days) from 1 September 2001 to 6 November 2001

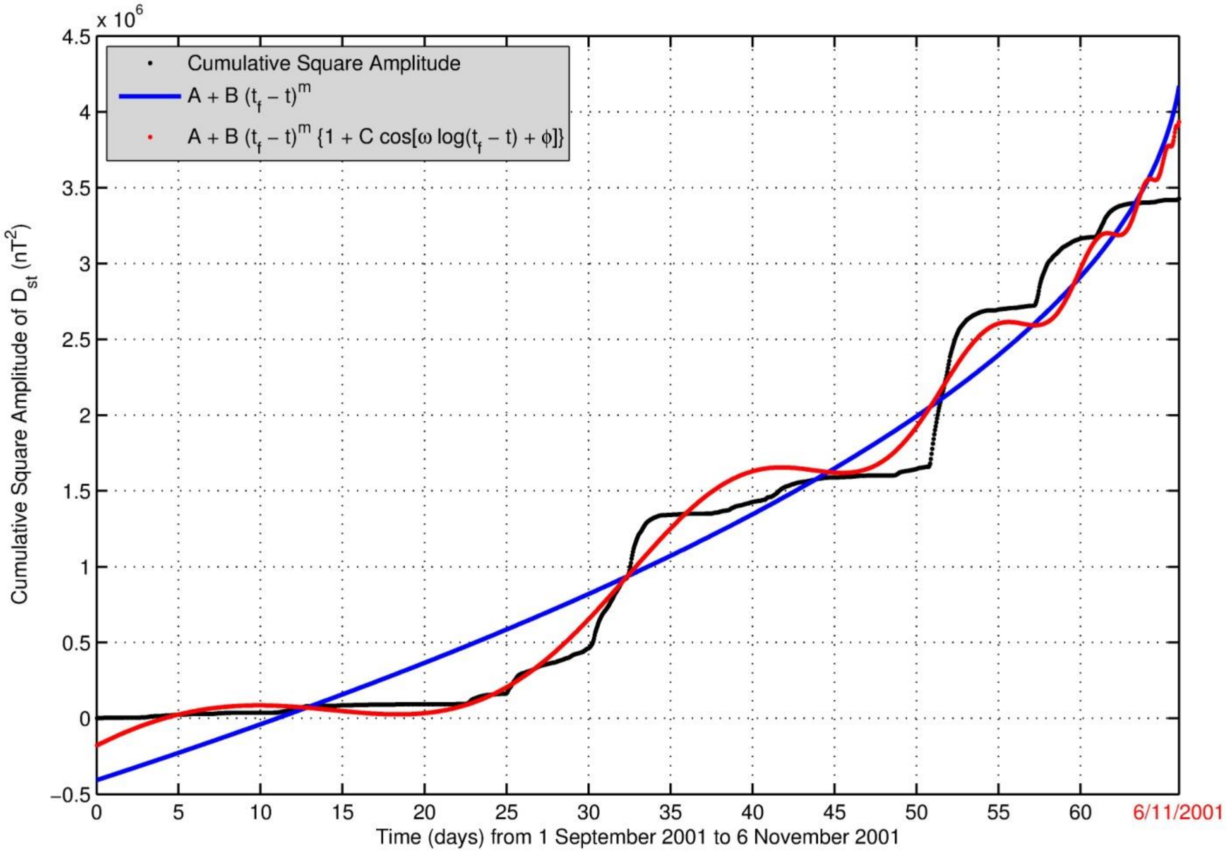

(Balasis et al., *GRL* 2011)

Summary

- Herein, the squares of the negative values of the Dst index increments have been taken as proxies of the energy dissipation rate in the Earth's magnetosphere.

- We have shown that a power law with log-periodic oscillations fits well the cumulative square amplitudes of Dst time series, which include an intense magnetic storm.

- Based on the theory of log-periodic corrections to scaling we have inferred a theoretical value for the time of the occurrence of the extreme magnetospheric event which is 1.92 hours ahead of the real time that the magnetic storm peak Dst value took place.

Summary

- The theoretical curve we have used is able to fit Dst data starting 66.25 days prior to the intense magnetospheric event.

- The last data used to achieve this theoretical occurrence time came from day 62.63, almost four days before the actual event (real occurrence time is at 66.38 days).

- We believe that the convergence of the results presented in this study with other well-established methods of Dst forecast (e.g., O'Brien and McPherron, 2000; Temerin and Li, 2002; Lundstedt et al., 2002; Balikhin et al., 2010) can potentially increase the reliability of forecasting techniques and can therefore improve space weather forecasting and modeling.

Earth's magnetic field: invisible but apparent

- ✓ produced to a large extend by a self-sustaining dynamo, operating in the fluid outer-core,
- ✓ also caused by magnetised rocks in the Earth's crust,
- ✓ electric currents flowing in the ionosphere, magneto-sphere and oceans
- ✓ and by currents induced in the Earth mantle by time-varying external fields.

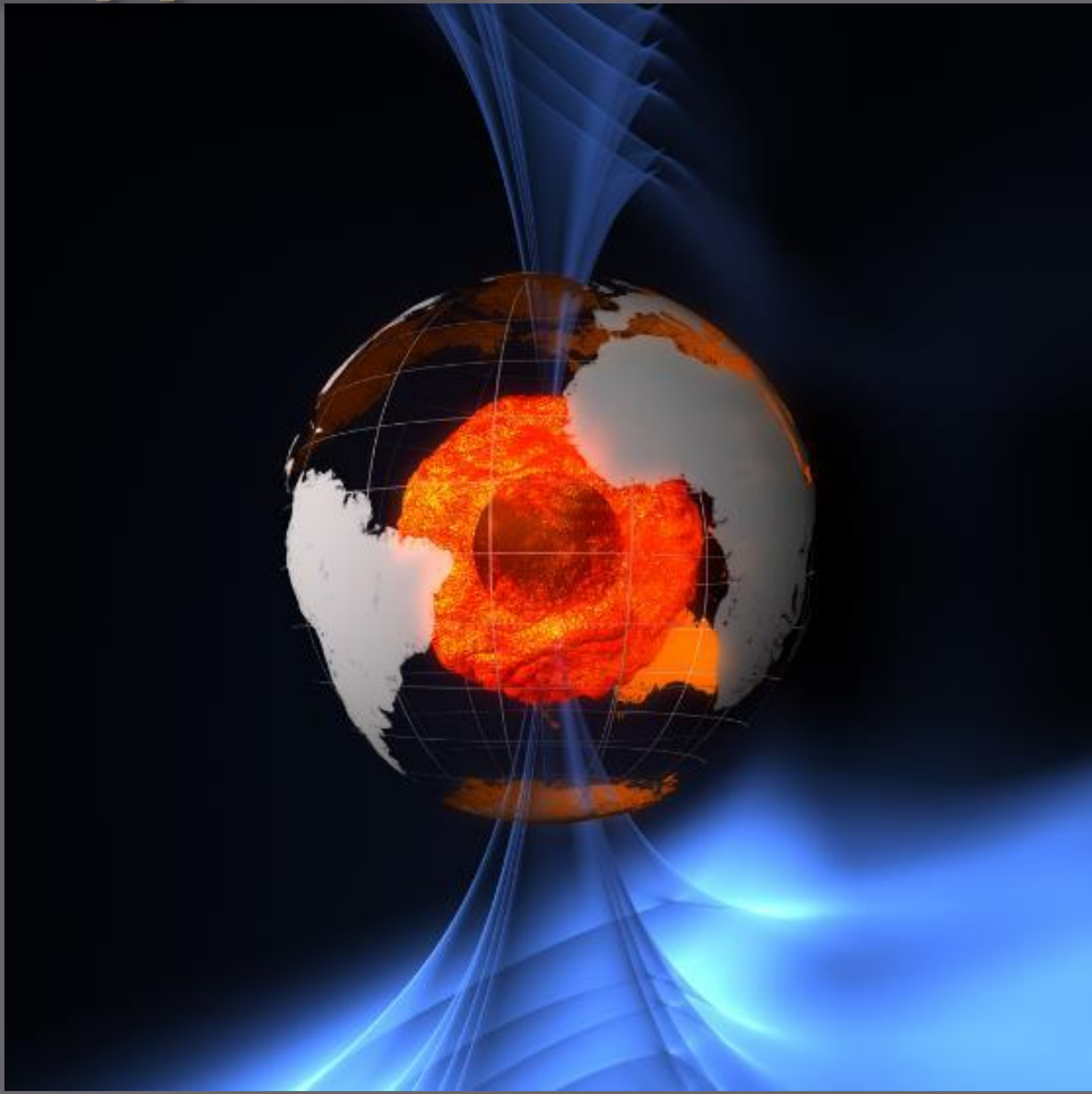

Investigating Dynamical Complexity of Geomagnetic Jerks Using Various Entropy Measures

- A geomagnetic jerk can be defined as a sudden change (a V-shape like change) in the slope of the geomagnetic secular variation, i.e., the first time derivative of the Earth's magnetic field. Geomagnetic jerks were first reported by Courtillot et al. (1978).

Geomagnetic time series (Balasis et al., *Frontiers* 2016)

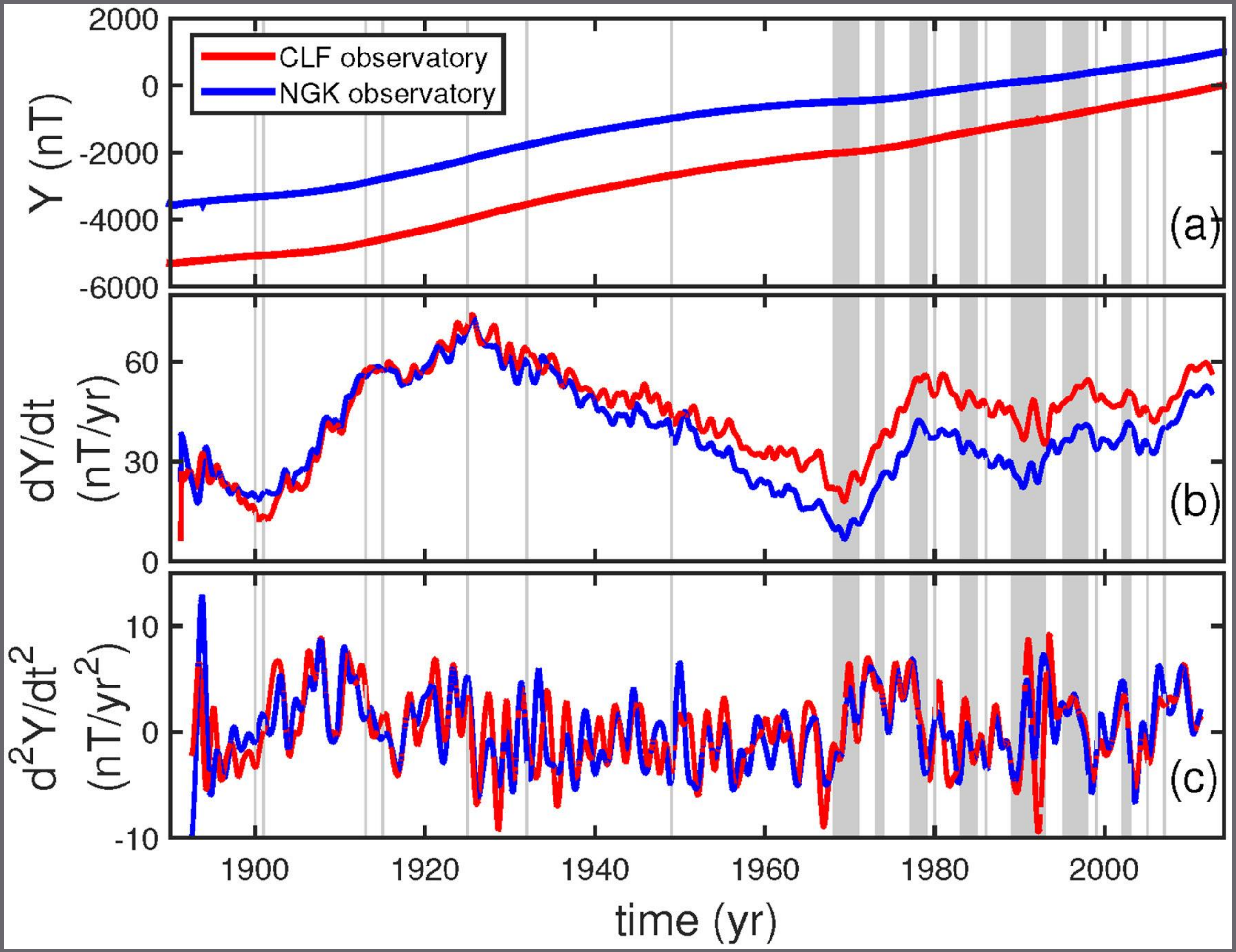

Fisher Information

- Fisher information was first introduced as a representation of the amount of information that can be extracted from a set of measurements (or the "quality" of the measurements) (Fisher, 1925; Mayer etal., 2006).

- Fisher information is also a powerful tool to investigate complex and non-stationary signals), permitting the detection of significant changes in the behavior of non-linear dynamical systems and the characterization of complex signals generated by these systems.

Fisher Information

$$I_x = \sum_{n=1}^{N-1} \frac{\left[p\left(x_{n+1}\right) - p\left(x_n\right)\right]^2}{p\left(x_n\right)}, \tag{5}$$

where $p(x_i)$ are the probabilities associated with the value bins x_i , as defined in Section 3.1, N is their total number, while $p(x_n)$ and $p(x_{n+1})$ are the probabilities corresponding to two successive bins.

Entropy analysis of geomagnetic field (Balasis et al., *Frontiers* 2016)

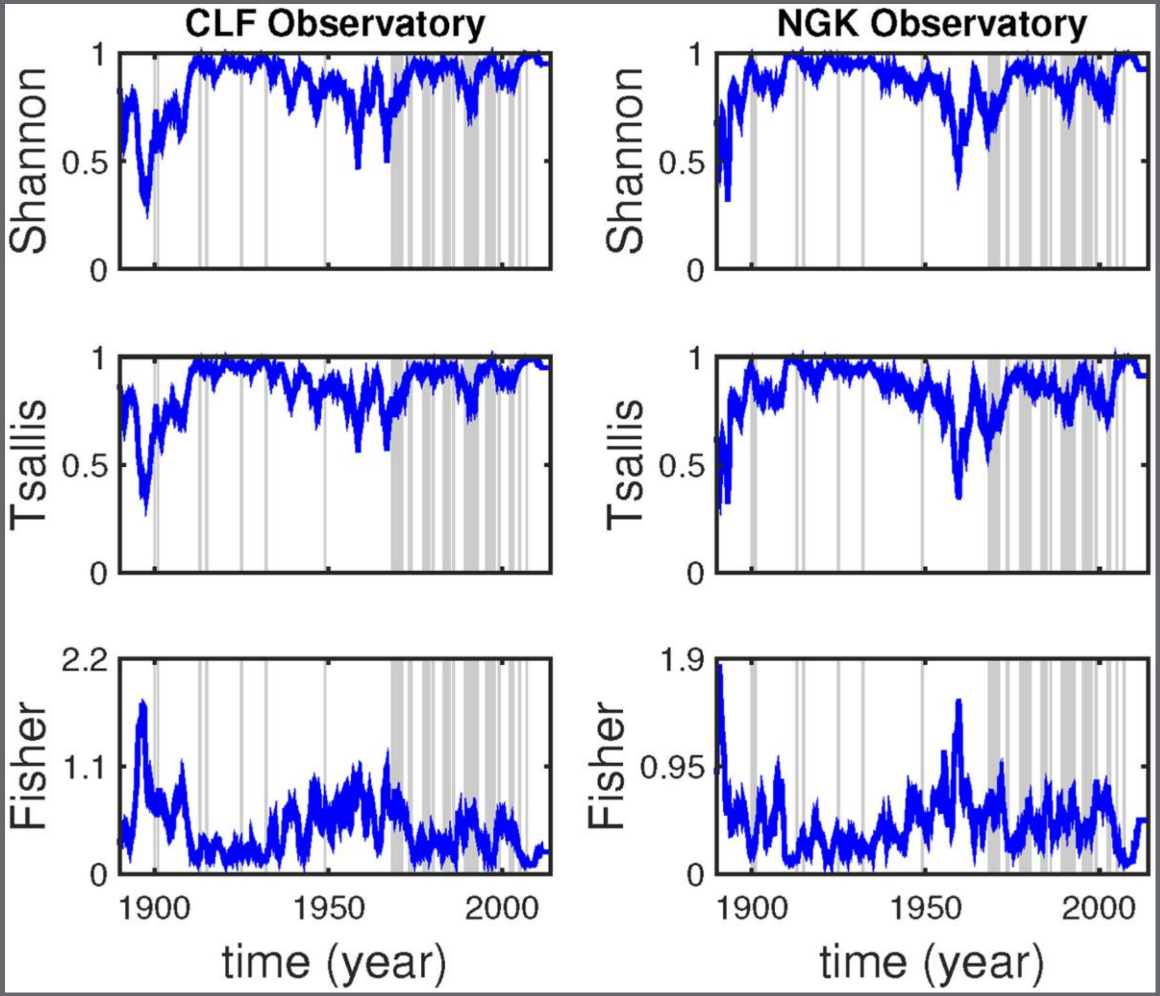

ESA Swarm mission

Each satellite is measuring:

- ✓ Strength and direction of the magnetic field
- ✓ Plasma conditions and characteristics
- ✓ Location

The Constellation:

- ✓ 3 identical satellites:
  - 2 side-by-side in low orbit (<460km)
  - 1 in higher orbit
  - (< 530km)
- ✓ three orbital planes for optimal coverage in space and time
- ✓ **Launch 22 November 2013: initially 4 years of operations, currently extended through 2021**

Copyright / ESA and AOES Medialab

IAASARS

The primary aim of the mission is to provide the best survey ever of the geomagnetic field and the first global representation of its variations on time scales from less than a second to several years.

Looking into the force that protects Earth

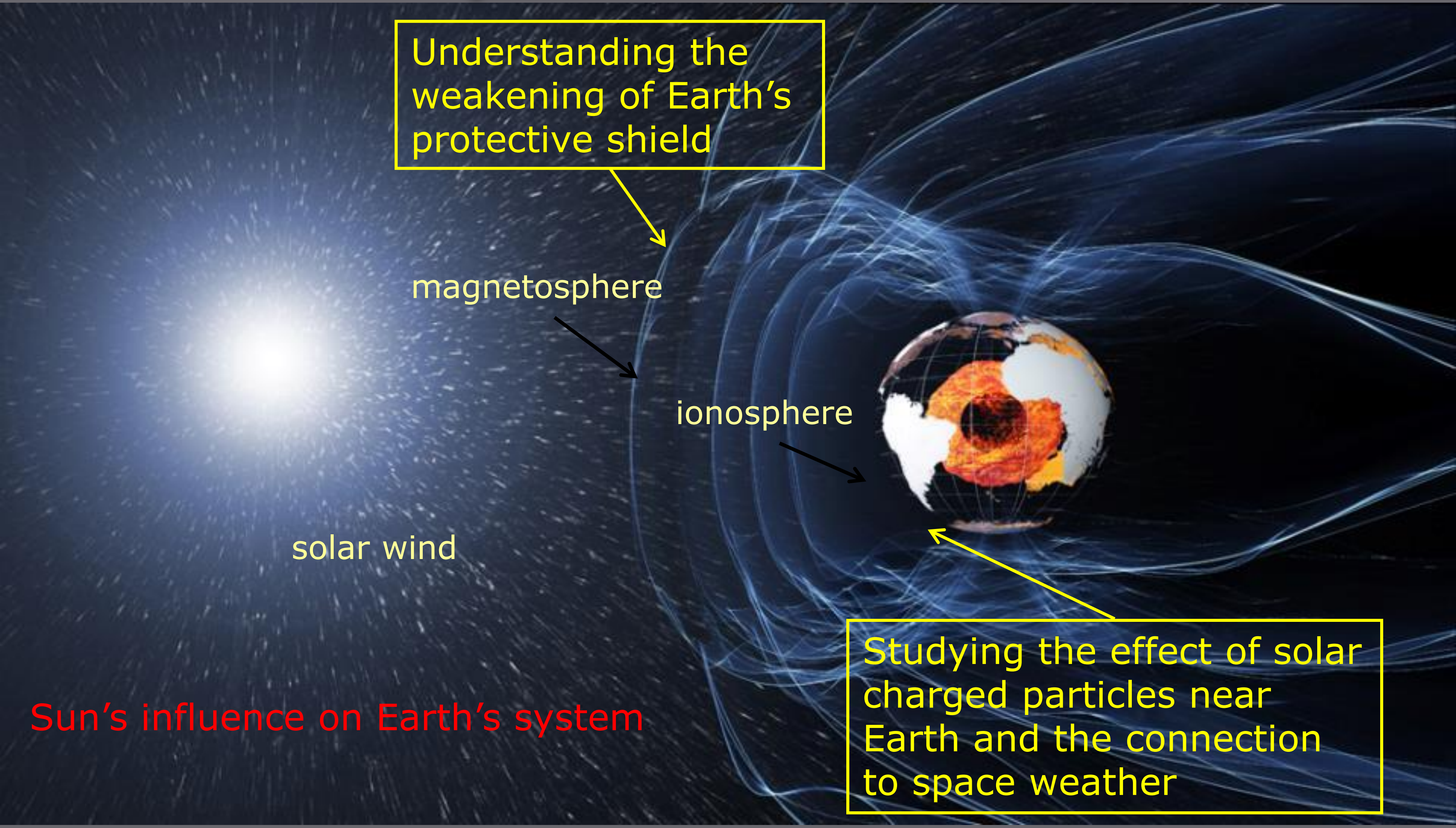

entropy

MDPI

Article

Dynamical Complexity of the 2015 St. Patrick's Day Magnetic Storm at Swarm Altitudes Using Entropy Measures

Constantinos Papadimitriou [1,2], Georgios Balasis [1,*], Adamantia Zoe Boutsi [1,3], Ioannis A. Daglis [1,3,4], Omiros Giannakis [1], Anastasios Anastasiadis [1], Paola De Michelis [5] and Giuseppe Consolini [6]

1. Institute for Astronomy, Astrophysics, Space Applications and Remote Sensing, National Observatory of Athens, Metaxa and Vas. Pavlou St., Penteli, 15236 Athens, Greece; constantinos@noa.gr (C.P.); zboutsi@noa.gr (A.Z.B.); iadaglis@phys.uoa.gr (I.A.D.); og@noa.gr (O.G.); anastasi@noa.gr (A.A.)
2. Space Applications & Research Consultancy, SPARC P.C., 10551 Athens, Greece
3. Department of Physics, National and Kapodistrian University of Athens, Panepistimiopolis, Zografos, 15784 Athens, Greece
4. Hellenic Space Center, 15231 Athens, Greece
5. Istituto Nazionale di Geofisica e Vulcanologia, 00143 Rome, Italy; paola.demichelis@ingv.it
6. INAF-Istituto di Astrofisica e Planetologia Spaziali, 00133 Rome, Italy; giuseppe.consolini@iaps.inaf.it

* Correspondence: gbalasis@noa.gr

Received: 14 April 2020; Accepted: 13 May 2020 ; Published: 19 May 2020

check for updates

Abstract: The continuously expanding toolbox of nonlinear time series analysis techniques has recently highlighted the importance of dynamical complexity to understand the behavior of the complex solar wind–magnetosphere–ionosphere–thermosphere coupling system and its components. Here, we apply new such approaches, mainly a series of entropy methods to the time series of the Earth's magnetic field measured by the Swarm constellation. We show successful applications of methods, originated from information theory, to quantitatively study complexity in the dynamical response of the topside ionosphere, at Swarm altitudes, focusing on the most intense magnetic storm of solar cycle 24, that is, the St. Patrick's Day storm, which occurred in March 2015. These entropy measures are utilized for the first time to analyze data from a low-Earth orbit (LEO) satellite mission flying in the topside ionosphere. These approaches may hold great potential for improved space weather nowcasts and forecasts.

Keywords: dynamical complexity; entropy; magnetic storm; space weather; Swarm mission

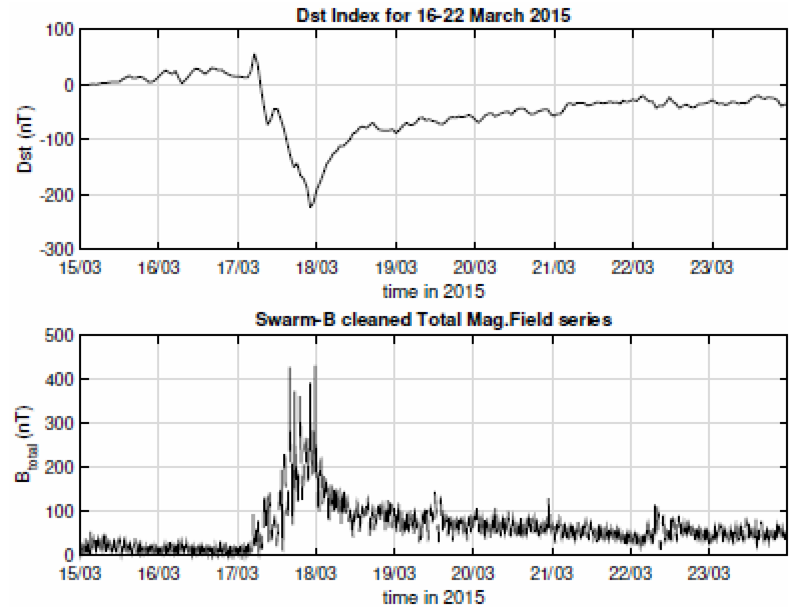

Figure 1. Comparison between the Dst index (**top panel**) and the pre-processed series of the total (external) magnetic field (**bottom panel**), as measured by Swarm B, during the March 2015 storm.

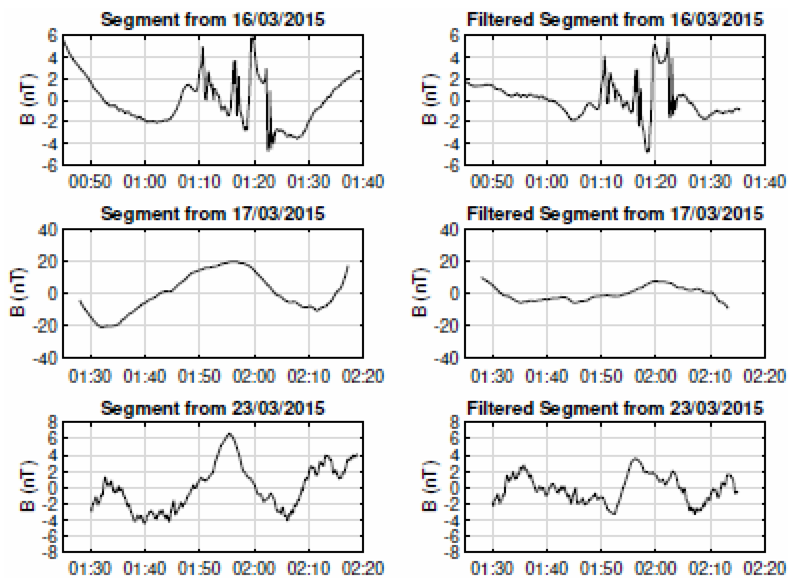

Figure 2. Example of three segments before (**left**) and after filtering (**right**), for the pre-storm phase (**top row**), the peak of the storm (**middle row**) and after the end of event (**bottom row**), respectively.

Case Study: March 2015 Storm

Swarm-A, Total Magnetic Field (MFA), after subtraction of CHAOS-6 model, 1 Hz sampling rate (VFM instrument).

Keeping only mid-to-low latitudinal measurements, segmented into daily, non-overlapping windows.

Histogram Entropy computed in 100 bins.

Block entropies computed on binary symbolic series (median threshold), up to m=5.

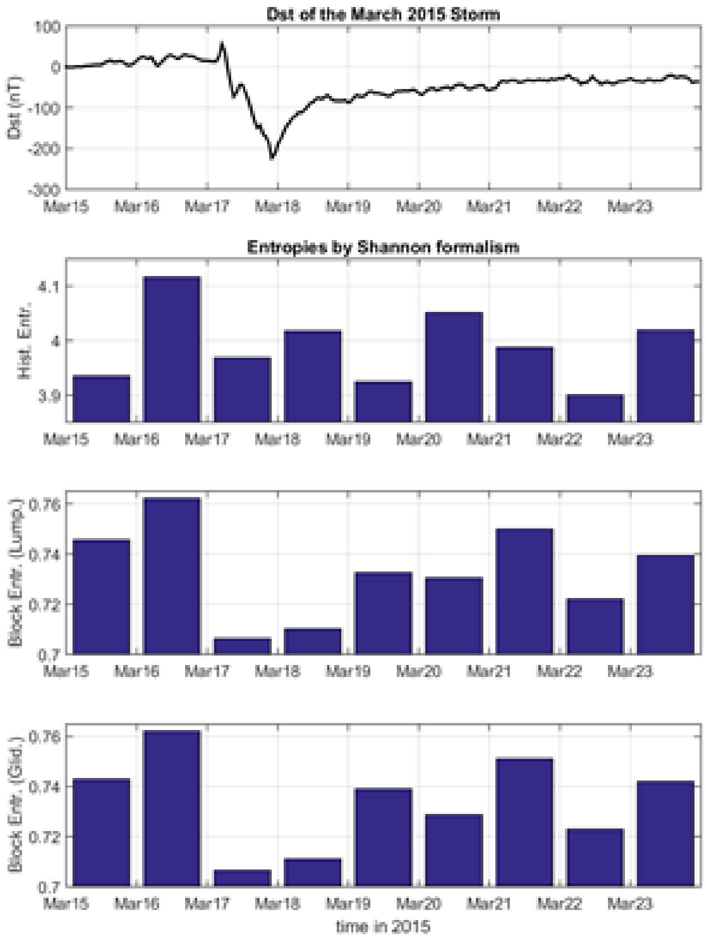

Case Study: March 2015 Storm

Swarm-A, Total Magnetic Field (MFA), after subtraction of CHAOS-6 model, 1 Hz sampling rate (VFM instrument).

Keeping only mid-to-low latitudinal measurements, segmented into daily, non-overlapping windows.

Histogram Entropy computed in 100 bins.

Block entropies computed on binary symbolic series (median threshold), up to m=5.

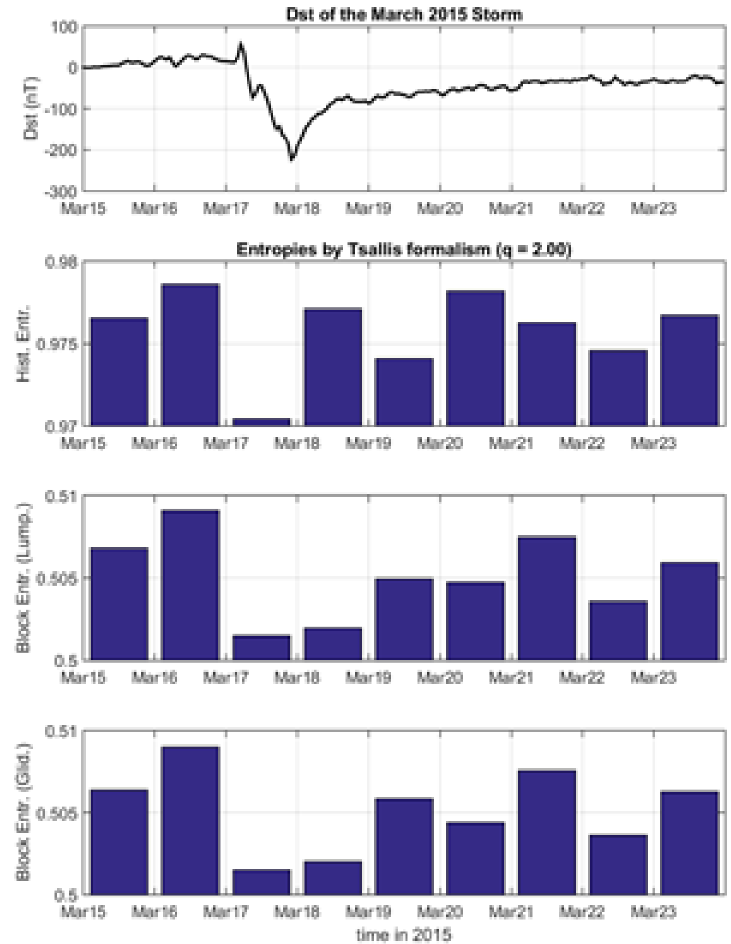

Case Study: March 2015 Storm

Swarm-A, Total Magnetic Field (MFA), after subtraction of CHAOS-6 model, 1 Hz sampling rate (VFM instrument).

Keeping only mid-to-low latitudinal measurements, segmented into daily, non-overlapping windows.

ApEn & SampEn using the Supremum Norm as a difference measure, with a parameter r=3std.

FuzzyEn using Gaussian Membership Function.

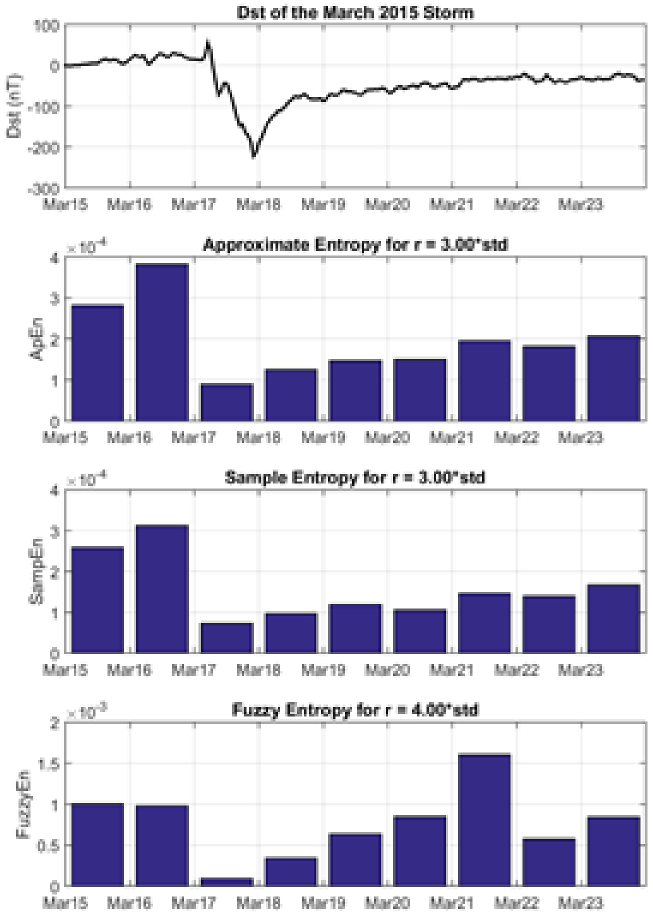

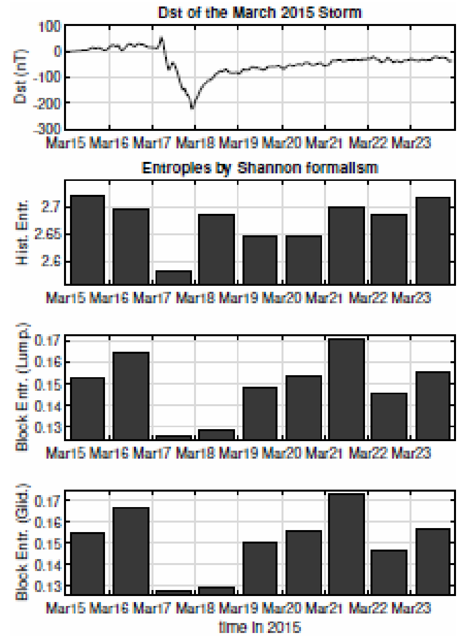

Figure 3. Entropy analysis according to Shannon formalism of the Swarm B total (external) field for the March 2015 magnetic storm.

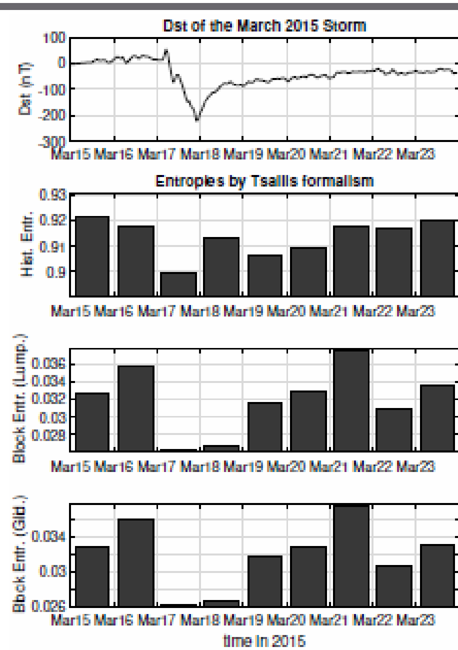

Figure 4. Entropy analysis according to Tsallis formalism of the Swarm B total (external) field for the March 2015 magnetic storm.

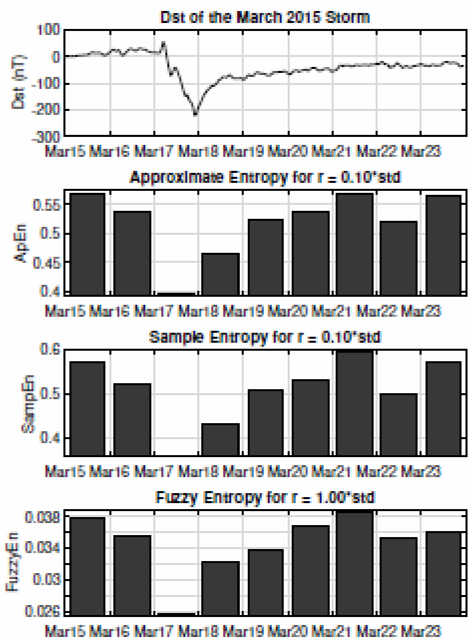

Figure 5. Approximate, Sample and Fuzzy entropy analysis of the Swarm B total (external) magnetic field for the March 2015 magnetic storm.

epl A LETTERS JOURNAL EXPLORING THE FRONTIERS OF PHYSICS

September 2020

EPL, **131** (2020) 69001
doi: 10.1209/0295-5075/131/69001

www.epljournal.org

Dynamical complexity in Swarm electron density time series using Block entropy

G. BALASIS[1], C. PAPADIMITRIOU[1,2], A. Z. BOUTSI[1,3], I. A. DAGLIS[3,4,1], O. GIANNAKIS[1], A. ANASTASIADIS[1], P. DE MICHELIS[5] and G. CONSOLINI[6]

[1] *Institute for Astronomy, Astrophysics, Space Applications and Remote Sensing, National Observatory of Athens Metaxa and Vas. Pavlou St., Penteli, 15236 Athens, Greece*
[2] *Space Applications & Research Consultancy, SPARC - 10551 Athens, Greece*
[3] *Department of Physics, National & Kapodistrian University of Athens - Panepistimiopolis, Zografos 15784 Athens, Greece*
[4] *Hellenic Space Center - 15231 Athens, Greece*
[5] *Istituto Nazionale di Geofisica e Vulcanologia - 00143 Rome, Italy*
[6] *INAF-Istituto di Astrofisica e Planetologia Spaziali - 00133 Rome, Italy*

received 18 June 2020; accepted in final form 14 September 2020
published online 2 November 2020

PACS 94.05.Sd – Space weather
PACS 94.30.Lr – Magnetic storms, substorms
PACS 89.75.-k – Complex systems

Abstract – Our goal in this study is to investigate the dynamical complexity of the electron density profiles in the topside ionosphere as measured by the Swarm mission, employing the use of symbolic information-theoretic techniques. We perform a Block entropy analysis for a time interval associated with the most intense magnetic storm of solar cycle 24, which occurred on 17 March 2015. We produce entropy maps for varying degrees of magnetospheric disturbance, resolving the different effects that the various geomagnetic activity levels have in the dynamics of the complex magnetosphere-ionosphere coupling system. Understanding the impact of these effects on the ionospheric plasma constitutes a crucial factor for the functionality of the modern technological infrastructure operating around the Earth and, thus, human welfare.

Motivation

- The Langmuir probes of the Electric Field Instrument on board the three satellites of the Swarm constellation (Knudsen et al., 2017) provide **electron density data** in the form of time series, as the satellites fly through the ionosphere.

- The data have a cadence of **2 per second**, but these measurements have been **downsampled to a 1 Hz** resolution, in order for them to be consistent with the rest of the magnetic field data and the other data products from the mission.

- Our goal in this study is to employ the use of **information-theoretic measures** in order to capture the turbulent nature of the electron density profiles and then produce **maps for varying degrees of magnetospheric disturbances**, in order to capture the effect that these conditions have in the dynamics of the ionospheric plasma.

- Attempting to capture the turbulent nature of the electron density series by means of entropic measures is a very complex task. Special care should be taken, since the temporal and spatial scale of these features can be significantly smaller compared to the ones encountered in similar studies using e.g. the Dst Index.

- Due to this, the analysis must be performed in significantly **smaller time windows** than the ones that have been employed so far, e.g. in the **scale of a few minutes**.

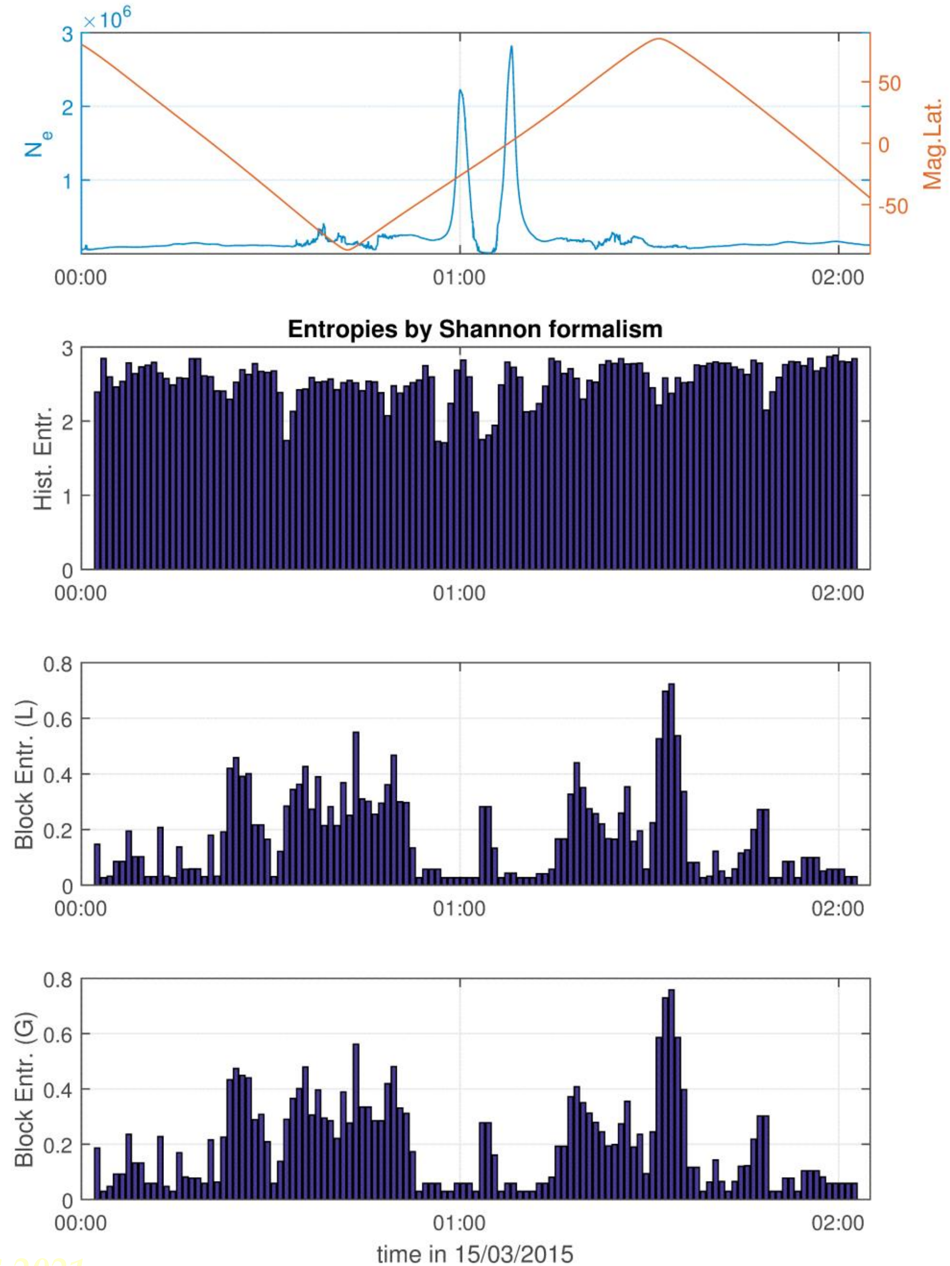

IAASARS

- **1 Hz** cadence, 5 min time window, **300 measurements**.
- Repeating the methods used in the case of the magnetic field data ad-hoc, is not enough to give meaningful results.
- A **couple of hours** of electron density data from Swarm-A on the 15th of March 2015 have been processed with **various entropy methods**, yielding disappointing results.
- Both the histogram entropy and the Block Entropy approach, with a binary symbolic representation (segmented at the window median) for both Lumping and Gliding parsing, all failed to capture any meaningful behavior. Similarly incomprehensible results were obtained for multi-symbol representations (up to 4-letter) and for various other types of entropies.

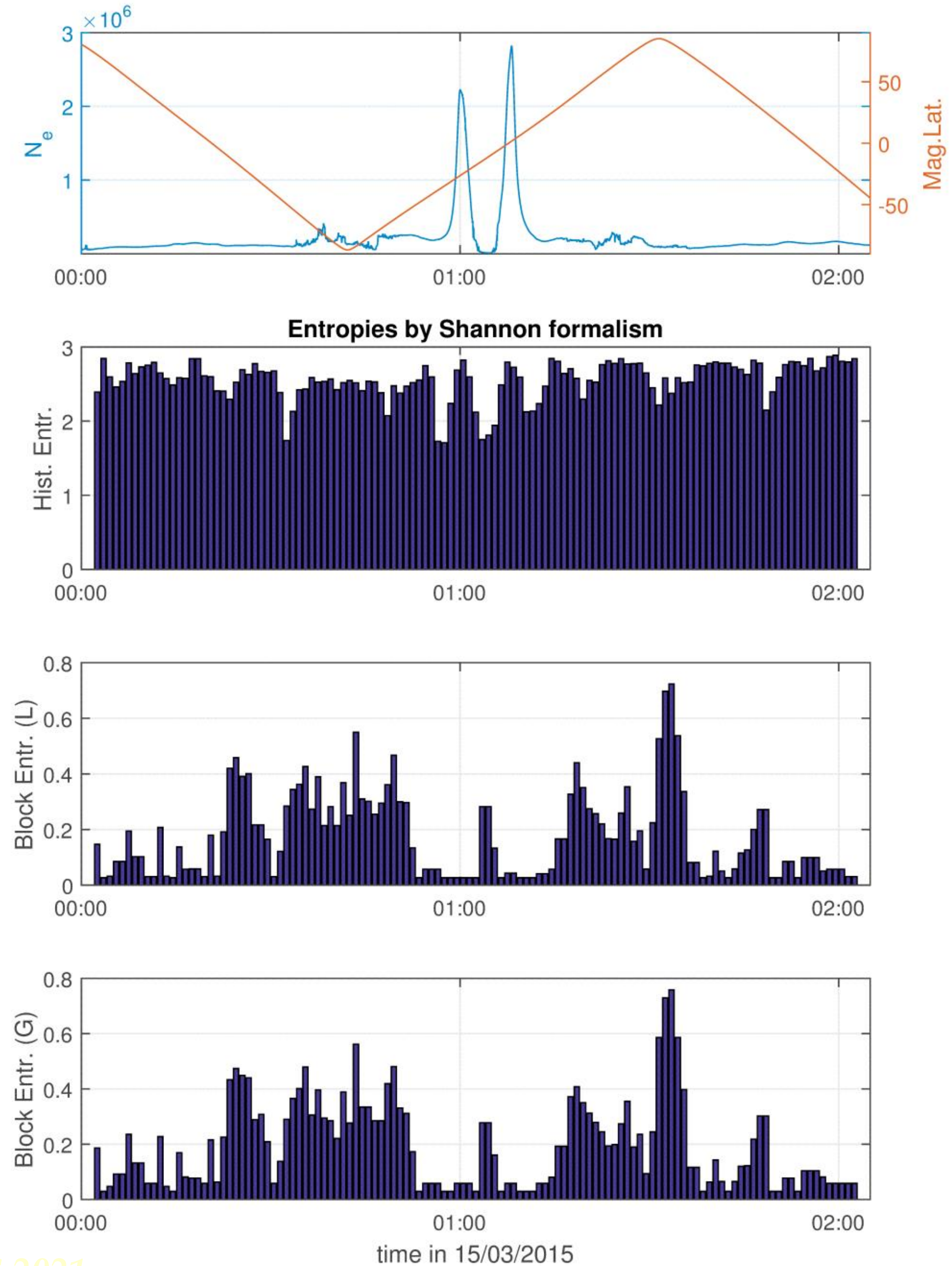

New strategy

- Based on the differential series of the electron density (on its absolute value) and then performing the binary symbolic representation using as a threshold a constant value (not window-dependent).
- Histogram entropy fails to produce any meaningful result.
- Both Block Entropies **successfully capture the turbulent nature of the plasma.**
- Near-zero values at windows where the satellite only measures smooth electron density profiles.
- High entropy values at the times when the satellite flies through disturbances (polar passes / equator - red line shows the satellite's latitude).
- Entropy is **normalized** (0→1) & given by the gradient of the H(n) values (n: 1 - 4).

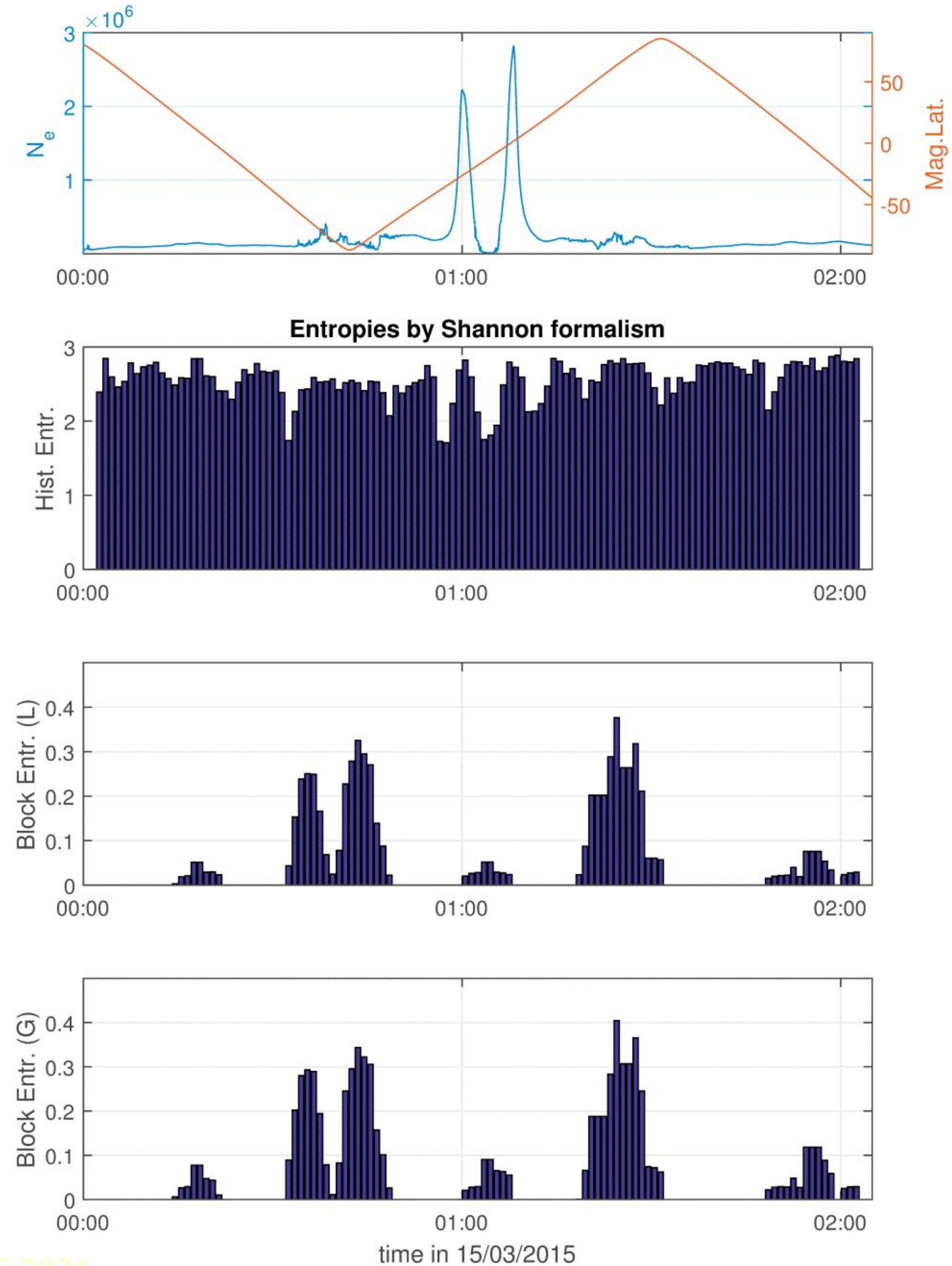

- The particular way with which this conversion takes place plays a critical role in capturing a specific portion of the information that is carried by the signal.

- In this case, the binarization was performed by a **constant threshold** value.

- The entropies of the windows encountered at high latitudes exhibited higher values.

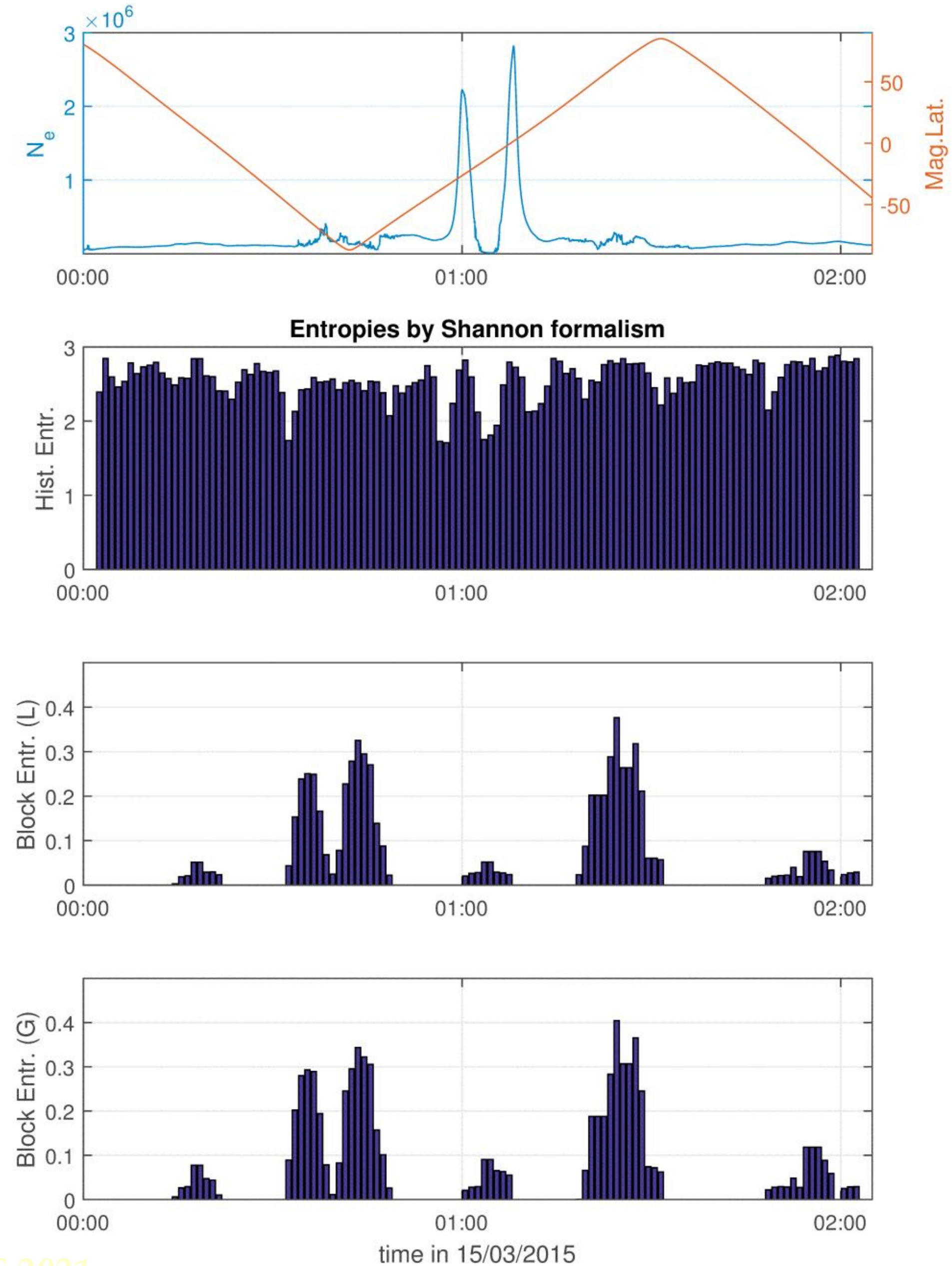

- Raising this threshold can inverse this behavior and thus produce a different image, with the low-latitude entropies taking the lead.

- In this manner, by changing the threshold of the binarization one can **switch the emphasis from low to high latitudes**!

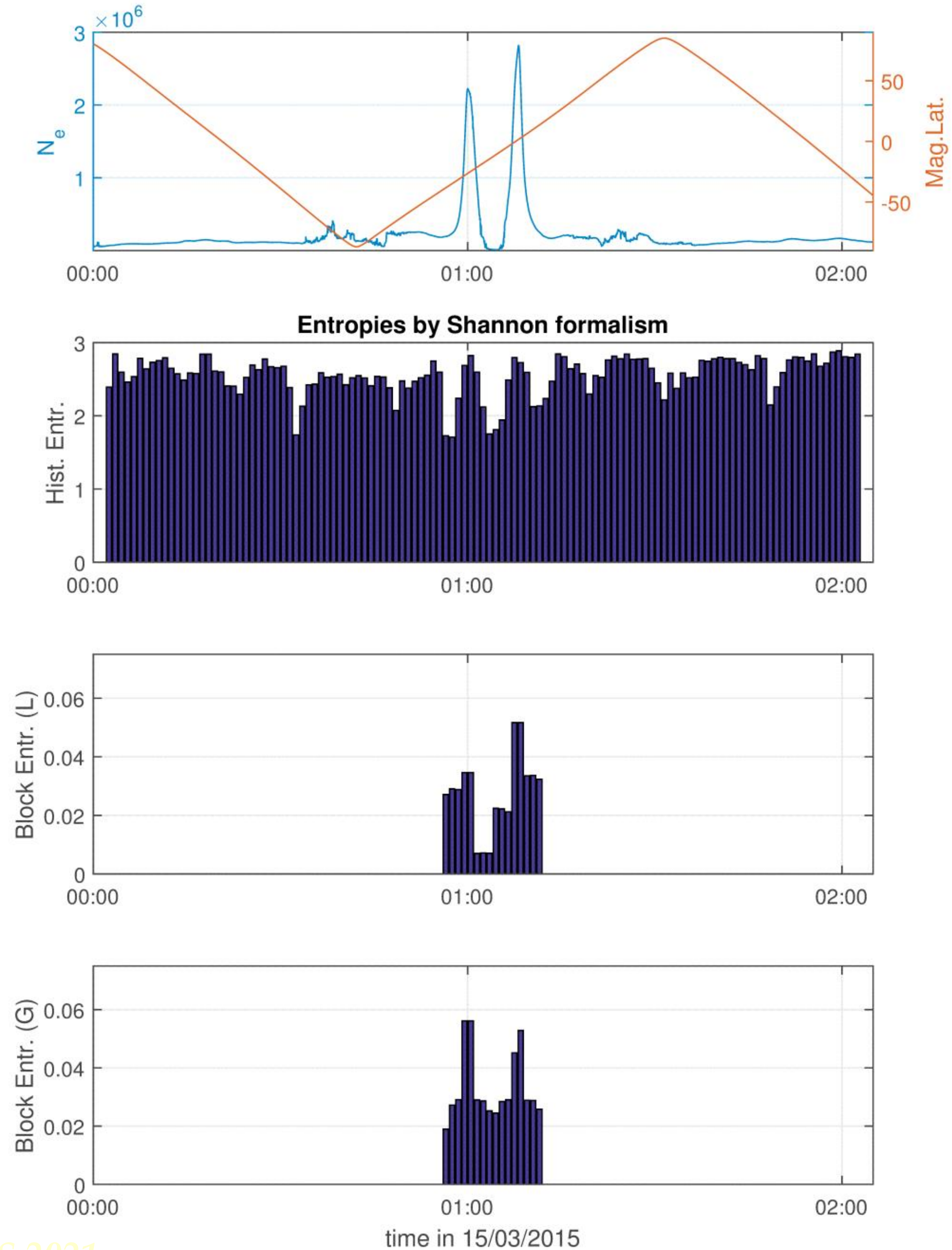

Non-linear analysis of the St. Patrick's storm

- Analysis performed (for simplicity only for Block Entropy(G)) for the entire time span of the March 2015 Geomagnetic Storm, using a **moving time window of 5 minutes** that slides forward by 1 min at a time.

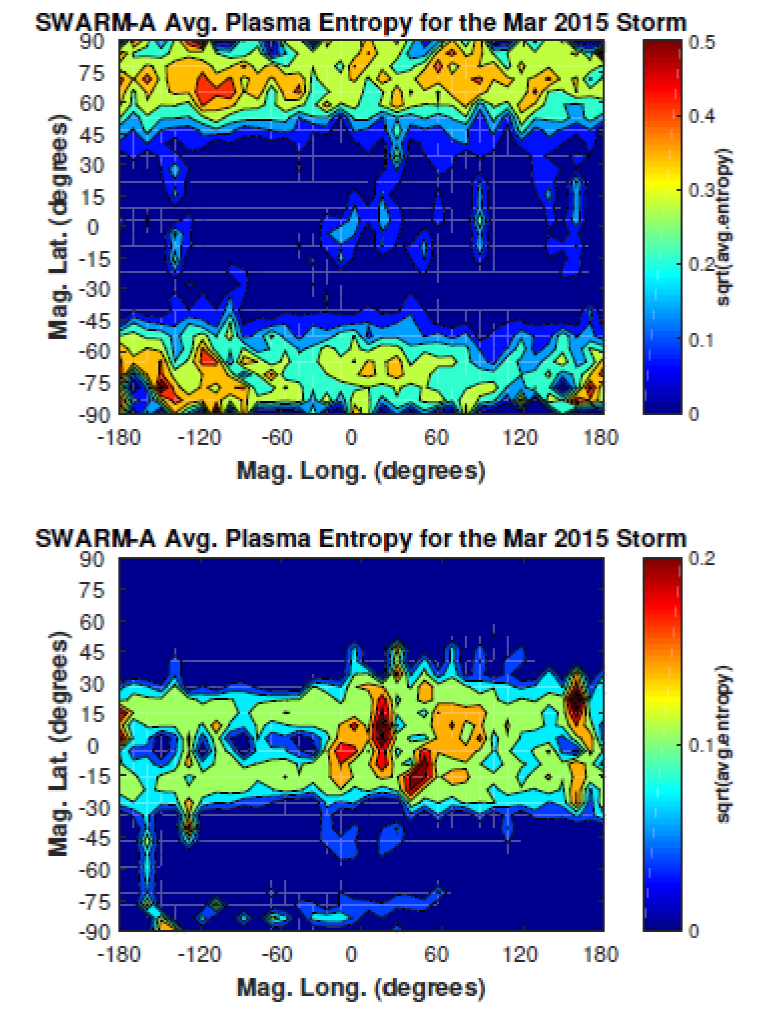

Fig. 5: Maps of the average entropy for Swarm A from 15 to 23 March 2015 [emphasizing (top) high and (bottom) low latitudes].

Non-linear analysis of the St. Patrick's storm

Since the satellite continuously moves in space, we also save the position of the satellite for each entropy calculation (by considering the median value of the lon. & lat. for each window) and thus are able to produce **maps of the average entropy values of the electron density** for the entire duration of the event (15-23 March).

Again, changing the threshold can produce two different versions of those maps, one emphasizing the low and another for the high latitudes.

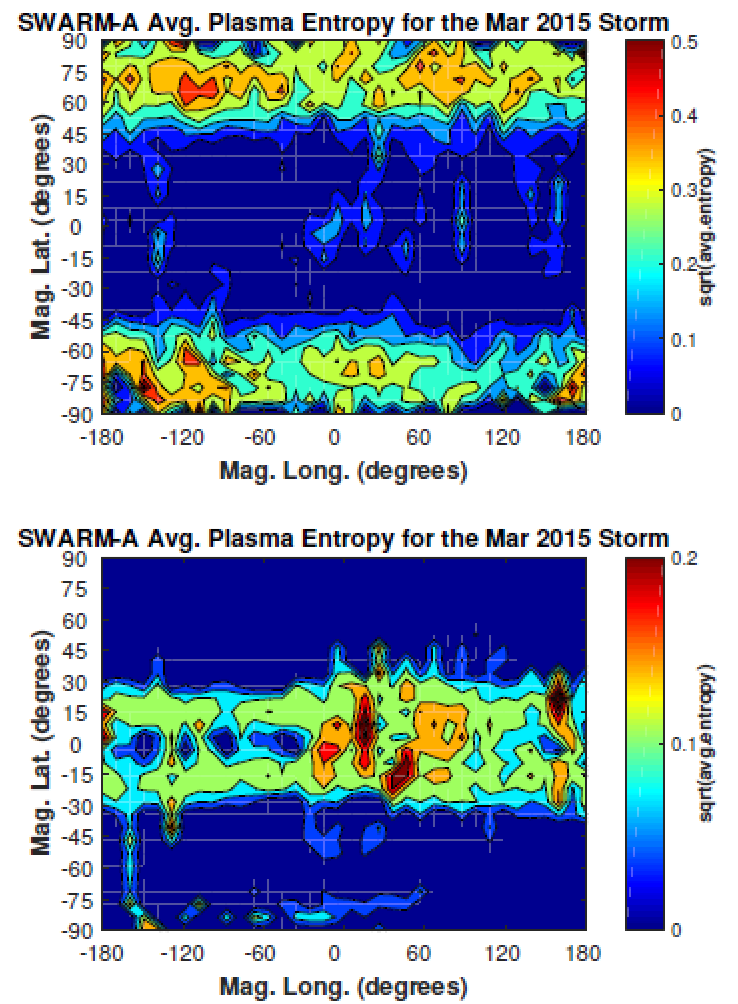

Fig. 5: Maps of the average entropy for Swarm A from 15 to 23 March 2015 [emphasizing (top) high and (bottom) low latitudes].

Non-linear analysis of the St. Patrick's storm

Pre-storm (March 1 to 15 of 2015) and Storm-time (March 16 to 31 of 2015) differences in the maps for high-threshold (low latitudes).

Again, as is always the case, one can see the drop in entropy values as we move from pre-storm period to the main phase and recovery phase of the storm (axes and colormaps are identical in the two plots).

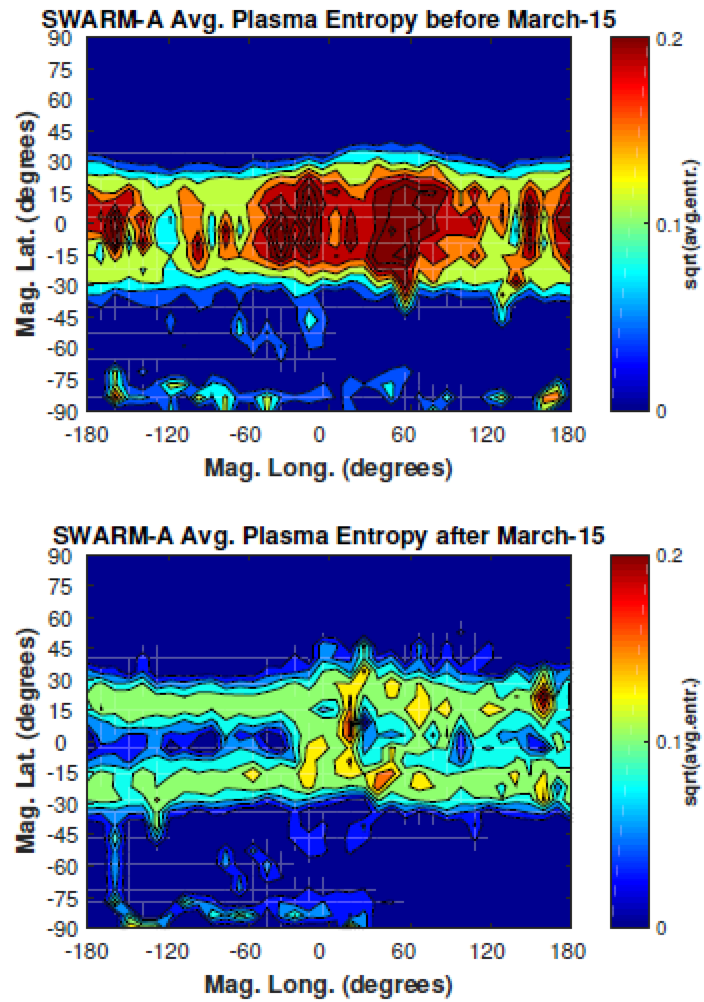

Fig. 6: Maps of average entropy between (top) pre-storm time (1-15 March 2015) and (bottom) storm-time as well as post-storm time (16-31 March 2015) for high-threshold (low latitudes).

Non-linear analysis of the St. Patrick's storm

Pre-storm (March 1 to 15 of 2015) and Storm-time (March 16 to 31 of 2015) differences in the maps for low-threshold (high latitudes).

Again, as is always the case, one can see the drop in entropy values as we move from pre-storm period to the main phase and recovery phase of the storm (axes and colormaps are identical in the two plots).

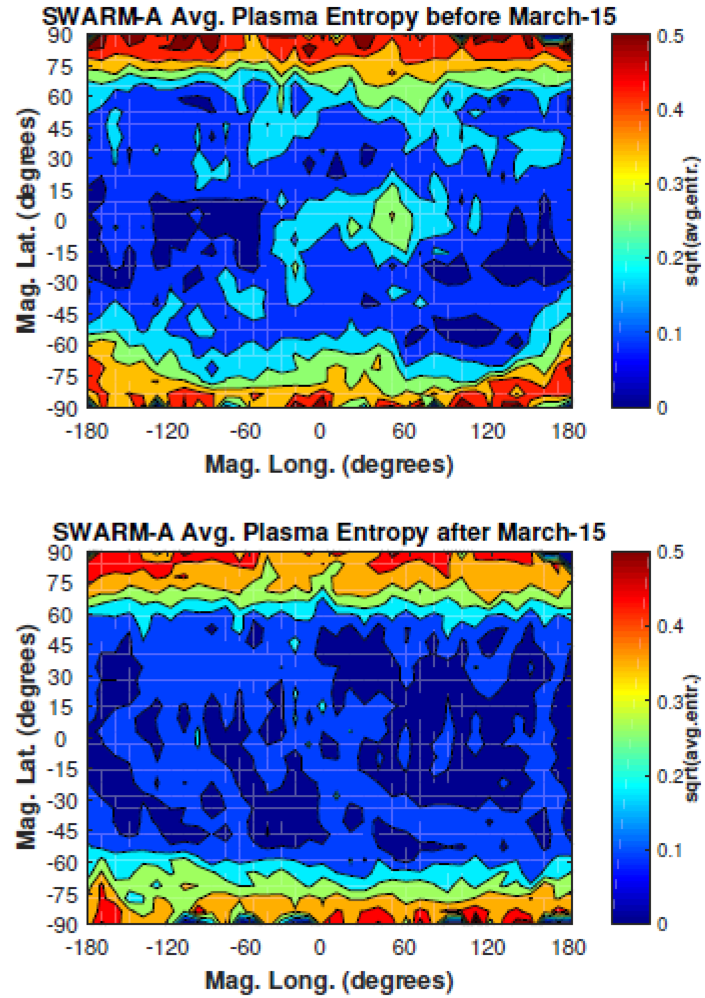

Fig. 7: Maps of average entropy between (top) pre-storm time (1-15 March 2015) and (bottom) storm-time as well as post-storm time (16-31 March 2015) for low-threshold (high latitudes).

IAASARS

Summary

- One can utilize different concepts
  - Histogram
  - Block Entropies on Symbolic Series
  - Non-symbolic Measures based on ApEn
- … as well as different entropy definitions
  - Shannon
  - Hartley
  - Rényi
  - Tsallis

to capture the changes in the Dynamics of a Complex System. Perhaps some of these ideas could be also useful in ML-based applications.

Dst Index

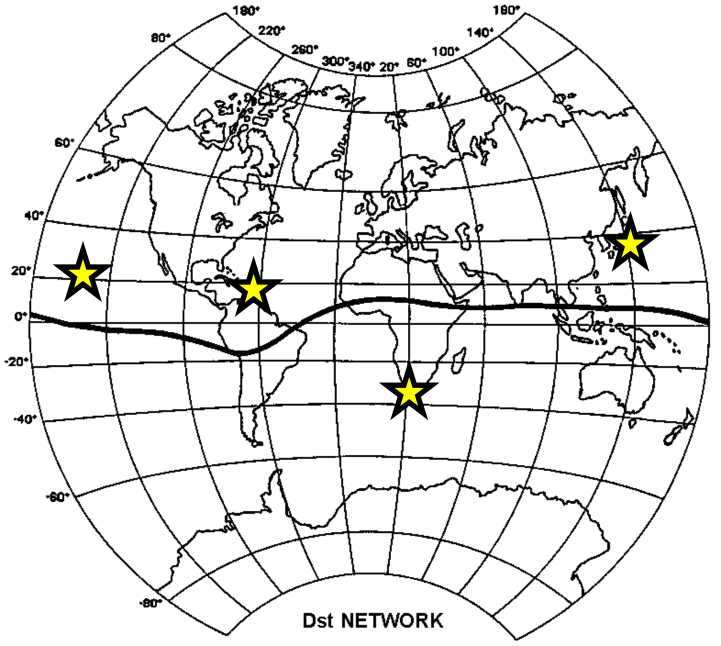

- Represents the axially symmetric disturbance (of the horizontal component) of the magnetic field at the dipole equator on the Earth's surface.

- Derived using data from 4 stations
  - Hermanus (South Africa)
  - Kakioka (Japan)
  - Honolulu (US-HI)
  - San Juan (Puerto Rico)

IAGA Bulletin N°40: http://wdc.kugi.kyoto-u.ac.jp/dstdir/dst2/onDstindex.html

Dst-like Index From Swarm Data

1. Extract Total Magnetic Field Series from MAG_LR (1 Hz) product (Swarm-A)
   - Both VFM and ASM measurements can be used

2. Subtract CHAOS-6 (Finlay et al., *EPS* 2016) Internal Field Model
   - The External component models the Ring Current which is what drives the Dst Index so it must remain in the data

3. Remove values that lie above ±40° in Magnetic Latitude

4. Remove spikes and interpolate small data gaps

Dst-like Index From Swarm Data

5. Apply a low-pass Chebysev Type I filter with a cutoff period of 13 hours
   - A 12-hour averaging provides **complete global coverage!**

     (better than the 4 stations used for Dst Index derivation!)
6. Remove seasonal effects and the Local Time drift of the satellites' orbit
   - Use a Chebysev Type I filter with a cutoff period of approx. 4 months to model this slowly varying component
   - Subtract it from the filtered series of step 5.

- Apply a linear transform to get the Swarm Index

$$S_{index} = 2.5\, B_{(6)} - 15$$

Dst-like Index From Swarm Data

Before Linear Transform

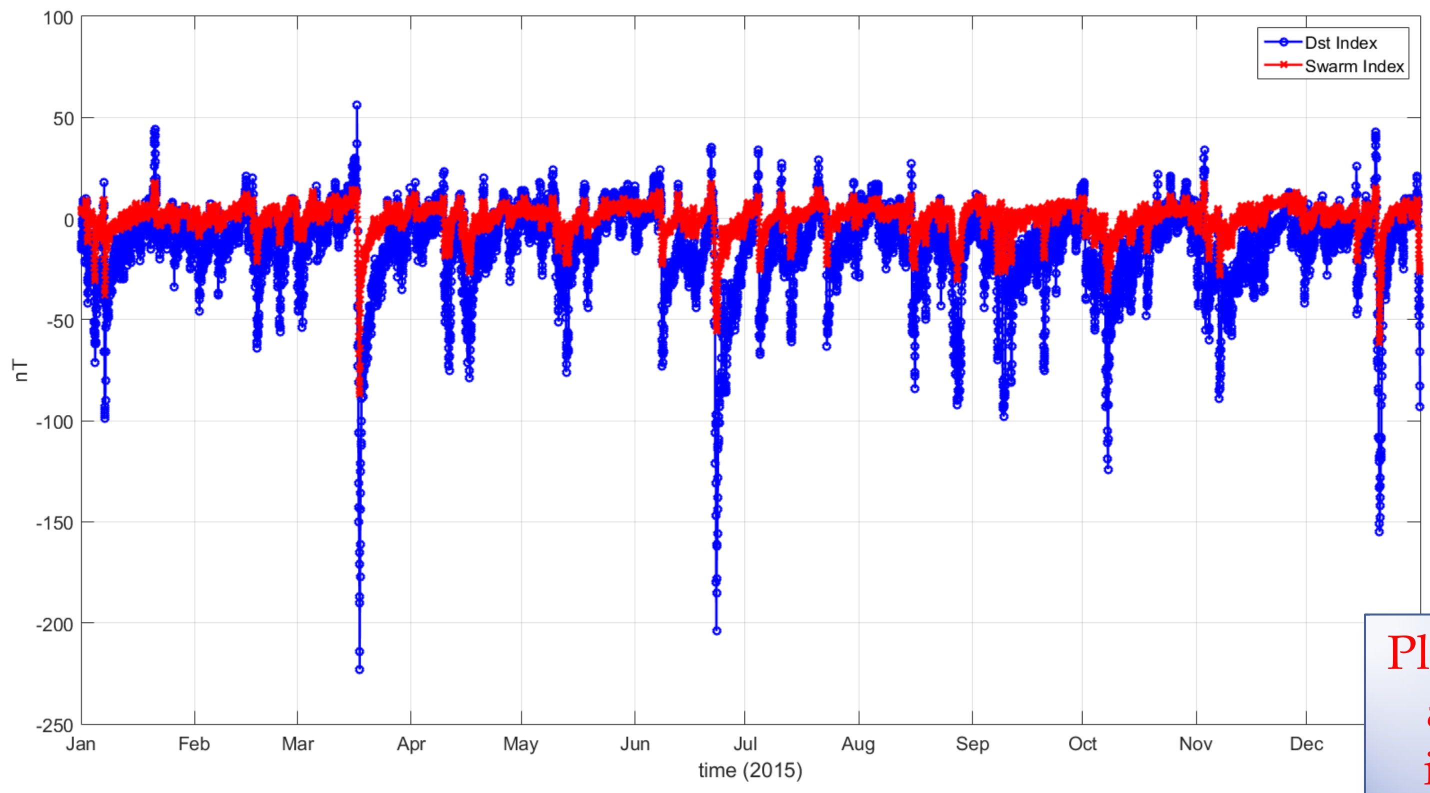

Plot markers at 1-hour intervals!

Dst-like Index From Swarm Data

After Linear Transform

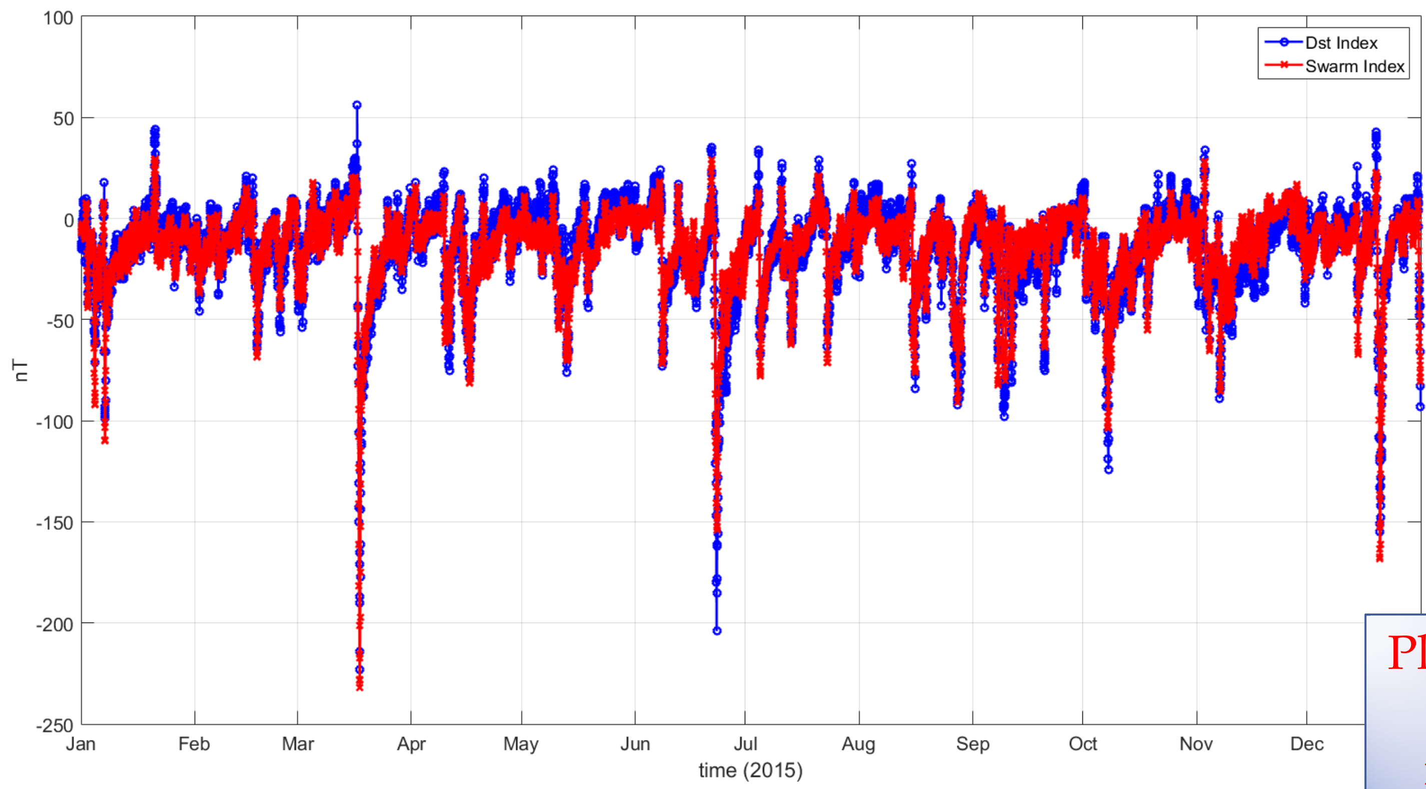

Plot markers at 1-hour intervals!

Swarm Index vs Dst Index for 2015

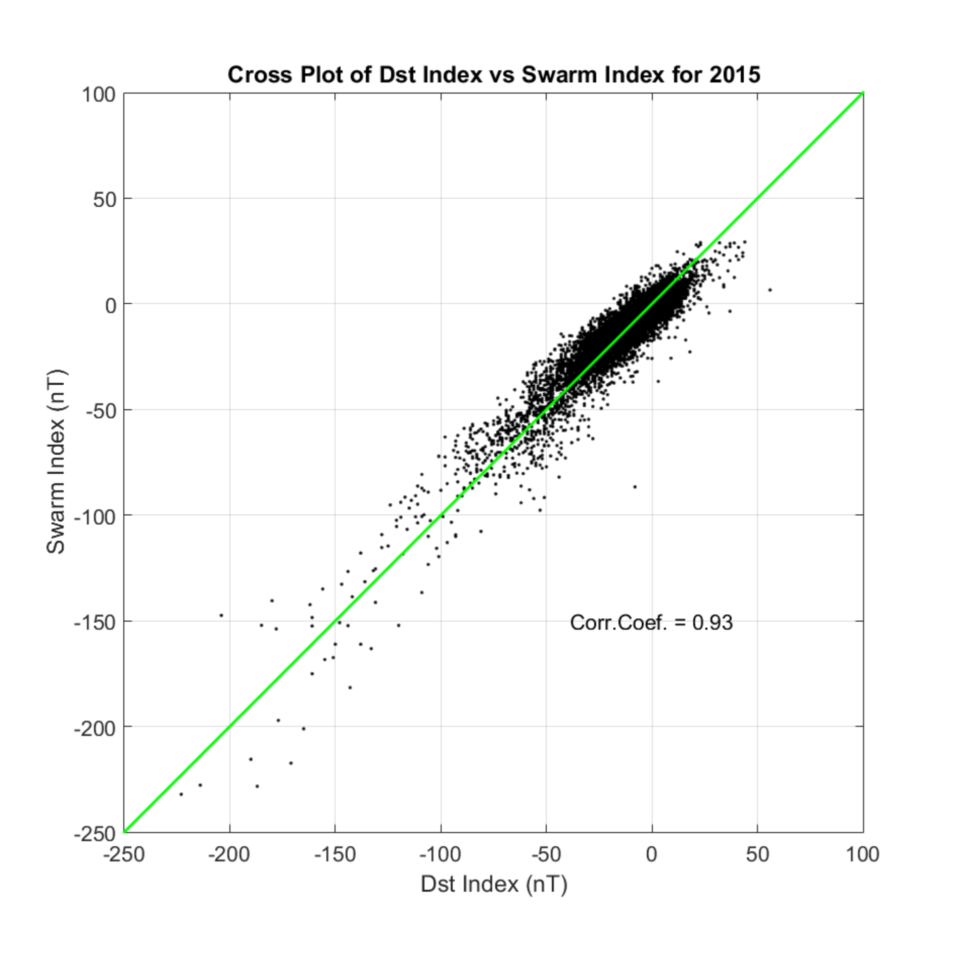

Correlation Study

- Up-sample Dst Index series to 1-sec sampling rate by linear interpolation
- Estimate Pearson's Correlation Coefficient for the entire 2015 time series
- Values >0.90 for a wide range of values for the free parameters

Swarm Index vs Dst Index for the March storm of 2015

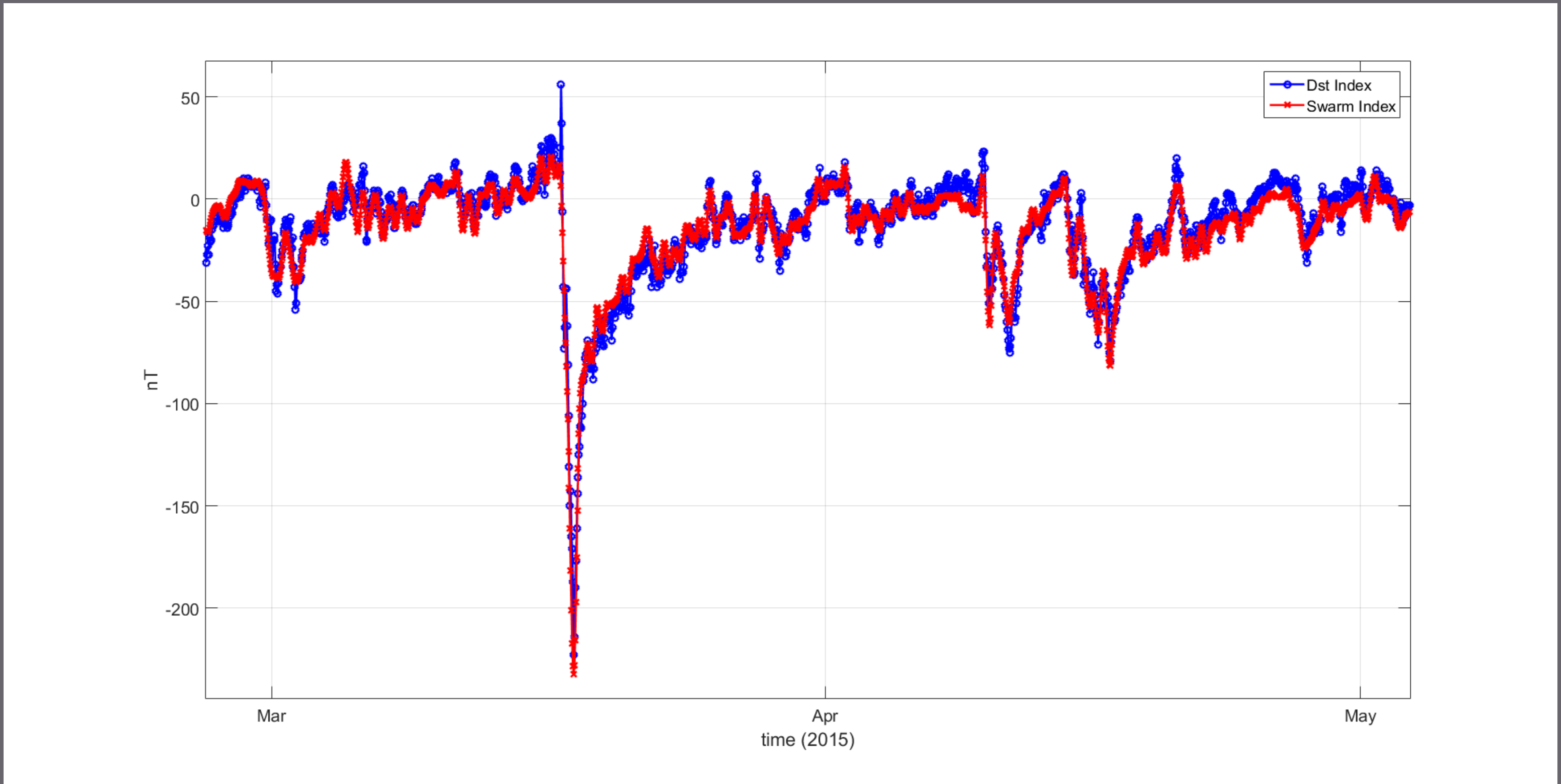

Swarm Index vs Dst Index for the June storm of 2015

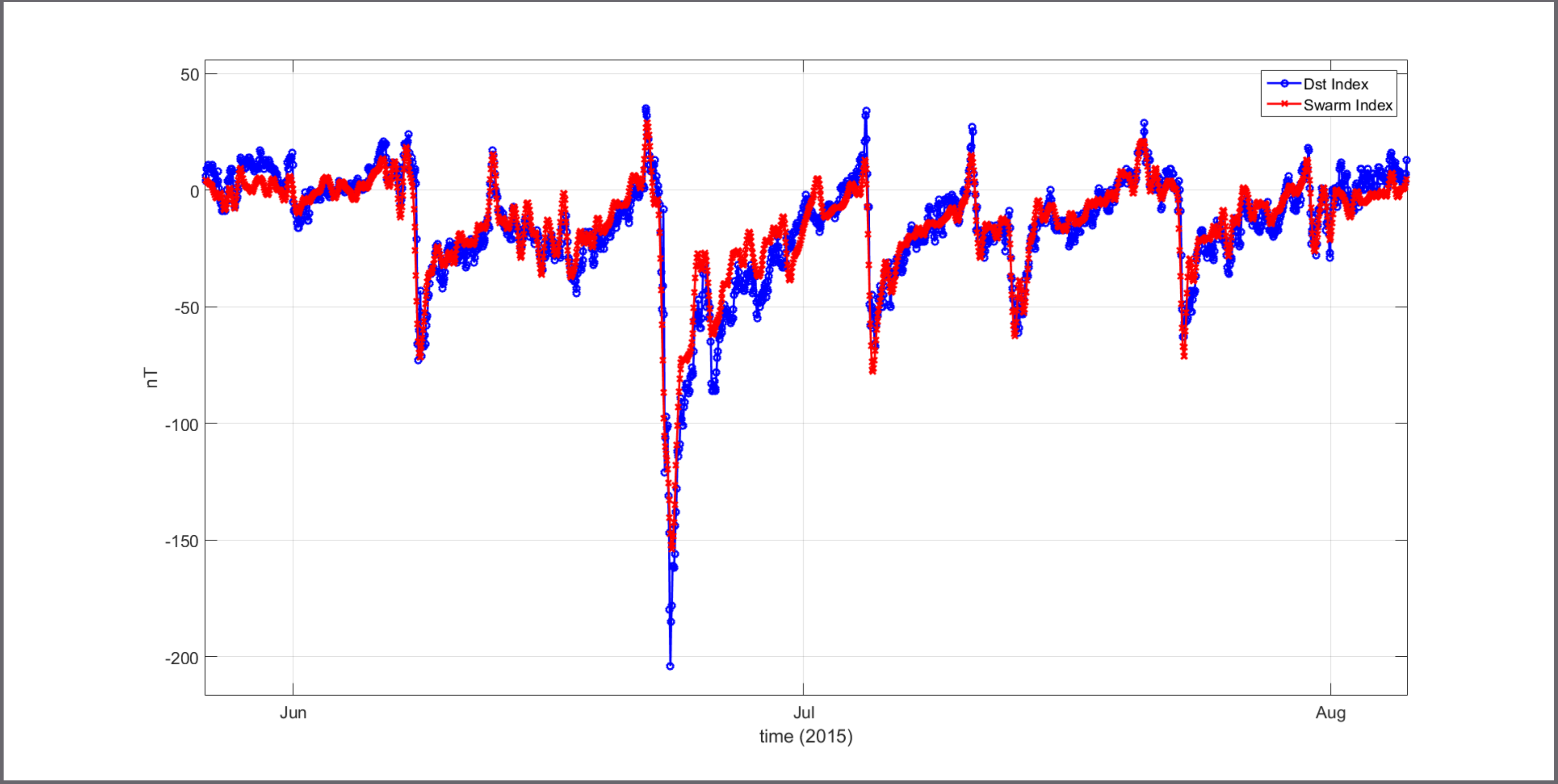

Swarm Index vs Dst Index for the December storm of 2015

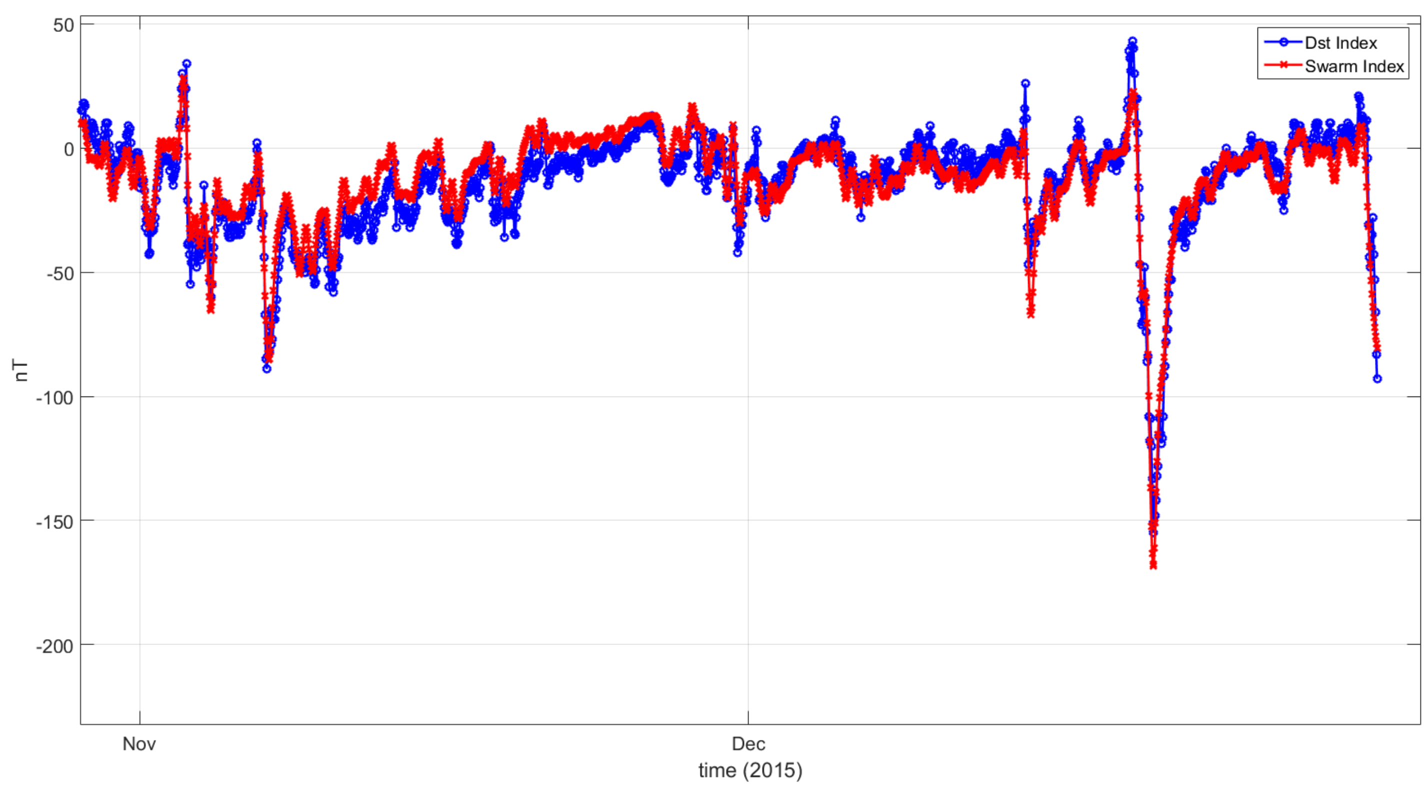

Model Training: The March 2015 Storm

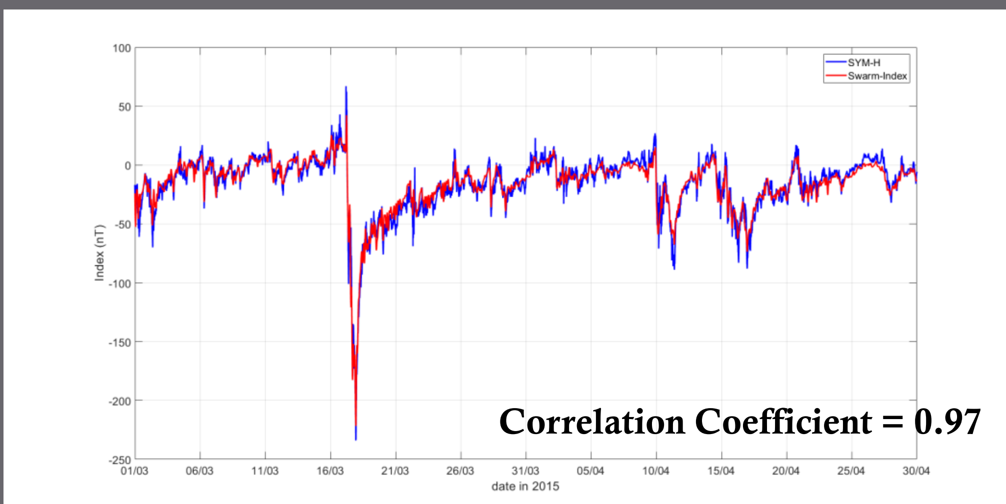

Application: The June 2015 Storm

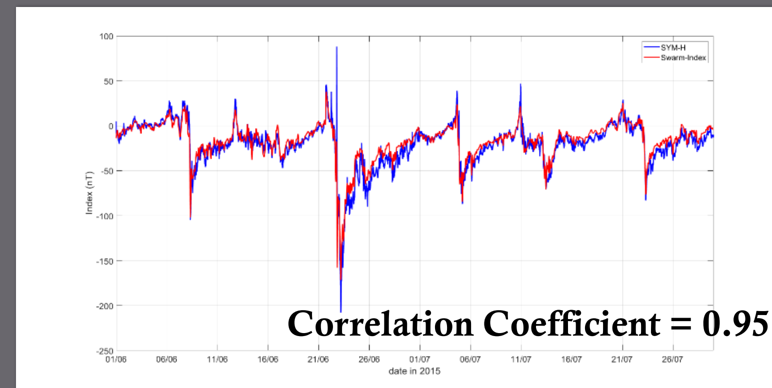

Application: The December 2015 Storm

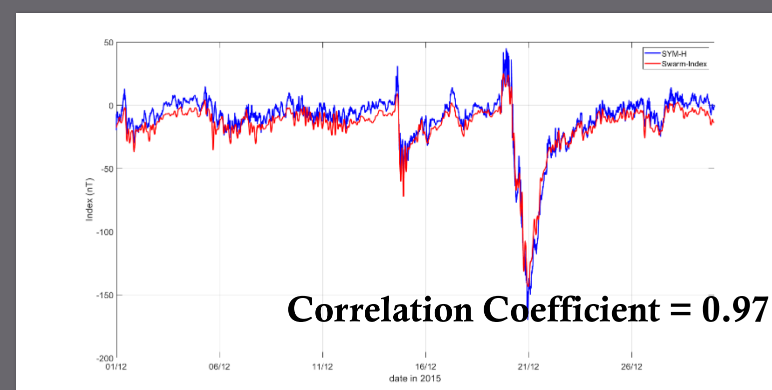

Key Reference

PHILOSOPHICAL TRANSACTIONS A

royalsocietypublishing.org/journal/rsta

Research

Check for updates

Cite this article: Balasis G, Papadimitriou C, Boutsi AZ. 2019 Ionospheric response to solar and interplanetary disturbances: a Swarm perspective. *Phil. Trans. R. Soc. A* **377**: 20180098.
http://dx.doi.org/10.1098/rsta.2018.0098

Accepted: 1 April 2019

One contribution of 9 to a theme issue 'Solar eruptions and their space weather impact'.

Subject Areas:
astrophysics, geophysics

Keywords:
ionosphere, low-Earth orbit satellites, plasma instabilities, magnetic storms

Author for correspondence:
G. Balasis
e-mail: gbalasis@noa.gr

Ionospheric response to solar and interplanetary disturbances: a Swarm perspective

G. Balasis[1], C. Papadimitriou[1,2] and A. Z. Boutsi[1,3]

[1]Institute for Astronomy, Astrophysics, Space Applications and Remote Sensing, National Observatory of Athens, Athens, Greece
[2]Space Applications & Research Consultancy – SPARC, Athens, Greece
[3]Department of Physics, National and Kapodistrian University of Athens, Athens, Greece

GB, 0000-0001-7342-0557

The ionospheric response to solar and interplanetary disturbances has been the subject of intense study for several decades. For 5 years now, the European Space Agency's Swarm fleet of satellites surveys the Earth's topside ionosphere, measuring magnetic and electric fields at low-Earth orbit with unprecedented detail. Herein, we study *in situ* the ionospheric response in terms of the occurrence of plasma instabilities based on 2 years of Swarm observations. Plasma instabilities are an important element of space weather because they include irregularities like the equatorial spread F events, which are responsible for the disruption of radio communications. Moreover, we focus on three out of the four most intense geospace magnetic storms of solar cycle 24 that occurred in 2015, including the St Patrick's Day event, which is the strongest magnetic storm of the present solar cycle. We examine the associated ionospheric response at Swarm altitudes through the estimation of a Swarm Dst-like index. The newly proposed Swarm derived Dst index may be suitable for space weather applications.

This article is part of the theme issue 'Solar eruptions and their space weather impact'.

Wavelet spectral analysis

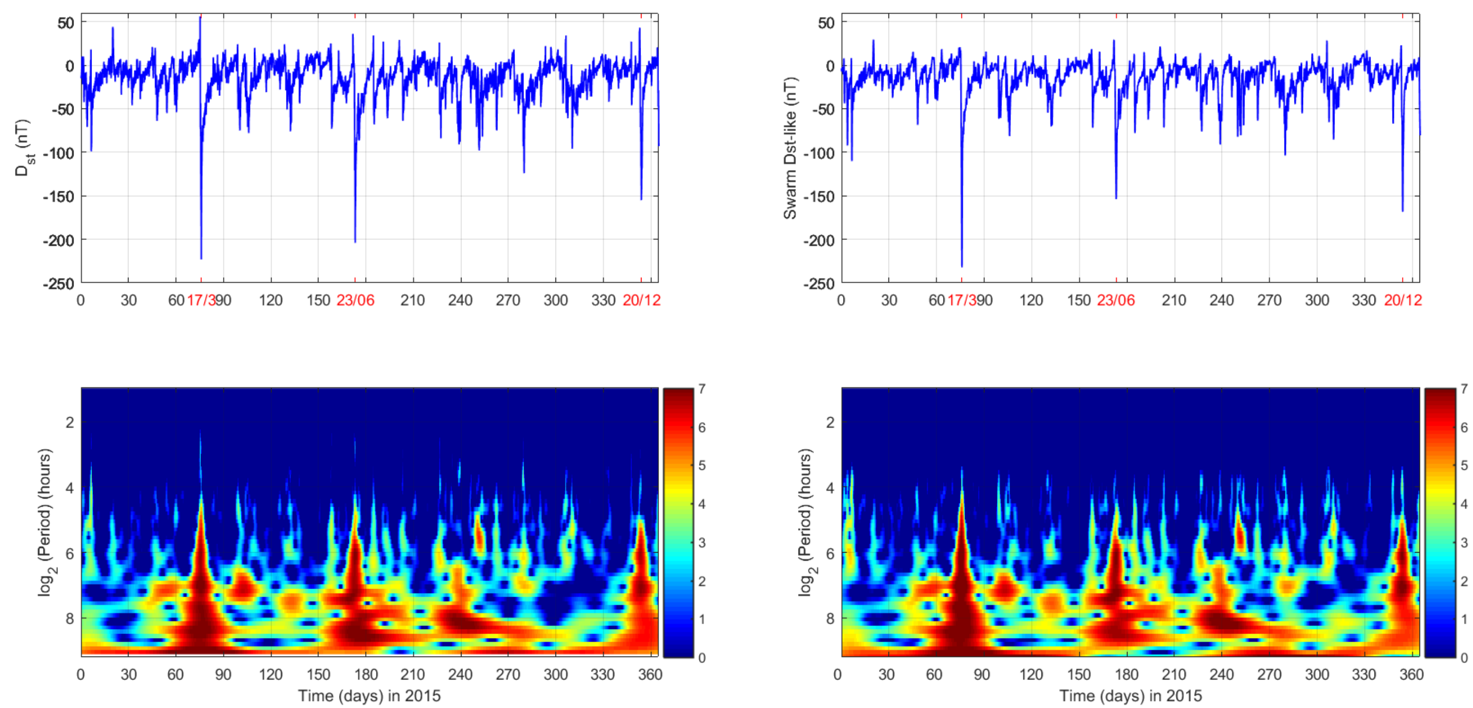

[Balasis et al., *under preparation]*

Temporal Variation of the *H* index

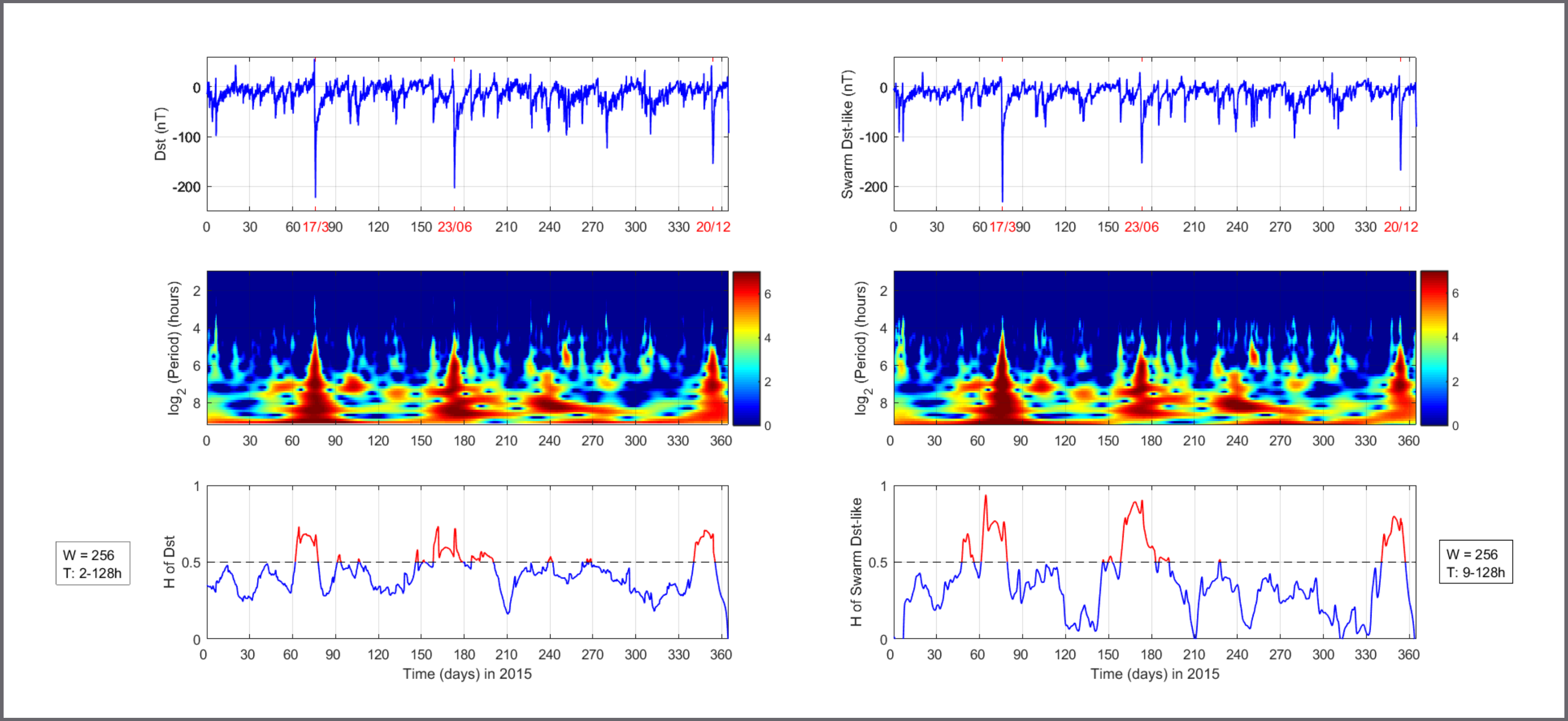

[Balasis et al., *under preparation*]

Entropies

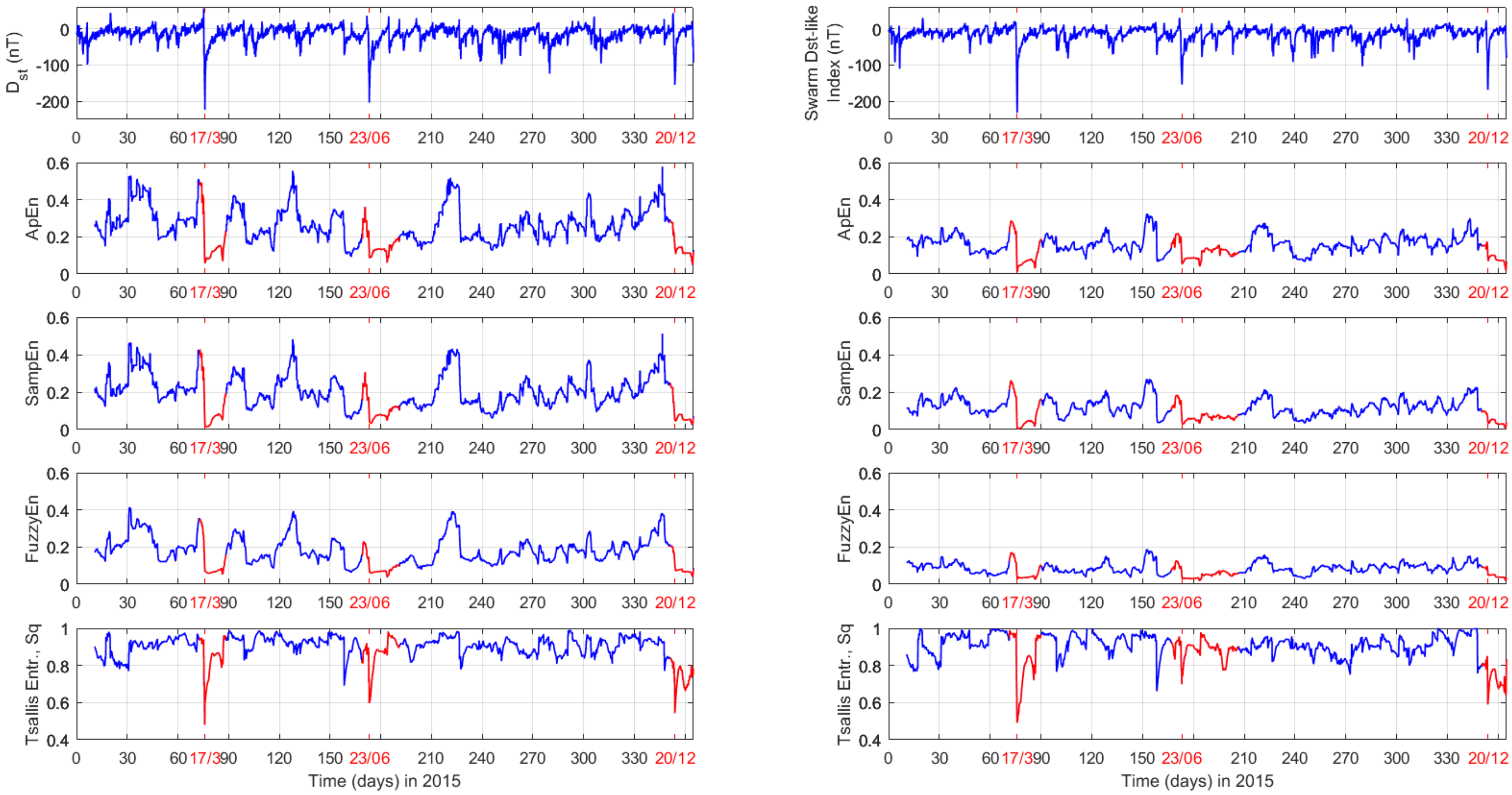

[Balasis et al., *under preparation*]

Auroral Electrojet (AE) Index

The AE index is derived from geomagnetic variations in the horizontal component observed at selected observatories along the auroral zone in the northern hemisphere.

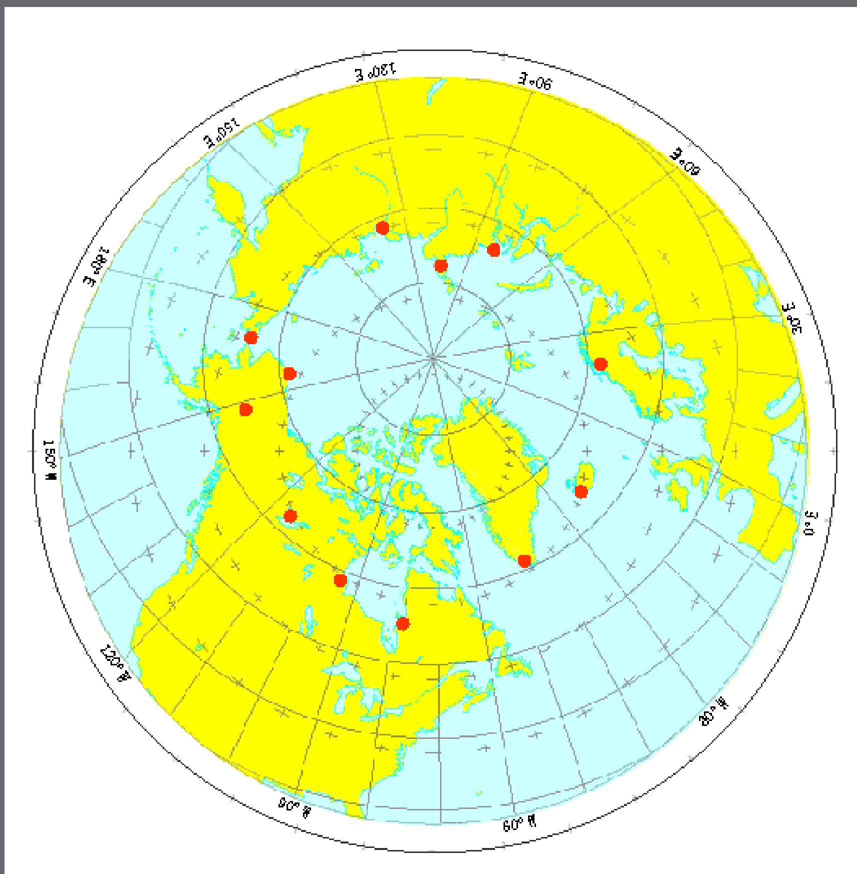

The AE index represents the overall activity of the electrojets

TABLE 1 - List of AE(12) Stations.

Observatory	IAGA Code	Geographic Coord. Lat.(°N)	Geographic Coord. Long.(°E)	Geomagnetic Coord. Lat.(°N)	Geomagnetic Coord. Long.(°E)
Abisko	ABK	68.36	18.82	66.04	115.08
Dixon Island	DIK	73.55	80.57	63.02	161.57
Cape Chelyuskin	CCS	77.72	104.28	66.26	176.46
Tixie Bay	TIK	71.58	129.00	60.44	191.41
Cape Wellen	CWE	66.17	190.17	61.79	237.10
Barrow	BRW	71.30	203.25	68.54	241.15
College	CMO	64.87	212.17	64.63	256.52
Yellowknife	YKC	62.40	245.60	69.00	292.80
Fort Churchill	FCC	58.80	265.90	68.70	322.77
Poste-de-la-Baleine	PBQ	55.27	282.22	66.58	347.36
Narsarsuaq (Narssarssuaq)	NAQ	61.20	314.16	71.21	36.79
Leirvogur	LRV	64.18	338.30	70.22	71.04

> 55˚ lat.

Davis and Sugiura, 1966

AE-like Index from Swarm Data

- Get Magnetic Field data in FAC (Bpar, Bper1, Bper2) after pre-processing and removal of the CHAOS-6 Model.
- Build the "horizontal" component, assuming that at high latitudes, this is mostly given by the perpendicular FAC components

$$B_{horz} = \sqrt{B_{per1}^2 + B_{per2}^2}$$

- Keep only values above 50˚ or below 50˚ in MLat
- Low-pass filter with a a cutoff period of 2.4 hours to get B_f
- Apply a linear transform to get the Swarm Index

$$S_{index} = 5.3\, B_f - 75$$

B_{horz} formula, Latitude & freq. cutoffs designed to maximize correlation coef.
Multiplicative factor designed to achieve similar variance with AE Index
Offset designed to minimize RMSE

Model Training with March 2015 data

AE Index from Swarm Data March 2015 Storm

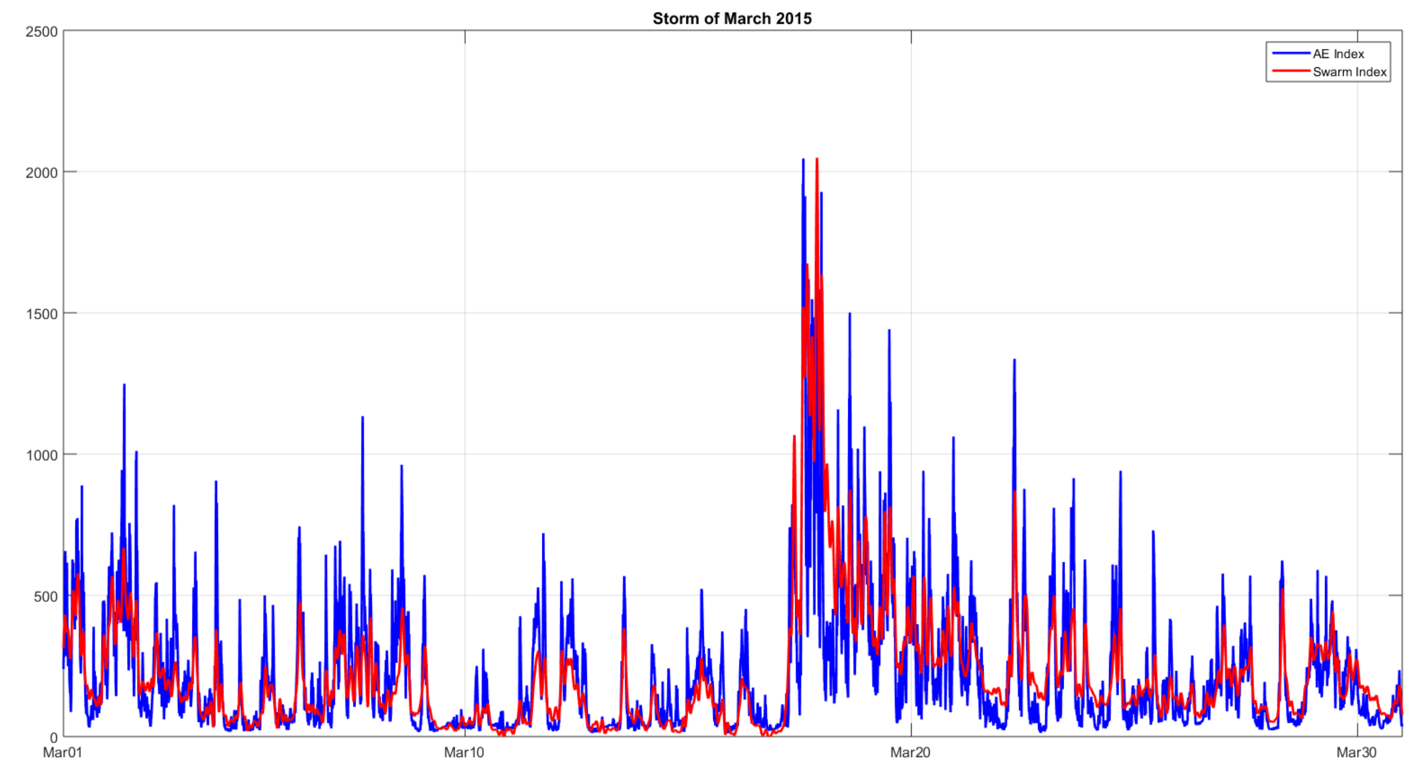

AE Index from Swarm Data June 2015 Storm

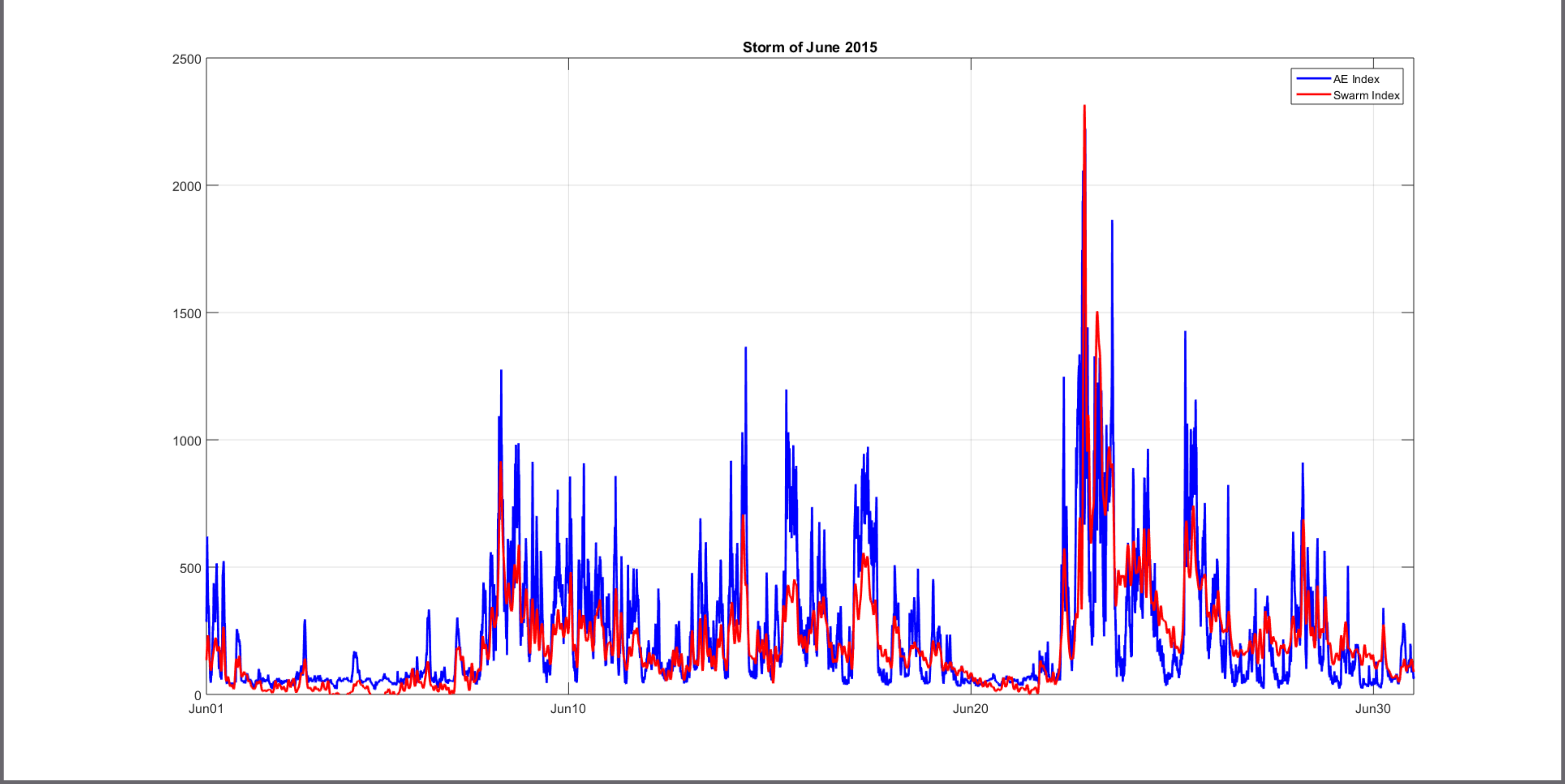

AE Index from Swarm Data December 2015 Storm

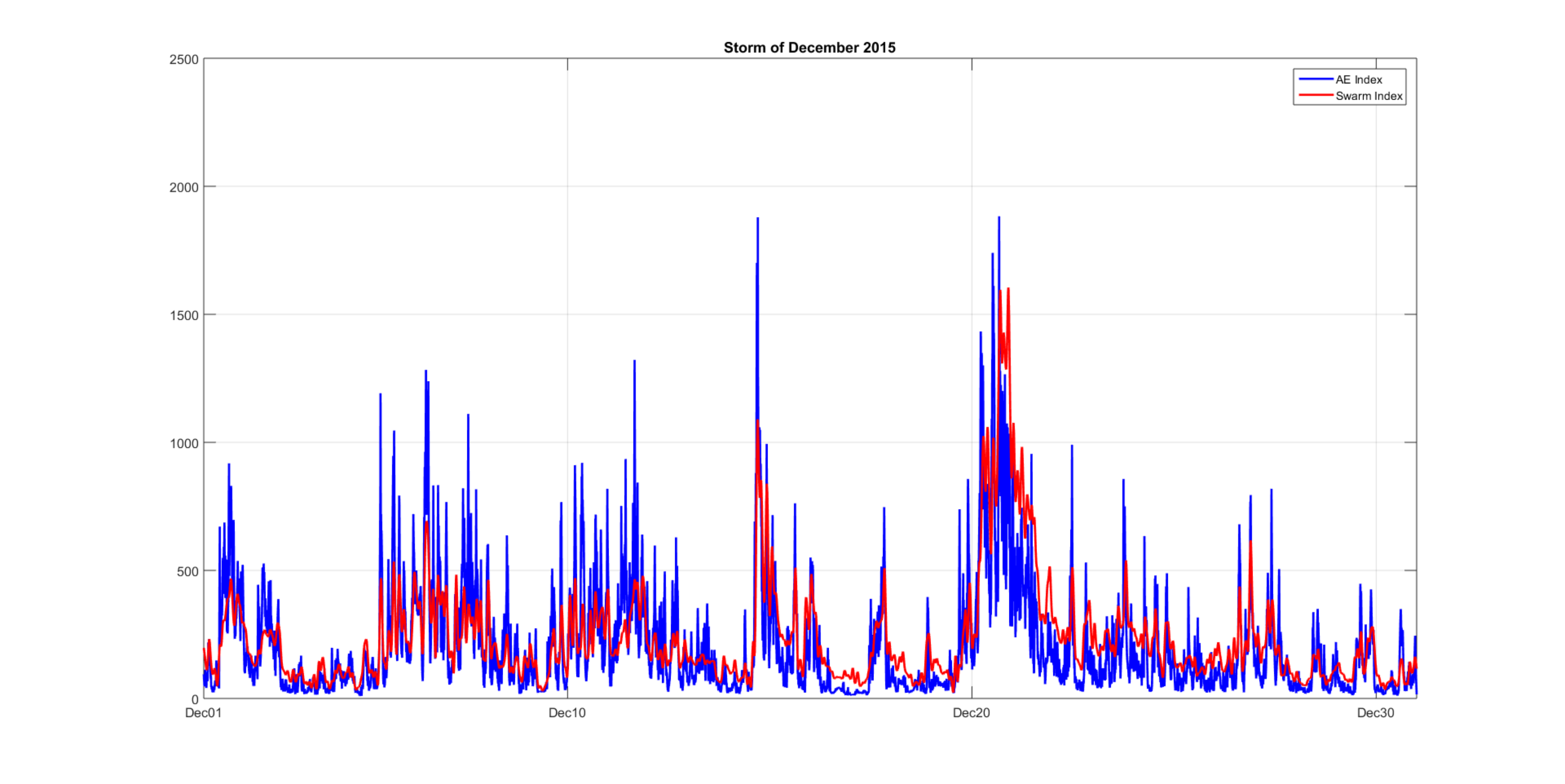

The March 2015 Storm

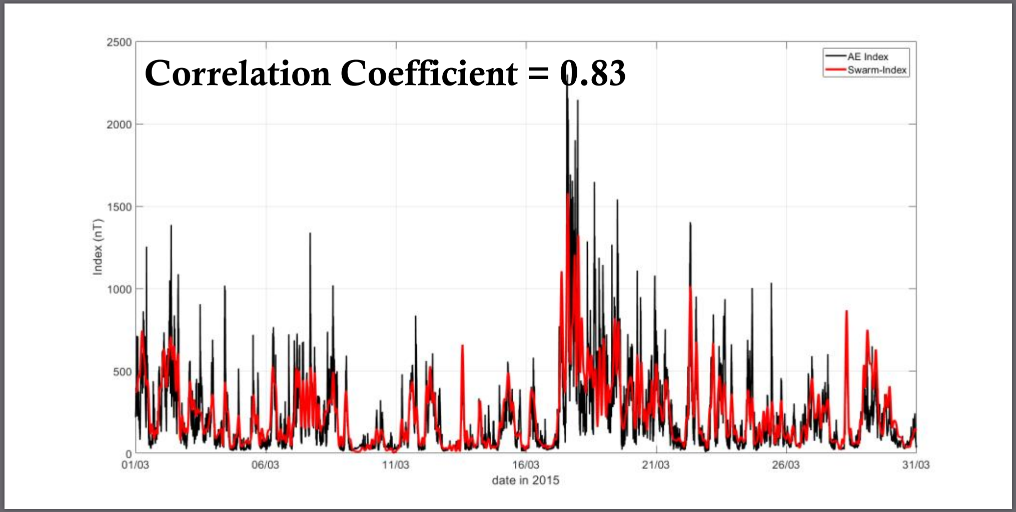

The June 2015 Storm

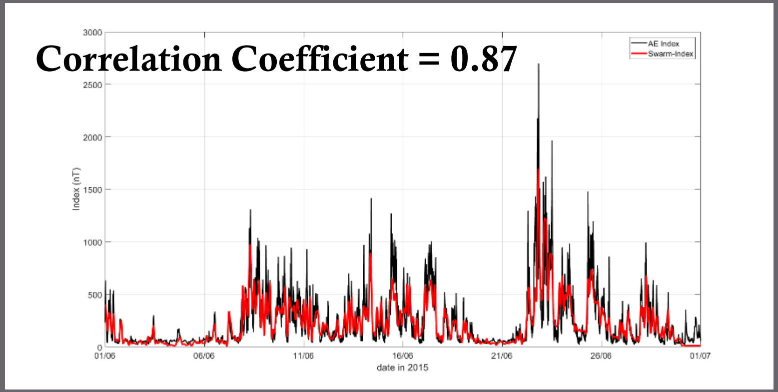

The December 2015 Storm

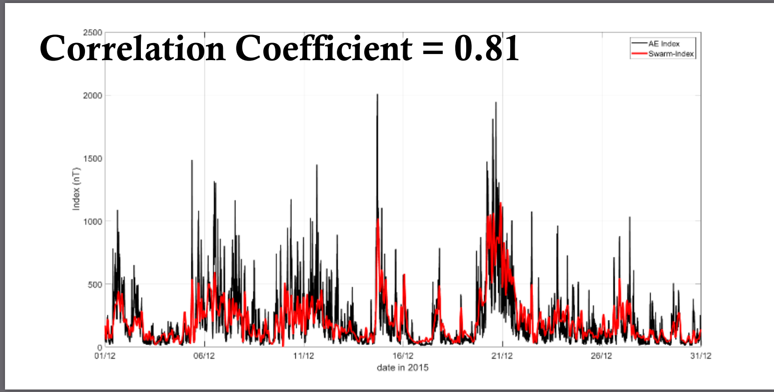

Entropies

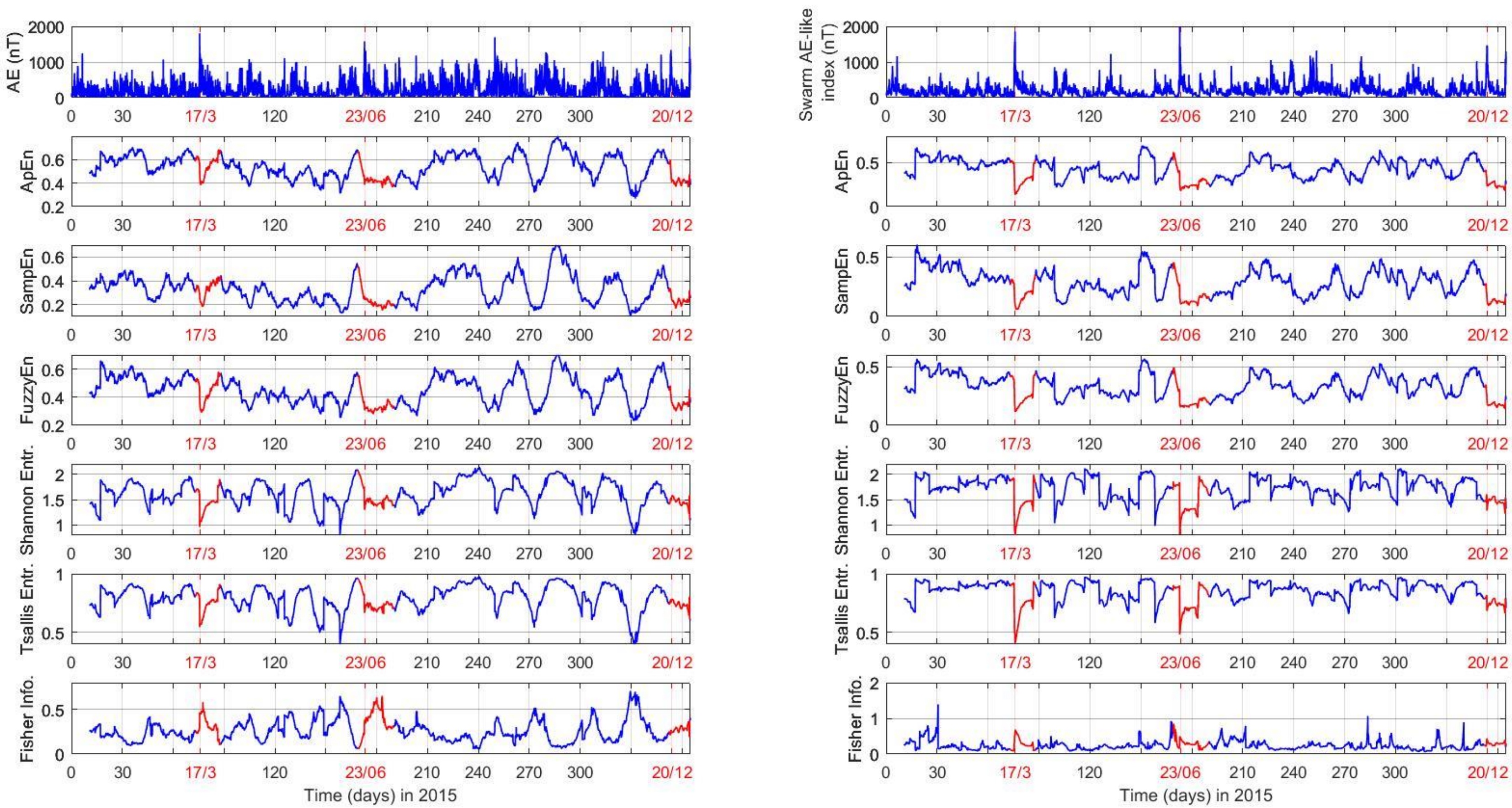

[Balasis et al., *under preparation]*

Summary

- The newly proposed Swarm-inspired Dst index [Balasis et al., *RSTA* 2019] monitors magnetic storm activity at least as good as the standard Dst / SYM-H indices.

- It yet remains to be investigated whether the standard Dst or the Swarm Dst index is a better representation of the currents contributing to the coupled ionosphere-magnetosphere system (e.g. ring current), especially during stormy periods.

- Due to the global coverage and superior sampling rate (1 Hz) of the Swarm Dst in comparison to the 4 / 6 stations coverage and inferior sampling rate (1 hour / 1 minute) of the standard Dst / SYM-H, the new index may be utilized for space weather forecasting purposes.

- The Hurst exponent and various entropy measures show the complexity dissimilarity among different "physiological" (normal) and "pathological" states (intense magnetic storms) of the magnetosphere. They imply the emergence of two distinct patterns: (i) a pattern associated with normal periods, which is characterized by a lower degree of organization / higher complexity, and (ii) a pattern associated with the intense magnetic storms, which is characterized by a higher degree of organization / lower complexity.

Multivariate information-theoretic method: causal inference approach

www.nature.com/scientificreports

SCIENTIFIC REPORTS

OPEN

Common solar wind drivers behind magnetic storm–magnetospheric substorm dependency

Received: 19 July 2017
Accepted: 2 November 2018
Published online: 19 November 2018

Jakob Runge[1,4,5], Georgios Balasis[2], Ioannis A. Daglis[3,2], Constantinos Papadimitriou[2] & Reik V. Donner[4,6]

The dynamical relationship between magnetic storms and magnetospheric substorms is one of the most controversial issues of contemporary space research. Here, we address this issue through a causal inference approach to two corresponding indices in conjunction with several relevant solar wind variables. We find that the vertical component of the interplanetary magnetic field is the strongest and common driver of both storms and substorms. Further, our results suggest, at least based on the analyzed indices, that there is no statistical evidence for a direct or indirect dependency between substorms and storms and their statistical association can be explained by the common solar drivers. Given the powerful statistical tests we performed (by simultaneously taking into account time series of indices and solar wind variables), a physical mechanism through which substorms directly or indirectly drive storms or vice versa is, therefore, unlikely.

IAASARS

ΕΘΝΙΚΟΝ ΑΣΤΕΡΟΣΚΟΠΕΙΟΝ ΑΘΗΝΩΝ * NATIONAL OBSERVATORY OF ATHENS *

Storm-substorm relationship

- The storm-substorm relationship is the more controversial aspect of magnetospheric dynamics where it is not clear whether and in which direction storms and substorms influence each other (Sharma et al., 2003).
- Although it has been traditionally assumed that the main phase of a magnetic storm is the interval in which many intense substorms take place successively a number of questions had been raised about the storm/substorm relationship (Gonzalez et al., 1994; Kamide et al., 1998).
- Daglis et al. (2003): No storms have been observed during which intense substorms did not occur. This implies that storms and substorms have a common cause, yet does not necessarily mean that one results in the other.

Substorms

- Akasofu coined the term "substorm" (Akasofu, 1964). His thesis advisor Sydney Chapman insisted that he use this term or else he wouldn't be allowed to publish (Bruce Tsurutani):
  - Brightening of equatorward most loop; Breakup and expansion; Recovery
  - The typical time scale is ~15 min to 1 hr

- Although the Akasofu 1964 scenario is "well accepted", in a recent private conversation with Bruce Tsurutani, he mentioned that this scenario is actually one of "typical features", not one of repeatable "check-list" items.
  - So one question is what are the variations from this norm, how frequently do they occur and are they externally or internally driven?

- Are Substorms An Incremental Unit of a Magnetic Storm?
  - Substorms can occur without magnetic storms and magnetic storms can occur without substorms.

Akasofu, S.-I.: The electric current approach in the solar–terrestrial relationship, Ann. Geophys., 35, 965-978, doi:10.5194/angeo-35-965-2017, 2017.

Multivariate information theoretical approach

- De Michelis et al. (2011) using transfer entropy (TE) suggested that there is information flow between storms and substorms and its direction depends upon the activity level.
- Wing et al. (2016) used mutual information (MI), conditional MI and TE to discovering solar wind drivers of the outer radiation belt (e.g. Vsw is found to be the most dominant driver of the geosynchronous MeV electron fluxes).
- Directional, multivariate causality measures using graphical models **(Runge et al., *PRL* 2012, *PRE* 2012, *Journal of Climate* 2014)** allow for the identification and statistical evaluation of linear as well as nonlinear causality between variables.
- Our goal is to detect which solar wind variables causally drives storm and substorm activity and whether and in which direction storms and substorms influence each other .

Substorm AL $\not\rightarrow$ Storm SYM-H

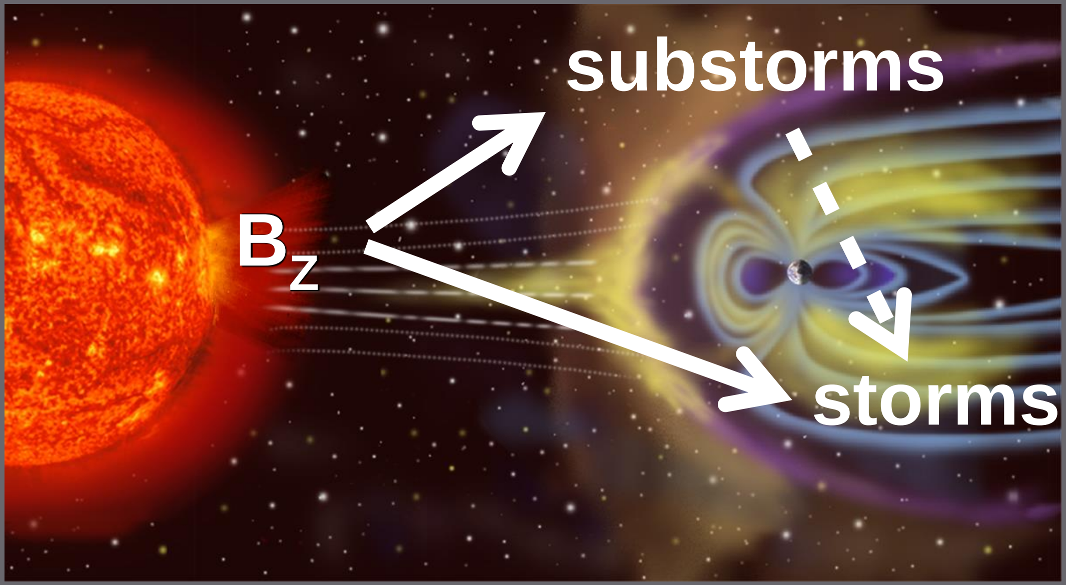

Data

2001 (near solar maximum)

Storm index: SYM-H [nT]
Substorm index: AL [nT]

Solar wind parameters:
B [nT]
B_Z (GSM) [nT]
V_{sw} [km/s]
P_{dyn} [nPa]

1 minute data aggregated to
20 minute time resolution

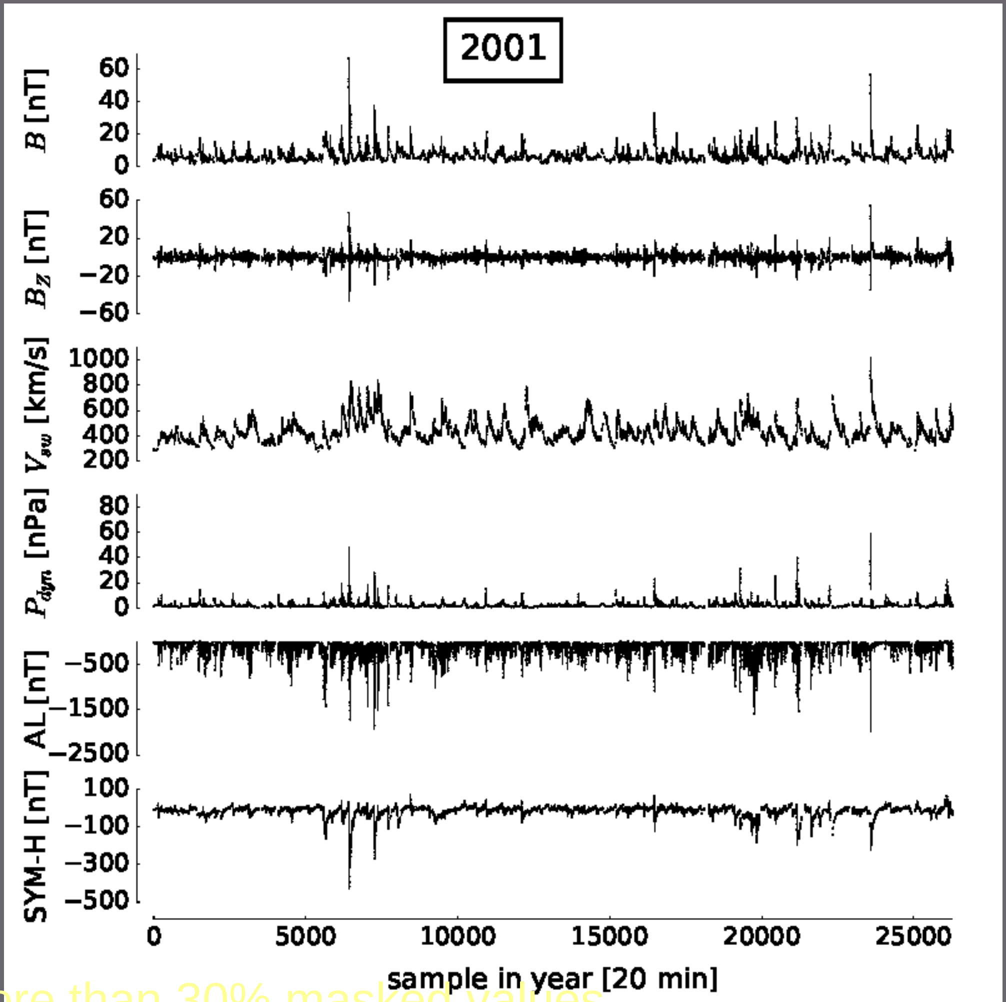

Neglecting 20 min. periods with more than 30% masked values

→ **20.000 – 26.000 samples**

SYM-H, AL indices: http://wdc.kugi.kyoto-u.ac.jp/
solar wind data: NASA omniweb

Causal reconstruction

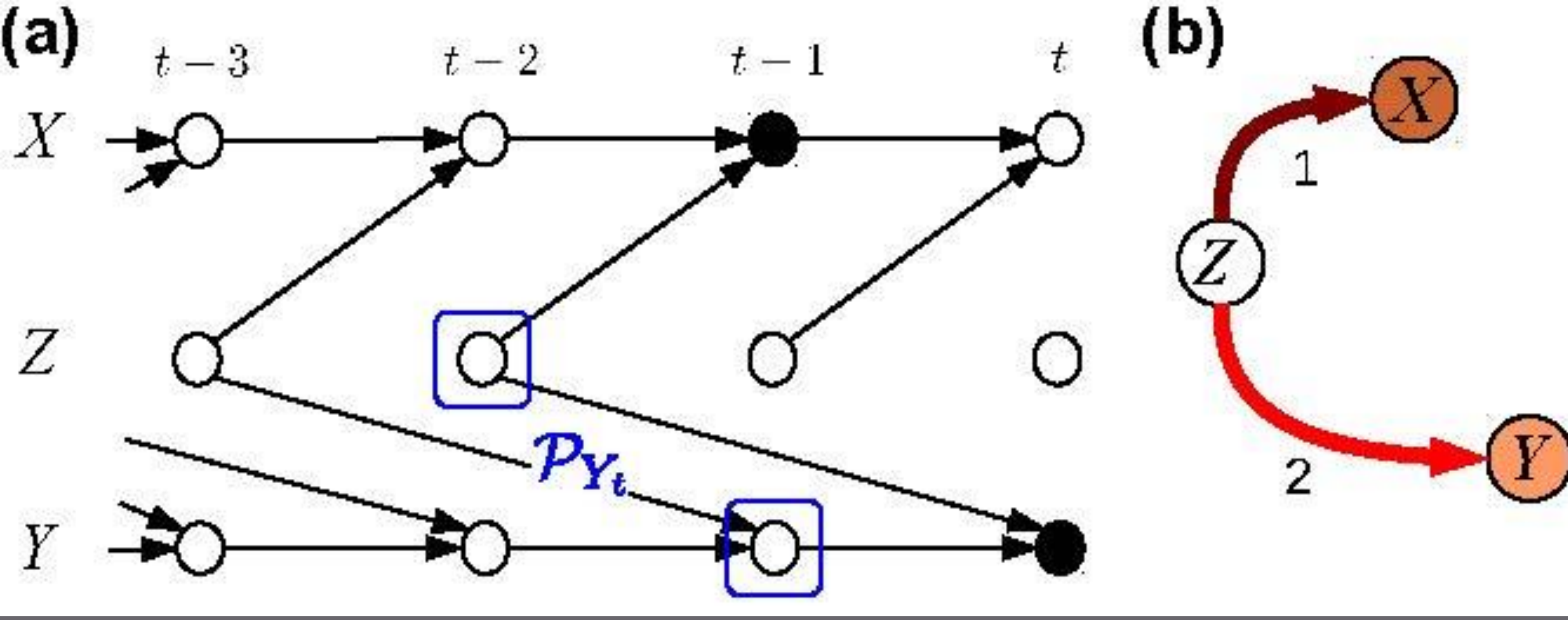

Lag functions of information-transfer measures

METHODS

1.) Lagged mutual information

k = 10 nearest-neighbor estimator (Kraskov et al. 2004)

Rescaled to correlation scale [0, 1]

Lag steps: 20 minutes
Max lag: 120 minutes

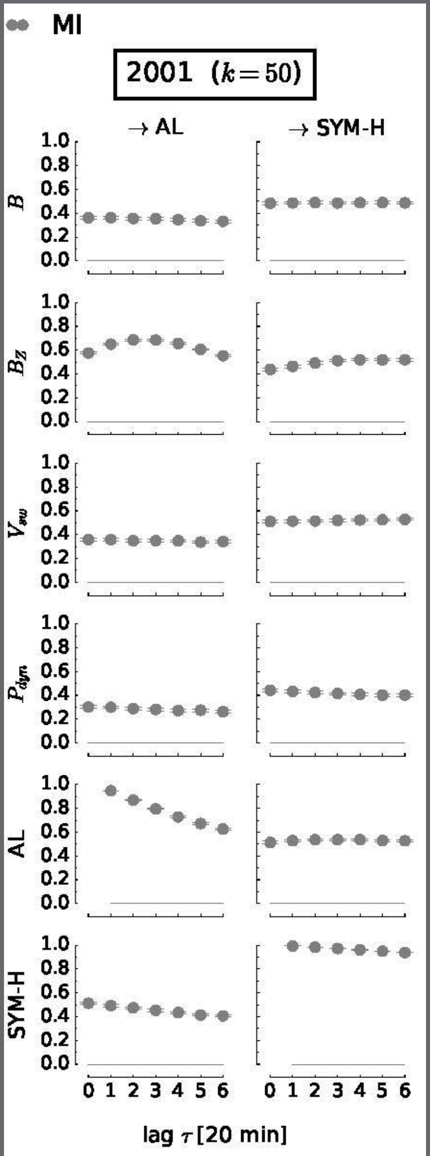

IAASARS

Lag functions of information-transfer measures

METHODS

2.) Bivariate Transfer Entropy / ITY

Condition on past:
$I(X_{t-\tau}; Y_t \mid Y_{t-1})$

k = 10 nearest-neighbor estimator
(Kraskov et al. 2004)

Rescaled to correlation scale [0, 1]

Lag steps: 20 minutes
Max lag: 120 minutes

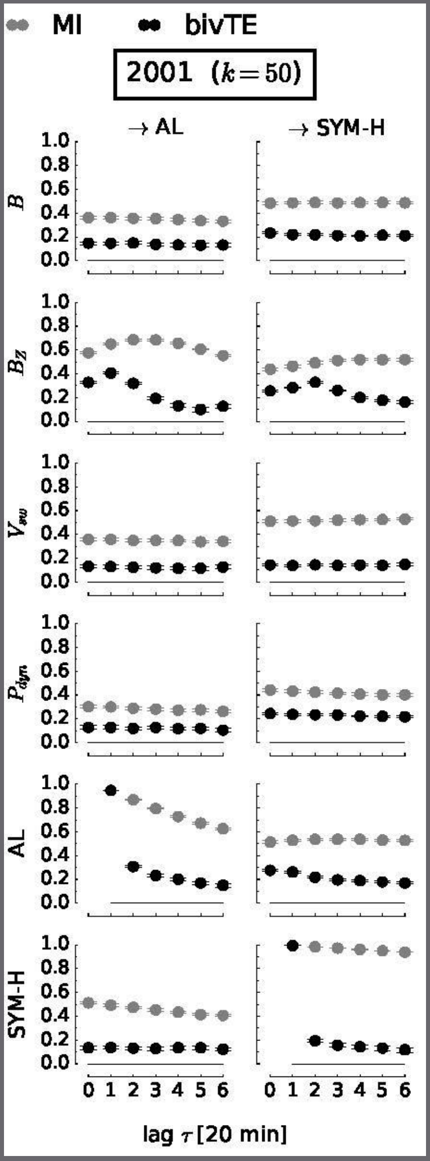

Lag functions of information-transfer measures

METHODS

3.) Multivariate ITY

Condition on past:
$I(X_{t-\tau}; Y_t \mid Parents(Y_t))$

k = 10 nearest-neighbor estimator
(Kraskov et al. 2004)

Rescaled to correlation scale [0, 1]

Lag steps: 20 minutes
Max lag: 120 minutes

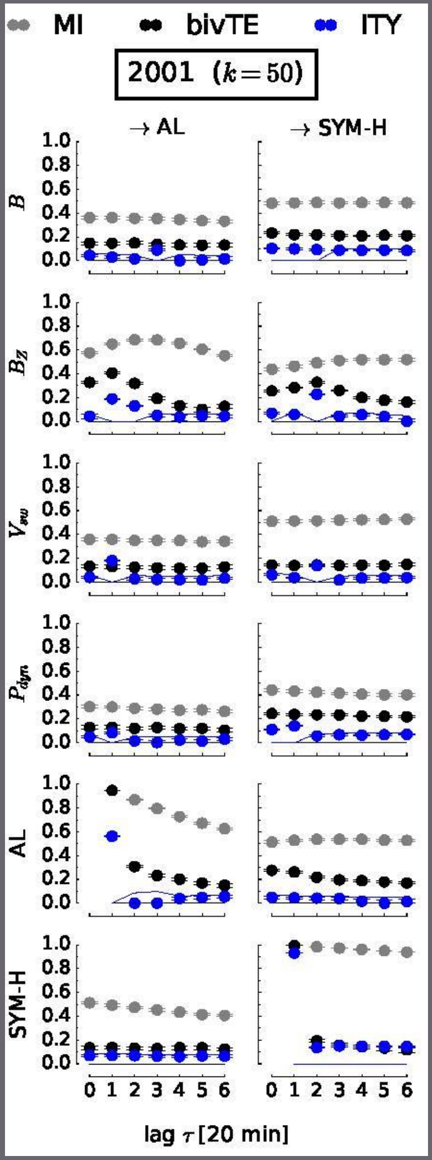

Results

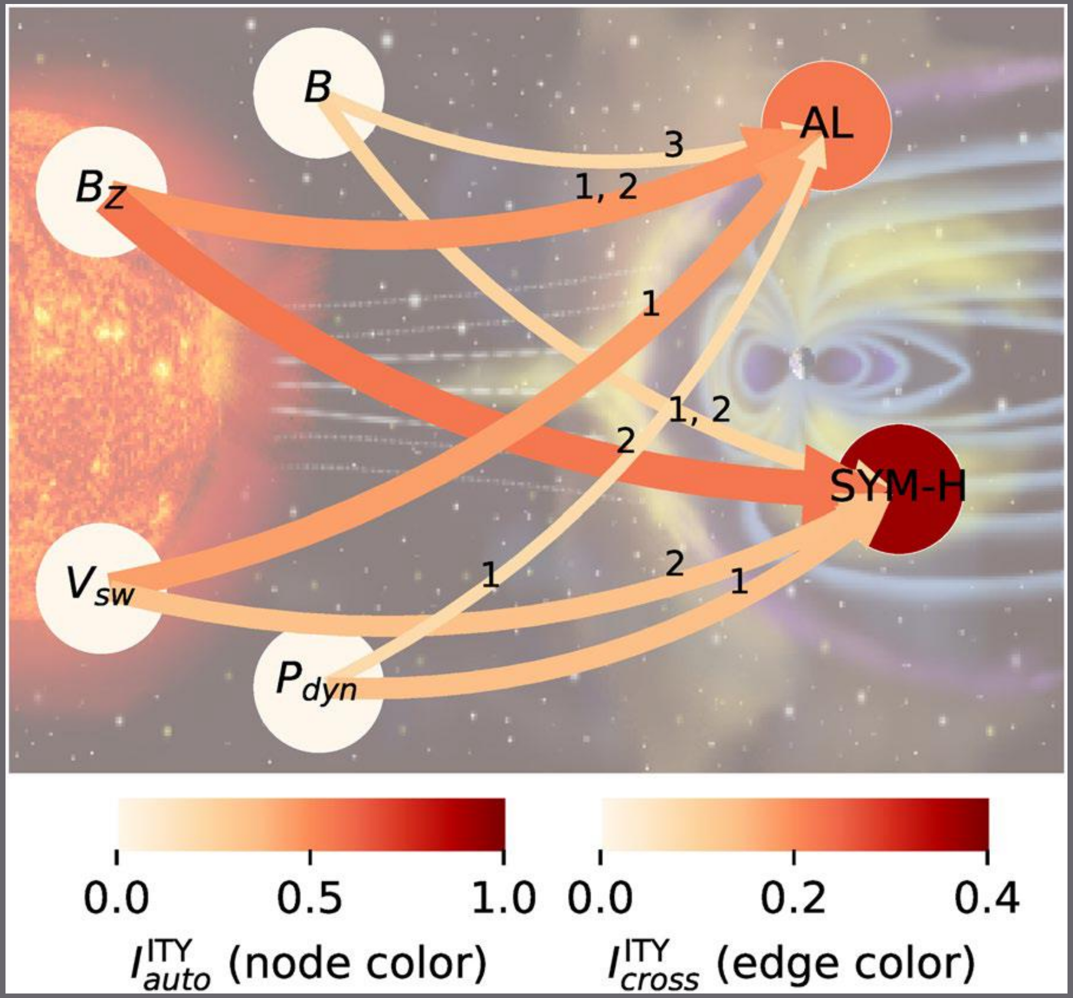

B
AL
B_Z
3
1, 2
1
1, 2
2
SYM-H
V_{sw}
1
2
1
P_{dyn}
0.0 0.5 1.0
I^{ITY}_{auto} (node color)
0.0 0.2 0.4
I^{ITY}_{cross} (edge color)

Summary

- The main driver of substorms as measured by AL is B_Z while V_{sw}. P_{dyn} and B are less relevant
  - Regarding time lags, the AL index first responds to B_Z (lag 20–40 min), then very weakly to B (20–40 min) and eventually to V_{sw} (80–120 min), while the lag of P_{dyn} is not very robust.

- B_Z and V_{sw} also drive storms as measured by SYM-H, but are less strong. P_{dyn} and B are also less relevant.
  - The SYM-H index also first responds to B_Z (lag 20–40 min) and earlier to P_{dyn} (20 min), then to V_{sw} (40-80 min) and rather weakly with non-robust lags to B.

- Most importantly, our iterative causal algorithm analysis suggests that B_Z , V_{sw} and P_{dyn} are sufficient to explain the previously found spurious link AL → SYM-H.

Take home messages

- Complex systems approaches are useful as complementary tools for many space weather - related problems of time series analysis and spatio-temporal data analysis.

- Here, complex systems-based methods have the potential to identify previously unrecognized precursory structures and, thus, contribute to a better understanding of dynamical processes manifested in observable magnetic field fluctuations prior to geospace magnetic storms and provide a novel way to anticipating and predicting incipient transitions in the dynamical regime of geomagnetic field variations in time and space.

- In addition to space weather forecasting, we expect a better understanding of the relationship between storms and substorms by disentangling the manifold processes interlinking both types of geospace phenomena.

Acknowledgements

Complex Systems Perspectives Pertaining to the Research of the Near-Earth Electromagnetic Environment

ISSI Team led by G. Balasis (GR)

Search

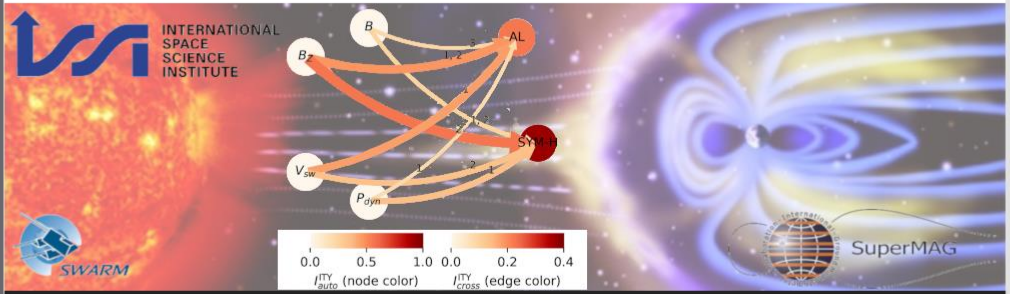

Home | Abstract | Team Members | Meetings | Internal

Summary

The Team attempts to combine advanced mathematical tools and identify key directions for future methodological progress relevant to space weather forecasting using Swarm, SuperMAG, and other space/ground datasets. By utilizing a variety of complementary modern complex systems based approaches, an entirely novel view on nonlinear magnetospheric variability is obtained. Taken together, the multiplicity of recently developed approaches in the field of nonlinear time series analysis offers great potentials for uncovering relevant yet complex processes interlinking different geospace subsystems, variables and spatio-temporal scales. The Team will provide a first-time systematic assessment of these techniques and their applicability in the context of geomagnetic variability.

International Space Science Institute | Hallerstrasse 6 | 3012 Bern | Switzerland | Tel +41 31 631 48 96

Acknowledgements

ISSI International Team members participating in *ISSS 2021* as lecturers:

- Giuseppe Consolini
- Tommaso Alberti
- Reik Donner
- Simon Wing
- Georgios Balasis

Acknowledgements

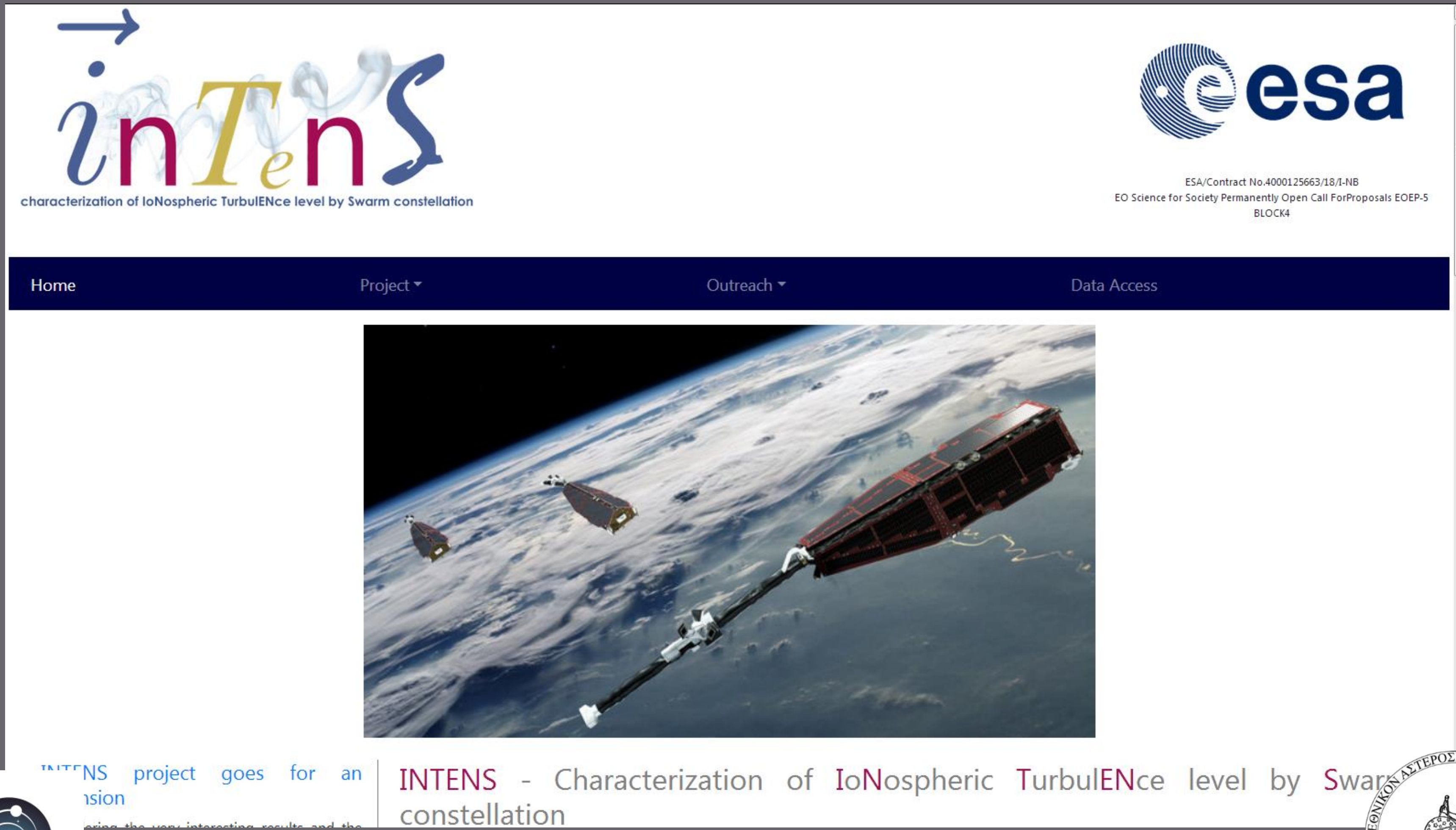

IAASARS